Aim and Scope

The objective of the *Journal of Residuals Science & Technology* (JRS&T) is to provide a forum for technical research on the management and disposal of residuals from pollution control activities. The Journal publishes papers that examine the characteristics, effects, and management principles of various residuals from such sources as wastewater treatment, water treatment, air pollution control, hazardous waste treatment, solid waste, industrial waste treatment, and other pollution control activities. Papers on health and the environmental effects of residuals production, management, and disposal are also welcome.

JOURNAL OF RESIDUALS SCIENCE & TECHNOLOGY—Published quarterly—January, April, July and October by DEStech Publications, Inc., 439 North Duke Street, Lancaster, PA 17602.

Indexed by Chemical Abstracts Service. Indexed/abstracted in Science Citation Index Expanded. Abstracted in Current Contents/Engineering, Computing & Technology. Listed in ISI Master Journal.

Subscriptions: Annual $219 per year. Single copy price $60. Foreign subscriptions add $45 per year for postage.

(ISSN 1544-8053)

DEStech Publications, Inc.
439 North Duke Street, Lancaster, PA 17602-4967, U.S.A.

CONTENTS

Research

Treatment of Wastewater Containing Crystal Violet Using Walnut Shell

YINGHUA SONG*, HE FANG, HUI XU, XUEMEI TAN and SHENGMING CHEN
Chongqing Key Lab of Catalysis & Functional Organic Molecules; Department of Chemistry and Chemical Engineering, Chongqing Technology and Business University, Chongqing 400067, China

ABSTRACT: Crystal violet (CV) was removed from aqueous solutions using walnut shell (WS) as an adsorbent. The effect of initial pH, contact time, adsorbent level and temperature on CV adsorption, were studied in batch mode. The results indicated that both the Langmuir and the Freundlich equations effectively described the adsorption equilibrium. A pseudo second-order kinetics provided a perfect fit for the studies. Intraparticle diffusion was also used to investigate the kinetic mechanisms. Intraparticle diffusion was a significant parameter in the regulation of adsorption. The thermodynamic parameters suggested a spontaneous endothermic reaction. The results suggest that WS is an inexpensive adsorbent for effective removal of CV.

1. INTRODUCTION

WASTEWATER contaminated with dyes is discharged into industrial effluents from textile, leather, plastic, printing, food, and cosmetic industries. More than 15% of the total dyes is released into the water bodies [1]. The discharge of dyes not only poses a serious environmental threat, but also toxic health hazards. Treatment of effluents before discharge into the environment is imperative. However, synthetic dyes are resistant to degradation due to their aromatic chemistry. The detoxification of synthetic dyes is important for the treatment of dye-based wastewater. Crystal violet (CV) is an important triphenylmethane cationic dye and is widely used to color paper, cotton, silk and leather. It is also used as a disinfectant and antiseptic in pharmaceutical industry. CV exposure leads to serious disease.

Among the various chemical and physical technologies available, adsorption is an inexpensive, fast and universal method to decontaminate water containing toxic dyes. Currently, activated carbon is used to eliminate dyes from wastewater. It is highly efficient, simple and feasible. However, it is an expensive process. Alternative techniques based on inexpensive raw materials such as rice husk [2], wheat husk [3], bagasse pith [4], saw dust [5], wheat straw [6], mango seed kernel [7], clay [8], apple pomace [6], peanut husk [9], and mazandaran wood [10] are desirable.

Walnut shell (WS) is an agricultural by-product generated in abundance in China, and is usually treated as an agricultural waste. The purpose of this study was to utilize WS to remove crystal violet from waste water. The study was conducted in batch mode to evaluate the effects of initial dye concentration, pH, adsorbent dose and temperature on adsorption. The equilibrium data were correlated with adsorption isotherms. The kinetic parameters were also calculated. The thermodynamic parameters were also determined.

2. MATERIALS AND METHODS

2.1. Adsorbent Preparation

WS was obtained from a farmers' market in Chongqing, China. After careful washing, it was dried at 333 K in an oven. It was ground to powder and sieved through different meshes before use.

2.2. Chemicals

A stock solution containing 0.5 g CV in 1000 mL of double-distilled water was prepared and diluted to obtain test solutions of the desired concentrations. Analytical-grade reagents were used. The initial pH of the dye solution was adjusted to pre-determined values using NaOH or HCl solutions (0.1 $mol \cdot L^{-1}$), before WS was added.

*Author to whom correspondence should be addressed.
Mailing Address: Department of Chemistry and Chemical Engineering, College of Environmental and Resources, Chongqing Technology and Business University, Chongqing 400067, China; Telephone: +86-023-62769785(office), Fax: +86-023-62769785, E-mail: yhswjyhs@126.com

1544-8053/16/03 243-07

doi:10.12783/issn.1544-8053/13/4/1

2.3. Adsorption Studies

Batch experiments were conducted with different concentrations of WS and 100 mL of CV solutions at constant temperature. The flasks containing the reagents were agitated on a shaker at 150 rpm. The residual dye levels in the system were monitored periodically. All the experiments were repeated and average values were obtained.

Equilibrium studies were conducted in a series of flasks containing 50 mL CV solution at concentrations ranging from 30 to 400 mg·L^{-1}. After addition of 0.01 g of WS to each flask, the mixtures were vortexed at 298K, 308K and 318K, respectively, for 6 h.

The adsorption capacity q(mg·g^{-1}) and the removal efficiency %R were calculated, respectively, as follows:

$$q = \frac{v(c_0 - c_t)}{m} \tag{1}$$

$$\%R = \frac{(c_0 - c_t)}{c_0} \times 100 \tag{2}$$

where c_0 denotes the initial CV concentration (mg·L^{-1}), c_t represents the CV concentration at t (mg·L^{-1}); v indicates the volume of CV solution (L); and m is the mass of the dry WS (g).

2.4. Analysis

The residual dye concentration in the solution was estimated spectrophotometrically. The maximum absorbance of CV was determined at 582 nm.

2.5. Adsorption Isotherms and Thermodynamic Parameters

Adsorption isotherms were used to correlate the equilibrium data. The linear form of the Langmuir isotherm is generally expressed as follows:

$$\frac{c_e}{q_e} = \frac{1}{K_L q_{\max}} + \frac{c_e}{q_{\max}} \tag{3}$$

where c_e denotes the equilibrium concentration (mg·L^{-1}), q_e represents the equilibrium capacity of CV on WS (mg·g^{-1}), K_L stands for the Langmuir adsorption constant (L·mg^{-1}), and $q_{\max}$ is the maximum value of monolayer adsorption potential of WS (mg·g^{-1}).

The Freundlich isotherm is expressed as follows:

$$\ln q_e = \ln k_F + \frac{1}{n} \ln C_e \tag{4}$$

where k_F (L·mg^{-1}) and n represent Freundlich constants.

Thermodynamic parameters are used to determine the role of temperature in CV removal. Changes in isosteric enthalpy ΔH at different degrees of adsorption were determined using the Clasius-Clapeyron equation [11]:

$$\ln c_e = \frac{\Delta H}{RT} + cons\tan t \tag{5}$$

where R is a constant (8.314 J·mol^{-1}·K^{-1}), and T is the absolute temperature (K). The lnc_e vs. 1/T plot yields a straight line with a slope equal to $\Delta H/R$.

The Freundlich isotherm provides an ideal fit for adsorption systems, and the Gibbs free energy function ΔG (kJ·mol^{-1}) is estimated using [12]:

$$\Delta G = -nRT \tag{6}$$

where n denotes the Freundlich constant.

The entropy ΔS (J·mol^{-1}·K^{-1}) is determined using the Gibbs-Helmholtz equation:

$$\Delta S = \frac{(\Delta H - \Delta G)}{T} \tag{7}$$

2.6. Adsorption Kinetics

The rate-determining step was determined using kinetic equations correlating the experimental data.

The pseudo-first order kinetics of adsorption systems according to Lagergren [13] is expressed by the following equation:

$$\ln(q_e - q_t) = \ln q_e - k_1 t \tag{8}$$

where q_t(mg·g^{-1}) represents the adsorption capacity at time t(min^{-1}) and k_1(min^{-1}) is the rate constant.

Further data analysis was conducted using Ho's pseudo-second order kinetics [14], assuming second-order chemical adsorption. It is expressed as follows:

$$\frac{t}{q_t} = \frac{t}{q_e} + \frac{1}{k_2 q_e^2} \tag{9}$$

where k^2(g·mg^{-1}·min^{-1}) denotes the rate constant.

Intraparticle diffusion resistance on adsorption is evaluated by a diffusion kinetics [15]:

$$q_t = k_p t^{1/2} + C \tag{10}$$

where k_p(mg·min$^{-1/2}$·g^{-1}) represents the rate constant and C(mg·g^{-1}) is a constant.

The intraparticle diffusion coefficient D(cm^2·s^{-1}) was calculated using the Wünwald-Wagner intraparticle diffusion model [16]:

$$\lg\left(1-\frac{q_t}{q_e}\right) = \lg\left(\frac{6}{\pi^2}\right) - \frac{4\pi^2 D}{2.303 d^2} t \tag{11}$$

where d(cm) denotes the average diameter of the WS particles.

3. RESULTS AND DISCUSSION

3.1. Effect of Initial pH

The initial pH of the working solutions was adjusted between pH 2–11, and its effect on adsorption of CV is shown in Figure 1.

The adsorption capacity increased sharply when the pH of the initial CV solution increased from 2.0–3.0. It remained almost constant between 3.0 and 6.0, and declined rapidly.

The poor elimination of CV at lower pH is attributed to excessive H^+ ions, which bind to the negatively charged WS surface, and prevent adsorption. Rising pH reduces proton generation, and increases the number of negatively charged adsorption sites. The attraction between WS and CV is dominant [17]. However, at pH greater than 6.0, flocculent precipitation occurs, indicating damage to the molecular structure of CV, resulting in a decline in adsorption capacity.

3.2. Contact Time

The role of contact time was determined using a CV concentration of 200 mg·L^{-1} at 303K, 313K and 323K, respectively.

At similar concentrations, the equilibrium adsorption capacity was directly correlated with temperature. The adsorption capacity of WS for CV increased from 339.2 mg·g^{-1} at 303 K to 349.8 mg·g^{-1} at 323 K. CV removal was faster initially and slower before finally reaching an equilibrium. Vacant sites on the surface of WS facilitate rapid adsorption. Eventually, fewer vacant sites prevent binding due to increased repulsion [18].

3.3. Effect of Adsorbent Dosage

As shown in Figure 3, the efficiency of removal increased from 25.6% up to 83.7% in proportion to the increase in adsorbent dosage from 1–6 g·L^{-1}, as vacant sites are available for adsorption on WS surface. The surface area and vacant adsorption sites are proportional to WS dosage under constant particle size.

3.4. Adsorption Isotherm Parameters

As shown in Figure 4, the adsorption capacity increased from 99.8–502.6 mg·g^{-1} at 298K, from 111.5–514.0 mg·g^{-1} at 308K, and from 108.0–631.3 mg·g^{-1} at 318 K with increasing CV concentration. At constant temperature, the increase in initial CV concentration resulted in a higher driving force for mass transfer [5] and higher interaction between CV and WS.

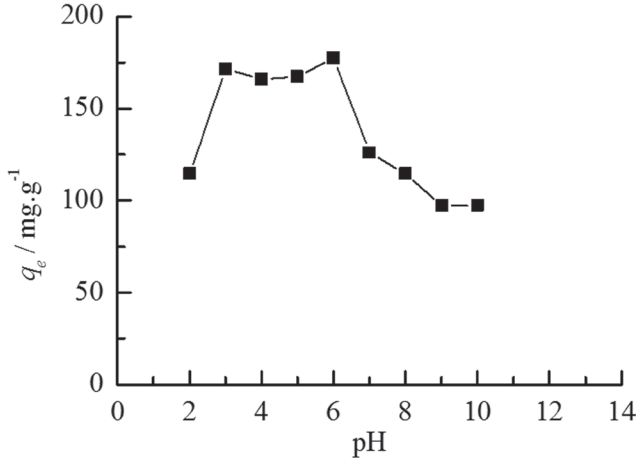

Figure 1. *Role of pH (c_0 = 500 mg·L^{-1}, T = 303K, WS concentration = 0.1 g·L^{-1}, adsorption time = 6 h, rpm = 150).*

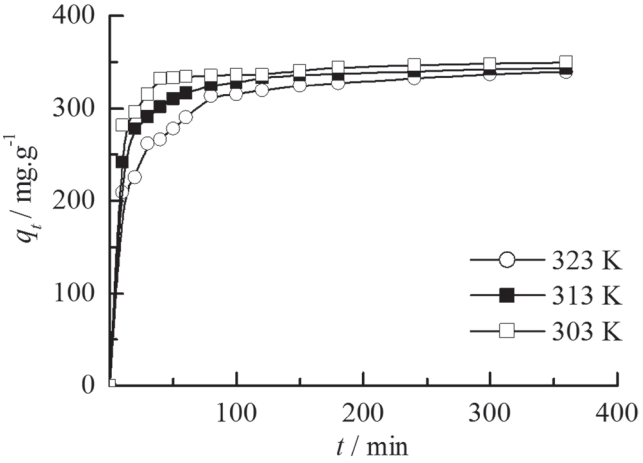

Figure 2. *Role of contact time (c_0 = 200 mg·L^{-1}, pH = 6.0, WS concentration = 2 g·L^{-1}, rpm = 150).*

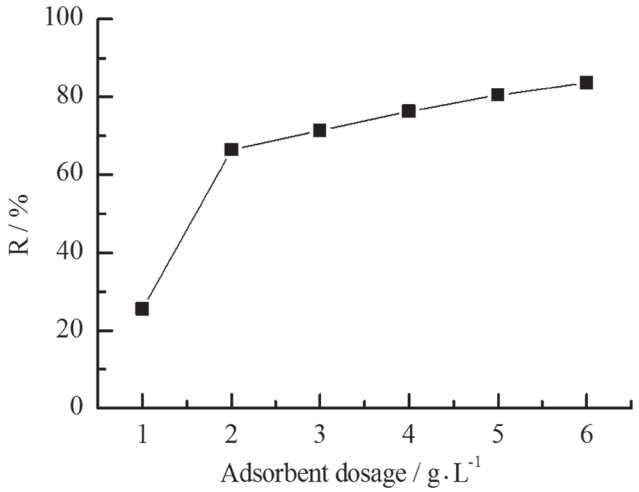

Figure 3. *Absorbent levels (c_0 = 500 mg·L^{-1}, T = 308K, pH = 6.0, adsorption time = 6 h, rpm = 150).*

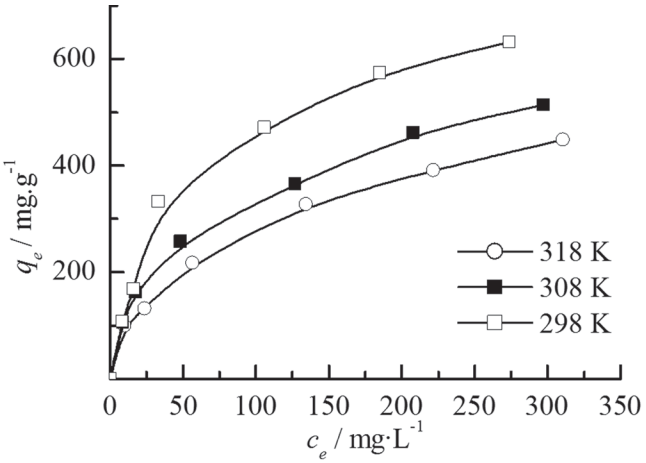

Figure 4. *Adsorption isotherms of CV for WS (pH = 6.0, adsorbent dosage = 0.2 g·L^{-1}, adsorption time = 6 h, rpm = 150).*

Adsorption of CV on WS was increased with temperature from 298K to 318K at different initial concentrations of the dye. The equilibrium adsorption capacity increased with temperature.

Equilibrium data displayed in Figure 4 were fitted with Langmuir and Freundlich isotherms. The Langmuir and Freundlich constants are listed in Table 1. The values of R^2 suggest that the equilibrium data were consistent with the adsorption models. The maximum monolayer capacities of WS were 526.3, 588.2, 714.3 mg·g^{-1} at 298K, 308K and 318K, respectively. The Freundlich constant, k_f, also showed an increase with temperature. Adsorption was favored at n values greater than 1 [5].

3.5. Thermodynamic Parameters

ΔH was determined from the slope of the Van't Hoff plot as shown in Figure 5 and Table 2. The Freundlich equation adequately defined the equilibrium data, and therefore, the Gibbs free energy ΔG (kJ·mol^{-1}) was calculated according to Equation (6). The changes in entropy were calculated using Equation (7).

The negative ΔG suggested spontaneous adsorption while the positive ΔH confirmed the endothermic features. It suggested that adsorption capacity increased with temperature. A positive ΔS suggests that WS was related to CV and also indicates entropy at the solid/liquid interface [19].

Table 1. Isotherm Constants.

	Langmuir Parameter			Freundlich Parameter		
T/K	q_{max}/mg·g^{-1}	K_L/L·mg^{-1} (10^{-2})	R^2	k_F	n	R^2
298	526.3	1.49	0.9836	33.65	2.20	0.9953
308	588.2	1.86	0.9856	38.40	2.27	0.9918
318	714.3	2.04	0.9960	43.85	1.94	0.9899

3.6. Kinetic Parameters

Pseudo first- and second-order kinetics, and intraparticle diffusion were used to investigate the rate-controlling steps. The constants of these models were reported in Table 3.

Low correlation coefficients (near 0.90) and large differences in equilibrium adsorption capacity (q_e) suggest poor first-order kinetics. Different temperatures yielded straight lines of pseudo-second order kinetics with high correlative coefficients (> 0.99). Further, the calculated q_e values of pseudo-second order kinetics were consistent with the experimental data, suggesting chemical adsorption.

Intraparticle diffusion was also observed (Figure 6). The time dependence of q_t was represented by three straight lines. Multi-linearity supported the presence of intraparticle diffusion [20] corresponding to the second straight line. The k_p values were directly calculated from the second regression line, with correlation coefficients exceeding 0.96 as shown in Table 3. However, the linear plots failed to pass through the origin of co-

Table 2. Thermodynamic Parameters.

q_e	ΔH	ΔG (kJ·mol^{-1})			ΔS (J·mol^{-1}·K^{-1})		
(mg·g^{-1})	(kJ·mol^{-1})	298K	308K	318K	298K	308K	318K
200	32.24				126.49	123.56	117.52
300	38.52	–5.45	–5.81	–5.13	147.56	143.95	137.27
400	51.41				172.52	166.92	161.67

Table 3. Kinetic Models of Adsorption.

Model			Temperature, K		
			303	313	323
First-order reaction	$k_1(10^{-3})$	First-order rate constant, min^{-1}	8.21	7.30	5.58
	$q_{e,cal}$	Equilibrium capacity, $mg \cdot g^{-1}$	97.19	60.14	41.87
	R^2	Correlation coefficient	0.9157	0.8589	0.8072
Second-order reaction	$k_2(10^{-4})$	Second-order rate constant, $g \cdot mg^{-1} \cdot min^{-1}$	2.77	5.16	7.61
	$q_{e,cal}$	Equilibrium capacity, $mg \cdot g^{-1}$	344.83	344.83	357.14
	R^2	Correlation coefficient	0.9998	1	0.9999
Intraparticle diffusion	k_p	Rate constant, $mg \cdot min^{-1/2} \cdot g^{-1}$	3.50	4.99	1.40
	R^2	Correlation coefficient	0.9800	0.9600	0.9818
Wünwald-Wagner intraparticle diffusion	$D(10^{-10})$	Effective diffusion coefficient, $cm^2 \cdot s^{-1}$	8.15	0.14	4.84
		Intercept	–0.798	–0.738	–1.094
	R^2	Correlation	0.9817	0.9793	0.9838
$q_{e,exp}$	–	Equilibrium capacity, $mg \cdot g^{-1}$	346.17	349.9	356.91

ordinates, suggesting simultaneous film diffusion and intraparticle diffusion [21–23].

As shown in Table 3, the results of Wünwald-Wagner diffusion model suggest that the internal diffusion coeffcient ranged in magnitude between 10^{-11} and 10^{-8}. Intraparticle diffusion mediated CV adsorption by WS [16].

3.8. Comparison of q_{max} of Various Adsorbents

The adsorption capacities of different materials for CV are depicted in Table 4, suggesting a maximum adsorption capacity of WS for CV (714.3 $mg \cdot g^{-1}$). The value was greater than any other adsorbent listed, suggesting that WS was a promising adsorbent for dye removal.

4. CONCLUSIONS

The CV adsorption capacity of WS was significantly affected by temperature, initial dye concentration and pH. The adsorption isotherms suggest that WS was a cost-effective agricultural by-product suitable for adsorption and removal of CV.

CV adsorption based on pseudo-first and pseudo-second order kinetics suggested the role of chemiadsorption and intraparticle diffusion. Thermodynamic constants, especially positive values of ΔH, suggested endothermic reaction. Negative ΔG demonstrated the spontaneous nature and positive ΔS suggested increasing entropy at the solid-liquid interface of adsorption.

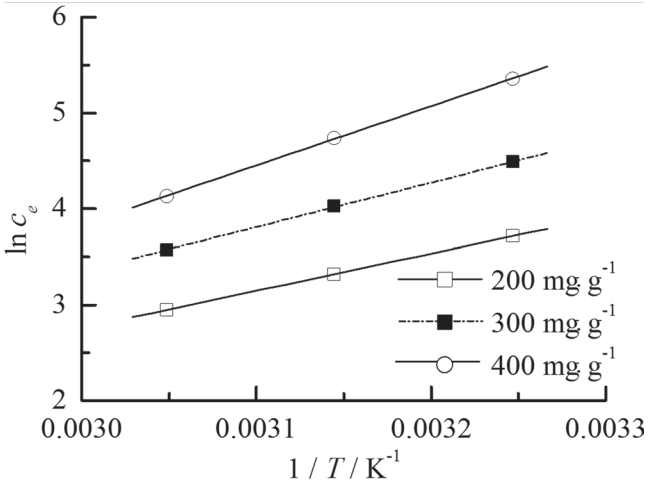

Figure 5. *Determination of isosteric enthalpy.*

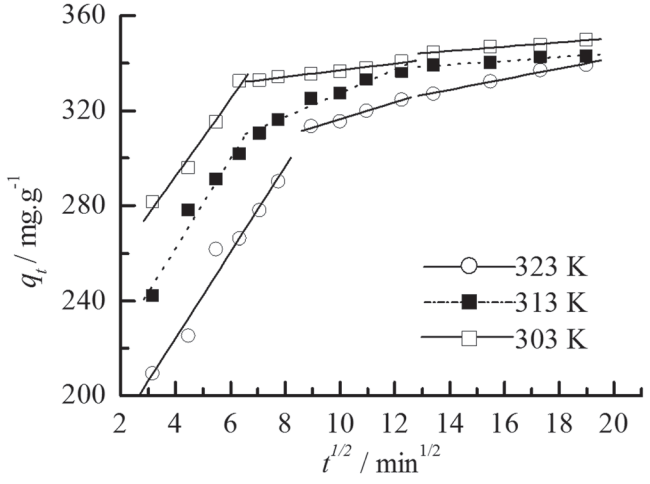

Figure 6. *Adsorption of CV via intraparticle diffusion.*

Table 4. Adsorbents for CV.

Adsorbent	Langmuir q_{max} (mg·g^{-1})	*T*(K)	Reference
Walnut shell	714.3	318	Present Work
Montmorillonite	160.6	–	[24]
Surfactant-treated nano-γ alumina	254.3	–	[25]
Amino silica	40.0	–	[26]
Acid-treated montmorillonite	400.0	–	[27]
Bacillus amyloliquefaciens biofilm	582.7	293	[28]
Nanocarbon derived from tomato paste	69.0	323	[29]
Acid-activated sintering process red mud	60.5	–	[30]

5. ACKNOWLEDGEMENT

The work was sponsored by the Project Foundation of Chongqing Municipal Education Committee (KJ110724).

6. REFERENCES

1. M.F. Attallah, I.M. Ahmed Hamed M.M., Treatment of industrial wastewater containing Congo Red and Naphthol Green B using low-cost adsorbent. *Environ. Sci. Pollut. Res.*, 2013, 20, 1106–1116. http://dx.doi.org/10.1007/s11356-012-0947-4
2. V.K. Gupta, A. Mittal, R. Jain, *et al.*, Adsorption of Safranin-T from wastewater using waste materials- activated carbon and activated rice husks. *J. Colloid Interf. Sci.*, 2006, 303(1), 80–86. http://dx.doi.org/10.1016/j.jcis.2006.07.036
3. V.K. Gupta, R. Jain, S. Varshney, Removal of Reactofix golden yellow 3 RFN from aqueous solution using wheat husk—An Agricultural waste. *J. Hazard. Mater.*, 2007, 142(1–2), 443–448. http://dx.doi.org/10.1016/j.jhazmat.2006.08.048
4. P. Sharma, H. Kaur, Sugarcane bagasse for the removal of erythrosin B and methylene blue from aqueous waste. *Appl. Water Sci.*, 2011, 1, 135– 145. http://dx.doi.org/10.1007/s13201-011-0018-x
5. R. Ansari, B. Seyghali, A. Mohammad-khah, *et al.*, Highly efficient adsorption of anionic dyes from aqueous solutions using sawdust modified by cationic surfactant of cetyltrimethylammonium bromide. *Surfact Deterg.*, 2012, 15, 557–565. http://dx.doi.org/10.1007/s11743-012-1334-3
6. T. Robinson, B. Chandran, P. Nigam, Removal of dyes from a synthetic textile dye effluent by biosorption on apple pomace and wheat straw. *Water Res.*, 2002, 36, 2824–2830. http://dx.doi.org/10.1016/S0043-1354(01)00521-8
7. K.V. Kumar, A. Kumaran, Removal of methylene blue by mango seed kernel powder. *Biochem. Eng. J.*, 2005, 27, 83–93. http://dx.doi.org/10.1016/j.bej.2005.08.004
8. A. Khenifi, Z. Bouberka, F. Sekrance, *et al.*, Adsorption study of an industrial dye by an organic clay. *Adsorption*, 2007, 13, 149–158. http://dx.doi.org/10.1007/s10450-007-9016-6
9. S. Sadaf and H.N. Bhatti, Batch and fixed bed column studies for the removal of Indosol Yellow BG dye by peanut husk, *J. Taiwan Inst. Chem. E.*, 2014, 45, 541–553. http://dx.doi.org/10.1016/j.jtice.2013.05.004
10. A. Azizi, M. R. Alavimoghaddam, M. Arami, Wood waste from mazandaran wood and the paper industry as a low cost adsorbent for removal of a reactive dye. *J. Residuals Sci. Tech.*, 2011, 8(1), 21–28.
11. R.A. Gracia-Delgado, L.M. Cotoruelo-Minguez, J.J. Rodriguez, Equilibrium study of single-solute adsorption of anion surfactants with polymeric XAD resins. *Sep. Sci. Technol.*, 1992, 27, 975–987. http://dx.doi.org/10.1080/01496399208019736
12. P.B. John, T. Marios, Removal of hazardous organic pollutants by biomass adsorption. *J. Water Pollut. Control Fed.*, 1987, 59, 191–198 .
13. S. Lagergren, About the theory of so-called adsorption of soluble substances. Kungliga Svenska Vetensk. *Handl*, 1898, 24, 1–39.
14. Y.S. Ho, G. McKay, Pseudo-second order model for sorption processes. *Process Biochem.*, 1999, 34, 451–465. http://dx.doi.org/10.1016/S0032-9592(98)00112-5
15. G. McKay, The adsorption of dyestuffs from aqueous solution using activated carbon: Analytical solution for batch adsorption based in external mass transfer and pore diffusion. *Chem. Eng. J.*, 1983, 27, 187–196. http://dx.doi.org/10.1016/0300-9467(83)80075-6
16. T.Y. Mustafa, K.S. Tushar, H.M. Ang., Equilibrium, kinetics, and thermodynamics of methylene blue adsorption by pine tree leaves. *Water Air Soil Pollut.*, 2012, 223, 5267–5282. http://dx.doi.org/10.1007/s11270-012-1277-3
17. H.S. Ghazi Mokri, N. Modirshahla, M.A. Behnajady, *et al.*, Adsorption of C.I. Acid Red 97 dye from aqueous solution onto walnut shell: kinetics, thermodynamics parameters, isotherms. *Int. J. Environ. Sci. Technol.*, 2015, 12, 1401–1408. http://dx.doi.org/10.1007/s13762-014-0725-6
18. C. T. Weber, E.L. Foletto, L. Meili, Removal of tannery dye from aqueous solution using papaya seed as an efficient natural biosorbent, *Water Air Soil Pollut.*, 2013, 224,1427–1437. http://dx.doi.org/10.1007/s11270-012-1427-7
19. Yinghua Song, Yi Liu, Shengming Chen, *et al.*, Sunset yellow adsorption by peanut husk in batch mode. *F. Environ. Bull.*, 2014, 23(4):1074–1079.
20. Yinghua Song, Yi Liu, Shengming Chen, *et al.*, Carmine adsorption from aqueous solution by crosslinked peanut husk. *Iran J. Chem. Chem. Eng.*, 2014, 33, 69–75.
21. Sen T.K., Afroze S., Ang H., Equilibrium, kinetics and mechanism of removal of methylene blue from aqueous solution by adsorption onto pine cone biomass of pinus radiata. *Water Air Soil Pollut*, 2011, 218, 499–515. http://dx.doi.org/10.1007/s11270-010-0663-y
22. X. Han, X. Niu, X. Ma, Adsorption characteristics of methylene blue on polar leaf in batch mode: equilibrium, kinetics and thermodynamics. *Korean J. Chem. Eng.*, 2012, 29(4), 494–502. http://dx.doi.org/10.1007/s11814-011-0211-5
23. M. Ghaedi, J. Tashkhourian, A.A. Pebdani, *et al.*, Equilibrium, kinetic and thermodynamic study of removal of reactive orange 12 on platinum nanoparticle loaded on activated carbon as novel adsorbent. *Ana F.N., Korean J. Chem. Eng.*, 2011, 28 (12), 2255–2261. http://dx.doi.org/10.1007/s11814-011-0142-1
24. L. Guz, G. Curutchet, R.M. Torres Sanchez, *et al.*, Adsorption of crystal violet on montmorillonite (or iron modified montmorillonite) followed by degradation through Fenton or photo-Fenton type reactions. *J. Environ. Chem. Eng.*, 2014, (2), 2344– 2351.
25. J. Zolgharnein, M. Bagtash, T. Shariatmanesh, Simultaneous removal of binary mixture of Brilliant green and crystal violet using derivative spectrophotometric determination, multivariate optimization and adsorption characterization of dyes on surfactant modified nano-γ-alumina. *Spectrochim.Acta Part A Mol. Biomol. Spectrosc*. 2015,137, 1016–1028. http://dx.doi.org/10.1016/j.saa.2014.08.115
26. H. Yang, D. Zhou, Z. Chang, *et al.*, Adsorption of Crystal violet onto amino silica: optimization, equilibrium, and kinetic studies. *Desalin. Water Treat*. 2014, 52(31–33), 6113–6121. http://dx.doi.org/10.1080/19443994.2013.811109
27. G. K. Sarma, S.S. Gupta, K.G. Bhattacharyy, Adsorption of Crystal violet on raw and acid-treated montmorillonite, K10, in aqueous suspension. *J. Environ. Manage.*, 2016, 171, 1–10. http://dx.doi.org/10.1016/j.jenvman.2016.01.038
28. Pengfei Sun, Cai Hui, Sheng Wang, *et al.*, Bacillus amyloliquefaciens biofilm as a novel biosorbent for theremoval of crystal violet from solution. *Colloid Surface B: Biointerfaces* 2016, 139, 164– 170. http://dx.doi.org/10.1016/j.colsurfb.2015.12.014

29. F. Guzel, H. Sayğılı, G. A. Sayğılı, *et al.*,Decolorisation of aqueous crystal violet solution by a new nanoporous carbon: Equilibrium and kinetic approach. *J. Ind. Eng. Chem.,* 2014, 20, 3375– 3386. http://dx.doi.org/10.1016/j.jiec.2013.12.023

30. Luyi Zhang, Huayong Zhang, Wei Guo, *et al.*,Removal ofmalachite green and crystal violet cationic dyes fromaqueous solution using activated sintering process red mud. *Appl Clay Sci.*, 2014, 93–94, 85–93. http://dx.doi.org/10.1016/j.clay.2014.03.004

Phytoavailability of Lead (Pb) for Corn and Sunflower as Affected by Pb-enriched Sewage Sludge and Cow Manure

AMIR HOSSEIN BAGHAIE[1,*], AMIR HOSSEIN KHOSHGOFTARMANESH[2] and MAJID AFYUNI[2]
[1]*Department of Soil Science, Arak Branch, Islamic Azad University, Arak, Iran*
[2]*Department of Soil Science, College of Agriculture, Isfahan University of Technology, Isfahan, 84156–83111, Iran*

ABSTRACT: This experiment was aimed to investigate the influence of Pb enriched sewage sludge and cow manure on Pb availability to sunflower (*Helianthus annuus* L.) and corn (*Zea mays* L. Single cross 704). A loamy sand soil was treated with organic and inorganic Pb salt. Lead was extracted in 1:2.5 soil: water using metal chelating exchange resin membranes. The VISUAL MINTEQ computer program was used to estimate concentrations of various soluble inorganic and organic species of Pb in the 1:2.5 soil: water extracts and chemical composition data obtained was considered as input data. Regardless of plant type, Pb bioavailability in soil amended with organic amendments was greater than in soil amended with $Pb(NO_3)_2$ salt. The soil Pb solution in sewage sludge and cow manure treatments was mainly complexed with dissolve organic carbon (Pb-DOC) and the other species of the metal in soil solution were low. A strong relationship between concentrations of soil Pb extracted by the Ca-saturated Chelex membrane with shoots and root corn Pb concentration showed that the resin membrane extraction can be used to estimate Pb phytoavailability of soil. According to the results, inorganic and organic components of organic treatments significantly affect Pb phytoavailability.

1. INTRODUCTION

ORGANIC matter content of soils in arid and semi-arid regions is often very low (less than 1%) [22]. Therefore, addition of organic amendments such as cow manure or sewage sludge to soils is highly recommended as an approach to increase soil organic content. Although, addition of organic fertilizer to soils affect soil physico- chemical properties and crop production [14], elevated heavy metals concentration in soils amended with some organic products has also been reported [2,8,13,28]. Therefore, knowledge on fractionation metals in organic amendment has to be understood for application of these products in agricultural soils [5,6].

Heavy metals are considered as one of the most serious pollutants due to their toxicity, persistence and bioaccumulation. Heavy metals uptake by plants is affected by solubility and availability of metals in the soil [31]. However, soil physico-chemical properties can affect soil metal availability. Despite relatively high amounts of metal added by organic amendments to the soil, formation of metal-organic matter complexes might reduce the availability of metals to plants [20,33]. On the other hand, many researchers reported the phytotoxicity critical concentration of metals by inorganic salts is much higher than that by organic amendments. These results indicate that organic amendments add adsorptive phases to soil and thereby change availability of metals to plants [6,10,18]. Baghaie *et al.* (2011) reported addition of cow manure or sewage sludge to the soil at a rate of 10% (w/w) significantly increased soil capacity of Pb sorption [6].

To better understand Pb phytoavailbility as affected by organic amendments in comparison with inorganic Pb salt, the metal species in soil solution has to be determined. Metal ions in soil are free, hydrated ions and the formation of soluble complexed with organic or inorganic ligands.

Trace metal free ion activities in soil solution play an important role in determining plant metal concentration. Because it is clear that heavy metal component and free ionic activity is more important in determining plant availability than total concentration in soil [15].

Metal speciation determination in soil solution is not easy and depending on soil physico-chemical properties. Computer programs can used to estimate chemical species of metals ions in solutions [21]. Although these programs are available to calculate metal speciation, they should be verified using experimental data.

*Author to whom correspondence should be addressed.
E-mail: a-baghaie@iau-arak.ac.ir

1544-8053/16/03 251-07

doi:10.12783/issn.1544-8053/13/4/2

Several experiments such as the ion exchange resins have used for determination of free ion and different species of metals in soil solution [17]. Khoshgftarmanesh *et al.* (2006) found significant correlation relationship between MINTEQA2 model and Amberlite resin to estimate soluble concentrations of the Cd^{2+} and Zn^{2+} ions in soil [4]. Significant relationship between the Amberlite resin and MINTEQA2 calculated free Zn^{2+} and Cd^{2+} showed that the MINTEQA2 model is appropriate for estimation of soluble Zn^{2+} and Cd^{2+} [17]. The resins can also be used for extraction of available metal pools in soil [17].

Chelating exchange resins are better than ion exchange resins for extraction of available pools of metals from soil [17]. Lee and Zheng (1994) reported the Ca-saturated Chelex membrane can easily be used for simultaneously extraction of soil available Cd, Cu and Pb in a wide range of soils [17].

Although the role of organic treatments on the changes in heavy metals availability in soils has largely been conducted [2,11,12], very little information is available about the speciation of heavy metal (e.g., Pb) in solution of soils amended with organic amendments and their relation correlation with plant metal concentration [1]. Therefore, the impact of organic and inorganic Pb sources on Pb speciation in soil solution and its concentrations in corn and sunflower was investigated.

2. MATERIALS AND METHODS

2.1. Soil Treated Characteristic

Loamy sand soil with a low in saline, calcareous and organic carbon (Typic Xerorthents) [30] was collected from the 0–15 cm layer of a wheat field around Shahr-e-kord, central Iran. The soil was transferred to laboratory, air dried and ground to pass 2 mm sieve. Some soil physico-chemical properties are presented in Table 1. In addition, free cation and anion soluble concentration in the soil: water extracted solutions (1:2.5) was shown in Table 2.

2.2. Treatments

Secondary, anaerobically digested municipal sewage sludge was selected from city of Isfahan, central Iran and cow manure was 8-months decomposed. Sewage sludge and manures were enriched with $Pb(NO_3)_2$ to 600 mg Pb kg^{-1} level. Soil incubated in greenhouse for 15 days. Some physico-chemical properties of the organic amendments are mentioned in Table 3.

Soil was sprayed with a similar rate of Pb (600 Pb kg^{-1}) through two organic treatments (enriched sewage sludge and manure) and an inorganic salt $Pb(NO_3)_2$. Enriched sewage sludge and manure were applied at a rate of 10% by weight to the soil. Four kilograms of treated soils were put into the plastic pots. Soil was irrigated till 80% water holding capacity during two weeks at 23–25°C for two weeks. Sunflower (*Helianthus annuus* L.) and corn (*Zea mays* L. single grass 704) seeds were sown with 3 seedlings kept in each pot.

2.3. Resin Membrane

According to the Lee and Zheng method (1993), Na-saturated chelating resin membrane sheets (Chelex 12″ × 12″ membrane sheets, Bio-Rex ion exchange mem-

Table 1. Some Physico-chemical Properties of Untreated, Sewage Sludge and Cow Manure Treated Soil.

Parameter	Unit	Unamended Soil	Sewage Sludge Amended Soil*	Cow Manure Amended Soil*
pH	–	7.3a**	6.8b	7.4a
Electrical Conductivity (EC)	dS m^{-1}	2c	3.3b	5a
Organic carbon	%	0.1c	2b	2.7a
Sand	%	70	–	–
Silt	%	18	–	–
Clay	%	12	–	–
Iron oxide	mg kg^{-1}	600a	620b	600a
Total P	%	0.01a	0.03b	0.02ab
$CaCO_3$	%	10a	10a	11a
Total Pb	mg kg^{-1}	3c	580a	570b
Cation exchange capacity (CEC)	cmolc (+)kg^{-1}	31.3c	33b	34.7a

*After enrichment.

**For each treatment, means with the similar letter in each row are not significantly different ($P \leq 0.05$, LSD test).

Table 2. Cation and Anion Soluble Concentration in the Soil: Water Extracted Solutions (1:2.5) (mmol/lit).

Treatment	DOC*** (mg/lit)	Pb	Na+	K+	Cl^-	NO3-	P
Pb salt	ND**	0.08a*	0.34c	0.02c	2.0c	14.0a	0.001c
Sewage sludge	28.0b	0.04b	1.41b	0.10b	8.0b	3.70b	0.01b
Cow manure	36.0a	0.02c	9.34a	3.0a	20.0a	0.60c	0.03a

*For each treatment, means with the similar letter in each column are not significantly different ($P \leq 0.05$, LSD test),
**ND: not detectable.
***DOC: Dissolve organic carbon.

brane sheets, Bio-Rad) were cut into 1 cm × 5 cm pieces and transformed into Ca-saturated form for use [16].

2.4. Soil Pb Uptake by Resin Membrane

The ion-exchange resin capsules were used to provide a simple, convenient, repeatable resin methodology to measure soil Pb bioavailability. For this purpose, according to the Lee and Zheng method (1994), 40 mL of deionized water added to four-gram of soil (grounded through 80 meshes), and one piece of Ca-saturated Chelex resin membrane (5 cm^2) in a polypropylene bag were placed in a 50-mL centrifuge tube. The tubes were centrifuged during 24 h. The soil suspensions were decanted and the resin membrane was recovered, rinsed thoroughly with distilled water, and air-dried. For the second time, a clean 50-mL centrifuge tube was used and 40-mL aliquots of 1 M HC1 were added. For cleaning Pb saturated membrane, the tube was centrifuged for 24 h to. The Pb desorption procedures were repeated once [17].

2.5. Soil Cd, Cu, and Pb

The Pb in organic and inorganic amended soil was also extracted by 0.01 M $CaCI_2$, DTPA (pH = 7.3), and DTPA (pH = 5.3) described by Lee and Zheng (1994) [17] and atomic absorption spectroscopy (Model 3030) was used for determining soil heavy metal concentration.

2.6. Soil Chemical Analysis

The soil pH of the treatments used in this research was measured in 1:2.5 soil: water suspension using a pH meter (Model EA940, Orion, USA) that was standardized with the three reference buffers (4, 7 and 9.2) [26]. Electrical cconductivity was determined by conductivity meter (Model, AZ 86503) [26]. Ammonium acetate extractable solution was used for extracting soil cations such as Na^+, K^+ and Ca^{2+} by repeated leaching procedure and then their concentrations were determined by Atomic Absorption Spectrophotometer (AAS) (Model 3030). The 1 M HC1 extractable was used for determining Pb concentrations by AAS [3]. Total organic carbon (TOC) analyzer (Model 1088) was used for determining dissolving organic carbon (DOC) [1]. The Soil phosphorous was measured according to the Olsen and Sommers [23].

2.7. Soil Pb Speciation

Soil cation and anion such as Na^+, Ca^{2+}, Mg^{2+}, K^+, HCO_3^-, SO_4^{2-}, Cl^- and DOC concentrations were used as input data to calculate concentrations of the soluble inorganic and organic species of Pb by the VISUAL MINTEQ computer program [11] in the 1:2.5 soil: water extracts [1]. The soil solution pH was fixed and equilibrium with atmospheric CO_2 was assumed. Comparing ion activity products (IAP) with the corresponding formation constant (K°) were used for determining Thermodynamic stabilities of select solid phases.

2.8. Statistics

A factorial experiment in the layout of completely randomized design with the three replications was used. The ANOVA procedures were performed for data statistical analyses [25]. The least significant difference (LSD) statistical analysis was used to determine the differences between the means.

Table 3. Selected Properties of Sewage Sludge and Cow Manure Used in this Experiment.

Characteristic	Unit	Sewage Sludge	Cow Manure
EC	dS m^{-1}	9	17
pH	–	6.7	8.9
Organic carbon	%	17.9	31.3
Fe_2O_3	mg kg^{-1}	730	73
Total Pb*	mg kg^{-1}	75	20
Total Zn	mg kg^{-1}	710	217
Total Cd	mg kg^{-1}	5	3

*Before enrichment.

3. RESULTS AND DISCUSSION

3.1. Soil Properties

Soil pH was not significant affected by adding 10% cow manure, while adding sewage sludge to the soil, significantly decrease soil pH (Table 1). It may be due to the dilution effect or the low amount of the applied cow manure. Slight decrease in soil pH by addition of sewage sludge is related to release of its acidic components during biodegradation [7].

Soil EC increased by addition of organic amendments (Table 1). In general, Soil treated with cow manure had higher EC than the soil treated with sewage sludge. Soil treated with cow manure and sewage sludge (10%) showed a significant increasing in carbon to nitrogen ratio (C/N) relative to the control soil (Figure 1). The greater organic carbon of cow manure relative to sewage sludge maybe caused a significant increasing in C/N ratio of the soils treated with cow manure relative to the soils treated with sewage sludge (Table 3). Soil CEC was affected by adding 10% cow manure and sewage sludge and showed a significant increasing by 2.9 and 1.5%, respectively.

3.2. Effect of Pb Enriched Sewage Sludge and Cow Manure on Soil Available Pb

The DTPA-Pb concentration was greater in the soil treated with $Pb(NO_3)_2$ than manure and sewage sludge-amended treatments (Table 4). This result is similar with the result of other researchers indicating that organic sources of heavy metals added to the soil are less available to plant than the soils treated by inorganic salts [10,18]. It has been shown that time has a significant effect on heavy metal availability. Long term application of organic treatments cause a significant decreasing in heavy metal availability and reach to a base level after several uses for extended time [6,10]. However, the sorption properties of inorganic components of the organic amendments such as carbonates or phosphates on the Pb sorption cannot be ignored [10].

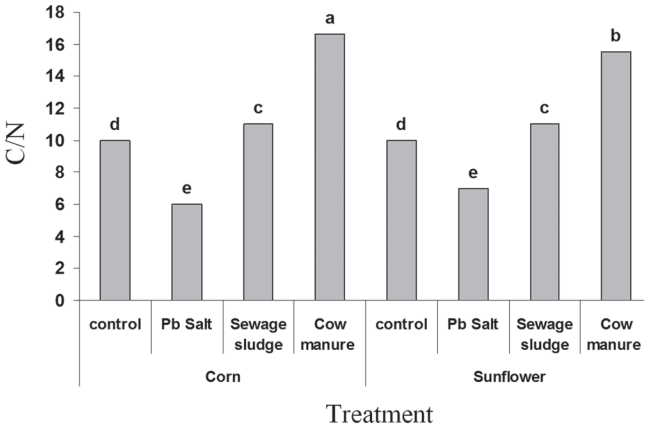

Figure 1. *Effect of organic and inorganic Pb sources on soil Carbon to nitrogen ratio (C/N), for each treatment, columns with the same letter are not significantly different (P ≤ 0.05, LSD test).*

Table 4. Effect of Cow Manure and Sewage Sludge on Soil Pb Under Corn and Sunflower Sultivation.

	Soil DTPA Extractable Pb(mg/kg)	
Treatment	**Corn**	**Sunflower**
Control soil	ND*	ND
Pb salt amended soil	87 ± 0.12a**	85 ± 0.17a
Sewage sludge amended soil	48 ± 0.09b	45 ± 0.13c
Cow manure amended soil	38 ± 0.21d	35 ± 0.10e

*ND: Not detectable by AAS.
**For each treatment, means with the similar letter are not significantly different ($P \leq 0.05$, LSD test).

Regardless of the plant species, soil DTPA-extractable Pb was lower at the cow manure than sewage sludge treatment. This might be related to higher pH and organic carbon content of the cow manure (Table 2). A reverse relationship was observed ($r = -0.9$, $p \leq 0.05$) between the soil DTPA extractable Pb and carbon to nitrogen ratio. Increasing carbon to nitrogen ratio of the soil amended with cow manure showed a decreasing in Soil DTPA extractable Pb in comparison with soil treated with sewage sludge. Tarighi *et al.* (2012) reported soil available Zn in the soil amended with cow manure significantly decreased relative to the soil treated with inorganic Zn sources. They found that cow manure application caused a significant increasing in the soil sorption capacity, thus, decreased the availability of soil Zn [32]. Organic amendments generally containing organic and inorganic matters such as organic matter, carbonate, phosphate, Fe, Mn, Al oxides and anions that increasing the sorption phases and adsorb or precipitate heavy metals. Many types of organic matters such as sewage sludge, cow manure, sewage sludge with a different properties have been used in agricultural land and have modified the soil physicochemical properties and thereby, heavy metal availability in soils. Addition of these amendments to the soil can change the chemical properties of metal- binding in the soil-residual mixture.

The result of the Table 4 showed that soil DTPA-extractable Pb of the corn rhizosphere was greater than that for the sunflower plant. It maybe related to the plant root rhizosphere that affect heavy metal availability in soil [32]. Corn relative to sunflower culti-

Table 5. Effect of Sewage Sludge, Cow Manure and $Pb(NO_3)_2$ on Shoot and Root Pb Concentration of Sunflower and Corn.

Treatment	Corn**		Sunflower	
	Shoot	Root	Shoot	Root
$Pb(NO_3)_2$-received soil	25.0 ± 0.21f	335 ± 0.42a**	23.2 ± 0.11g	323.2 ± 0.37b
Cow manure amended soil	7.7 ± 0.07i	91.5 ± 0.25d	12.25 ± 0.10h	92.0 ± 0.14d
Sewage sludge amended soil	ND*	99.2 ± 0.27c	22.2 ± 0.13g	31.5 ± 0.11e

*ND: not detectable.

**For each treatment, means with the similar letter are not significantly different ($P \leq 0.05$, LSD test).

vated under cow manure and sewage sludge amended soil showed significant differences by 3 units in the soil DTPA-extractable Pb. Similar to our results, Tarighi *et al.* (2012) concluded that with increasing application of organic and inorganic Zn sources, the soil DTPA-extractable Zn will significantly increase. In addition, they found that plant cultivars are very important in Zn efficiency, as, a greater soil DTPA extractable Zn was shown under cultivation for Alvand relative to Backcross cultivars. Plant root rhizosphere may be changed the soil chemical properties such as soil pH that affect soil Zn availability. However, the effect of plant cultivar cannot be ignored, as, the higher soil Zn availability was observed under the Alvand relative to Backcross cultivar [32].

3.3. Effect of Organic and Inorganic Sources on Plant Pb Concentration

Plant Pb concentration was largely affected by organic and inorganic treatments (Table 5). The corn Pb concentration under cow manure treated soil was lower than those cultivated under sewage sludge treatments (Table 5). This is most likely attributed to higher affinity of manure to adsorb Pb as compared to sewage sludge because of greater organic carbon content of manure. In addition, cow manure had a higher pH (Table 3) that may cause precipitation of Pb and thus decreasing its phyto-availability. However, root lead concentration in sunflower was lower in sewage sludge relative to cow amended soil. Negative sewage sludge composition may be caused to stunt the sunflower root growth (data was not shown).

The results of this study showed that cultivation of corn in soil treated with sewage sludge or cow manure caused a significant decreasing in root Pb concentration relative to the soil that received inorganic Pb salt (Table 5). Application of manure and sewage sludge decreased root Pb concentration of sunflower by 3.5 and 10.2 times in comparison with the inorganic Pb salt treated soil, respectively. However, for corn it was decreased 3.6 and 3.3 times, respectively.

Translocation factor (TF factor) is the measuring plant ability to translocate heavy metals from roots to shoots. The TF parameter for all the treatments was less than 1. The shoot and root Pb concentration of corn was significantly greater than the sunflower grown in inorganic Pb salt treatment, but the TF value did not show any differences. However, the Root Pb concentration of corn and sunflower grown in cow manure amended soil did not show any significant differences, but the TF value of sunflower was significantly greater than corn. It may be concluded that metal accumulation in roots may be dependent on plant physiology or soil rhizosphere condition that affect heavy metal availability or it may be due to binding heavy metal with sulphydryl groups that prevent the heavy metal translocation from root to shoot [29].

3.4. Soil Pb Extractable Methods

The results of Table 6 showed that DTPA and resin membrane is a good method for estimating root and shoot Pb concentration, as, all of the correlation coefficients between DTPA or resin membrane method and root and shoot Pb concentration were higher than 62% (Table 6).

Resin membrane extractable-soil Pb was a better

Table 6. Correlation Coefficients Between Root and Shoot Pb Concentration of Plants and Chemical Extraction Methods.

Extraction Method	Shoot Pb Concentration	Root Pb Concentration
Chelex resin membrane	0.85*	0.96*
0.01 M $CaCl_2$	0.77*	0.83*
DTPA (pH = 5.3)	0.75*	0.81*
DTPA (pH = 7.3)	0.62*	0.68*

*Significant, $p \leq 0.05$.

of indicator of root or shoot Pb concentration than Pb extracted by other methods in this research (Table 6). Lead extracted by DTPA method at the pH = 5.3 showed a greater significant differences relative to DTPA method at the pH = 7.3 methods. Lower pH affected the Pb solubility [19] and thereby affecting the soil Pb extracted. Lee and Zheng (1994) reported a high correlation between heavy metal concentration by plant and resin method. In addition, they founded a significant high correlation (> +0.9, $p \leq 0.05$) for Pb plant uptake and Pb-DTPA method at the pH = 5.3.

3.5. Predication of Pb Species by VISUAL MINTEQ Software

The greatest Pb concentration was measured in the Pb salt treatment as the greatest Pb plant concentration was also observed. The greatest NO_3^- was also measured in this treatment. The greater pH of cow manure relative to sewage sludge may be caused the decreasing Pb concentration of the soil solution by 50%. The lowest Phosphorous concentration was observed in Pb salt treatment that may be related to the interaction of Pb and Phosphorus. Applying the cow manure relative to sewage sludge caused a significant decreasing in P concentration by two times that maybe due to the greater percent of Al and Fe oxides (data was not shown) in the cow manure treatment.

Appling the 10% cow manure or sewage sludge caused a significant increasing in DOC (Table 7). Dissolve organic matter was not detectable in Pb salt treatment. The VISUAL MINTEQ software was used for estimating the different Pb chemical species of the soil solution [9] (Table 7).

The greatest Pb-DOC concentration was estimated in the organic treatments. Organic carbon made strong complexes with Pb, as, Pb-DOC was the greatest (more than of 99%) Pb complexes in the sewage sludge and cow manure treatments. Abbaspour *et al.* (2008) also concluded that the most prevalent species of dissolved Pb was belong to Pb-DOC in organic amended soil treatments [1]. However, the type of the elements and chemical condition of the soils can affected to the formation of the complexes cannot be ignored. 63.4%, 24% and 8.9% of the amount Pb in soil solution was belonged to Pb^{2+}, $Pb(OH)^+$ and $PbNO_3^+$ in the Pb salt treatment. Despite of the greater percentage of the Cl-complex (nearly 10 times) in the soil solution of the cow manure and sewage sludge relative to Pb salt treatment, a significant decreasing in the $PbCl^+$ complex was observed that maybe due to the formation of the Pb-DOC relative to $PbCl^+$ complexes.

4. CONCLUSION

Soil and organic amendments can directly affect soil sorption properties that change soil heavy metal availability. Soil physico-chemical properties such as soil pH, carbon to nitrogen ratio and organic and inorganic fractions of soil are important role controlling heavy metal availability systems. Our result showed that soil Pb availability in cow manure or sewage sludge amended soils is less available than those treated in inorganic Pb salt. However, the cow manure had shown more decreasing in soil Pb availability relative to sewage sludge that maybe related to the greater soil organic carbon percentage of cow manure relative to sewage sludge amended soil. High correlation between root and shoot concentration and resin membrane extractable-soil Pb showed that resin membrane was a better of indicator of root or shoot Pb concentration than Pb extracted by DTPA. Pb-DOC was the important Pb species in organic amendment soil estimated by VISUAL MINTEQ Software. However, the most important factor for soil Pb availability was belonged to the inorganic Pb salt treatment. Plant Pb concentration was largely affected by both organic treatments applied and plant species. In Pb salt treatment, shoot and root Pb concentration in corn was greater than in sunflower. However, the results of this study showed that corn and sun flower root Pb concentration was greater under inorganic Pb salt relative to those grown in organic treatments.

Table 7. Results of VISUAL MINTEQ Software for Estimation Pb Species Percentage in Soil Solution.

Treatment	Pb-DOC*	Pb^{2+}	$Pb(OH)^+$	$Pb(OH)_2$	$PbCl^+$	$PbNO_3^+$	$Pb(NO_3)_2$
Pb salt	ND**	63.40a***	24.0a	0.10	3.10a	8.90a	0.10
Sewage sludge	99.86a	0.06c	0.04b	–	0.03c	–	–
Cow manure	99.40a	0.40b	0.07b	–	0.08b	0.01b	–

*DOC: Dissolve organic carbon.

**ND: Not detectable.

***For each value, means with the similar letter in each column are not significantly different ($P \leq 0.05$, LSD test).

5. REFERENCES

1. Abbaspour, A., Kalbasi, M., Hajrasuliha, S., Fotovat, A., "Effect of organic matter and salinity on ethylenediaminetetraacetic acid-extractable and solution species of cadmium and lead in three agricultural soils", *Communications in Soil Science and Plant Analysis*, Vol. 39, 2008, pp. 983–1005. http://dx.doi.org/10.1080/00103620801925380
2. Afyuni, M., Rezaeinejad, Y., Schulin, R., "Extractability and plant uptake of Cu, Zn, Pb and Cd from a sludge-amended Haplargid in central Iran", *Arid Land Research and Management*, Vol. 20, 2006, pp. 29–41. http://dx.doi.org/10.1080/15324980500369343
3. Allen, S. E., Grimshaw, H. M., Rowland, A. P., "Chemical analysis", Moore, P. D. Chapman, S. B., *Methods in plant ecology*, Oxford, London, Blackwell Scientific Publication, 1986, pp. 285–344.
4. Allison, J. D., Brown, D. S., Novo-Gradac, K. J., "MINTEQA2/PRODEFA2. A geochemical assessment model for environmental system: ver. 3.0 User manual. Environ. Res. Lab., U.S. Environmental Protection Agency", 1991, Athens, GA 30613.
5. Alvarez, E. A., Mochon, M. C., Sanchez, J. C. J., Rodriguez, M. T., "Heavy metal extractable forms in sludge from wastewater treatment plants", *Chemosphere*, Vol. 47, 2002, pp. 765–775. http://dx.doi.org/10.1016/S0045-6535(02)00021-8
6. Baghaie, A., Khoshgoftarmanesh, A. H., Afyuni, M., Schulin, R., "The role of organic and inorganic fractions of cow manure and biosolids on lead sorption", *Soil Science and Plant Nutrition*, Vol. 57, 2011, pp. 11–18. http://dx.doi.org/10.1080/00380768.2010.548309
7. Bergkvist, P., Jarvis, N., Berggren, D., Carlgren, K., "Long term effects of sewage sludge applications on soil properties, cadmium availability and distribution in arable soil.", *Agriculture, Ecosystems and Environment*, Vol. 97, 2003, pp. 167–179. http://dx.doi.org/10.1016/S0167-8809(03)00121-X
8. Cai, Q.-Y., Mo, C.-H., Wu, Q.-T., Zeng, Q.-Y., Katsoyiannis, A., "Concentration and speciation of heavy metals in six different sewage sludge-composts", *Journal of Hazardous Materials*, Vol. 147, 2007, pp. 1063–1072. http://dx.doi.org/10.1016/j.jhazmat.2007.01.142
9. Gustafsson, J. P., "Visual MINTEQ 2.50", 2007, Software Manual, KTH, Department of land and water resources engineering, Stockholm, Sweden.
10. Hettiarachchi, G. M., Ryan, J. A., Chaney, R. L., La Fleur, C. M., "Sorption and desorption of cadmium by different fractions of biosolids-amended soils", *Journal of Environmental Quality*, Vol. 32, 2003, pp. 1684–1693. http://dx.doi.org/10.2134/jeq2003.1684
11. Jamali, M. K., Kazi, T. G., Arain, M. B., Afridi, H. I., Jalbani, N., Adil, R. S., "The correlation of total and extractable heavy metals from soil and domestic sewage sludge and their transfer to maize (*Zea mays* L.) plants", *Toxicological and Environmental Chemistry*, Vol. 88, 2006, pp. 619–632. http://dx.doi.org/10.1080/02772240600875052
12. Jamali, M. K., Kazi, T. G., Arain, M. B., Afridi, H. I., Jalbani, N., Memon, A. R., "Heavy metal contents of vegetables grown in soil, irrigated with mixtures of wastewater and sewage sludge in Pakistan, using ultrasonic-assisted pseudo-digestion", *Journal of Agronomy and Crop Science*, Vol. 193, 2007, pp. 218–228. http://dx.doi.org/10.1111/j.1439-037X.2007.00261.x
13. Kandpal, G., Ram, B., Srivastava, P. C., Singh, S. K., "Effect of metal spiking on different chemical pools and chemically extractable fractions of heavy metals in sewage sludge", *Journal of Hazardous Materials*, Vol. 106, 2004, pp. 133–137. http://dx.doi.org/10.1016/j.jhazmat.2003.10.006
14. Karami, A., Homaee, M., Afzalinia, S., Ruhipour, H., Basirat, S., "Organic resource management: Impacts on soil aggregate stability and other soil physico-chemical properties", *Agriculture, Ecosystems and Environment*, Vol. 148, 2012, pp. 22–28. http://dx.doi.org/10.1016/j.agee.2011.10.021
15. Khoshgoftarmanesh, A. H., Shariatmadari, H., Karimian, N., Kalbasi, M., Zee, S. E. A. T. M. v. d., "Cadmium and zinc in saline soil solutions and their concentrations in wheat", *Soil Science Society of America Journal*, Vol. 70, 2006, pp. 582–589. http://dx.doi.org/10.2136/sssaj2005.0136
16. Lee, D. Y., Zheng, H. C., "Chelating resin membrane method for estimation of soil cadmium phytoavailability", *Communications in Soil Science and Plant Analysis*, Vol. 24, 1993, pp. 685–700. http://dx.doi.org/10.1080/00103629309368833
17. Lee, D. Y., Zheng, H. C., "Simultaneous extraction of soil phytoavailable cadmium, copper, and lead by chelating resin membrane", *Plant and Soil*, Vol. 164, 1994, pp. 19–23. http://dx.doi.org/10.1007/BF00010106
18. Li, Z., Ryan, J. A., Chen, J. L., Al-Abed, S. R., "Adsorption of cadmium on biosolids-amended soils", *Journal of Environmental Quality*, Vol. 30, 2001, pp. 903–911. http://dx.doi.org/10.2134/jeq2001.303903x
19. Lindsay, W. L., Norvell, W. A., "Development of a DTPA soil test for zinc, iron, manganese, and copper", *Soil Science Society of America Journal* Vol. 42, 1978, pp. 421–428. http://dx.doi.org/10.2136/sssaj1978.03615995004200030009x
20. Liphadzi, M. S., Kirkham, M. B., "Availability and plant uptake of heavy metals in EDTA-assisted phytoremediation of soil and composted biosolids", *South African Journal of Botany*, Vol. 72, 2006, pp. 391–397. http://dx.doi.org/10.1016/j.sajb.2005.10.010
21. Luo, X.-S., Zhou, D.-M., Liu, X.-H., Wang, Y.-J., "Solid/solution partitioning and speciation of heavy metals in the contaminated agricultural soils around a copper mine in eastern Nanjing city, China", *Journal of Hazardous Materials*, Vol. 131, 2006, pp. 19–27. http://dx.doi.org/10.1016/j.jhazmat.2005.09.033
22. Mahmoodabadi, M., Amirabadi, Z., Amini, S., Khazaeipoul, K., "Fertilization of soybean plants with municipal solid waste compost under leaching and non-leaching conditions", *American-Eurasian Journal of Agricultural and Environmental Science*, Vol. 8, 2010, pp. 55–59.
23. Olsen, S. R., Sommers, L. E., "Phosphorus", Page, A. L., Miller, R. H. Keeney, D. R., Methods of soil analysis, Madison, Wisconsin, USA, *American Society of Agronomy*, 1982., pp. 403–431.
24. Rhoades, J. D., "Salinity: electrical conductivity and total dissolved solids", Sparks, D. L., Page, A. L., Helmke, P. A., Loeppert, R. H., Soltanpour, P. N., Tabatabai, M. A., Johnston, C. T. Sumner, M. E., Methods of soil analysis, Madison, Wisconsin, USA, *American Society of Agronomy*, 1996, pp. 417–435.
25. SAS, "Statistical analysis system, user's guide: statistics", 2002, SAS® Institute Inc., Cary, USA.
26. Scialdone, R., Scognamiglo, D., Ramunni, A., "The short and medium term effects of organic amendments on lead availability", *Water Air and Soil Pollution*, Vol. 13, 1980, pp. 267–274. http://dx.doi.org/10.1007/BF02145472
27. Singh, R. P., Agrawal, M., "Effects of sewage sludge amendment on heavy metal accumulation and consequent responses of Beta vulgaris plants", *Chemosphere*, Vol. 67, 2007, pp. 2229–2240. http://dx.doi.org/10.1016/j.chemosphere.2006.12.019
28. Singh, R. P., Agrawal, M., "Variations in heavy metal accumulation, growth and yield of rice plants grown at different sewage sludge amendment rates", *Ecotoxicology and Environmental Safety*, Vol. 73, 2010, pp. 632–641. http://dx.doi.org/10.1016/j.ecoenv.2010.01.020
29. Singh, S., Saxena, R., Pandey, K., Bhatt, K., Sinha, S., "Response of antioxidants in sunflower (*Helianthus annuus* L.) grown on different amendments of tannery sludge: its metal accumulation potential", *Chemosphere*, Vol. 57, 2004, pp. 1663–1673. http://dx.doi.org/10.1016/j.chemosphere.2004.07.049
30. Soil Survey Staff, "Keys to Soil Taxonomy", U.S. Department of Agriculture, Natural Resources Conservation Service, 2006, USDA, NRCS, Washington DC.
31. Stanhope, K. G., Young, S. D., Hutchinson, J. J., Kamath, R., "Use of isotopic dilution techniques to assess the mobilization of nonlabile Cd by chelating agents in phytoremediation", *Environmental Science and Technology*, Vol. 34, 2000, pp. 4123–4127. http://dx.doi.org/10.1021/es0010812
32. Tarighi, H., Majidian, M., Baghaie, A. H., Gomarian, M., "Zinc availability of two wheat cultivars in soil amended with organic and inorganic Zn sources", African Journal of Biotechnology, Vol. 11, 2012, pp. 436–443.
33. Yoo, M. S., James, B. R., "Zinc extractability as a function of pH in organic waste-amended soils.", Soil Science, Vol. 167, 2002, pp. 246–259. http://dx.doi.org/10.1097/00010694-200204000-00002

Distribution and Contamination Hazards of Heavy Metals in Solid Residues from the Pyrolysis and Gasification of Wastewater Sewage Sludge

YANJUN HU[1,*], GUANYI CHEN[2,**], WENCHAO MA[2], MI YAN[1] and LONG HAN[1]
[1]*Zhejiang University of Technology, Chaowang Road 18#, 310014, HangZhou, China*
[2]*Tianjin University, Weijin Road 92#, Nankai District, 300072, Tianjin, China*

ABSTRACT: Most of the targeted heavy metals (HMs) in sewage sludge ended up in solid residues after pyrolysis and gasification, such as Cu, Zn, Cr, Ni and Pb, which their residual rates were over 70%. The bioavailability of the HMs in residues decreased despite their concentrations being higher compared with in sludge. The potential eco-toxicity of each HM were ceased after pyrolysis and gasification of sludge. It was particularly noted that HMs in steam gasification residue exhibited the lowest contamination levels. In addition, the modification of pyrolysis temperature could pose a significant reduction on contamination level and environmental risk of HMs.

1. INTRODUCTION

MUNICIPAL wastewater treatment results in the production of a huge amount of sewage sludge (SS), the disposal of which is of serious environmental concern. In recent years, the amount of the SS generated in China has increased dramatically, and this trend is expected to increase many folds in the years to come [1]. Nowadays, the main approaches of disposing of SS can be classified into land use, incineration and landfill. Land use is one of the most economic ways because it can provide many easily available nutrient sources like N, P, K and organic matters [2,3]. However, SS also carries undesirable components, such as heavy metals (HMs), polycyclic aromatic hydrocarbons (PAHs), and polychlorinated dibenzo-P-dioxins and dibenzofurans (PCDD/Fs) which restrict its use as a fertilizer [4,5]. It was reported that the total concentration of HMs in SS (dry weight) was 0.5–2% and in some cases may increase to 4%, especially for Cu and Zn [6–8]. The reutilization of contaminated SS may release toxic pollutants into soil and underground water along with the decomposition of sludge organic matter. Sludge incineration and landfill similarly raises environmental concerns with the relevant accumulations of HMs and toxic organic pollutants in SS. Sludge incineration can result in emissions of dioxins and HMs into fly ash and flue gas [9,10]. Sludge landfill has already been banned by "Landfill Directive" in some European countries and China. Alternatively, SS can be thought of as a potential bio-resource due to its high content of organic matter. In this respect, to develop suitable technologies that can simultaneously combine material recycling and sludge disposal is become essential and expectable.

Pyrolysis and gasification technologies of recovering sustainable energy from SS are gaining more and more of interest [11–14]. The influences of various operation parameters (e.g., reaction temperature, residence time, moisture content, and catalysts) on by-product yields and hydrogen-rich syngas production have been systematically investigated [15–18]. Solid residue is an important by-product after pyrolysis and gasification treatment of SS. Recently, the residue is attracting an increasing interest, since its reutilization can potentially improve soil productivity [19], restore contaminated soils [20], reduce carbon dioxide emissions and adsorb contaminants [21].

A prediction of the ecological impact of the solid residue can be regarded as one of the essential points to confirm whether various approaches for the recovery of energy from SS can cause a secondary pollution problem [22]. In particularly, some problems need to be further investigated, such as the mitigation of the

*Author to whom correspondence should be addressed.
Yanjun Hu (Y. J. Hu), Institute of Power and Energy Engineering, School of Mechanical Engineering, Zhejiang University of Technology, China. Tel.:+86 571 88320942. E-mail address: huyanjun@zjut.edu.cn.
**Corresponding author:
Guanyi Chen (G.Y. Chen), School of Environmental Science and Engineering, Tianjin University, China. Tel. +86 27 87402075, E-mail address: chen@tju.edu.cn.

1544-8053/16/03 259-10

doi:10.12783/issn.1544-8053/13/4/3

potential ecological risks and pollution levels caused by HMs in SS after pyrolysis and gasification. Agrafioti *et al.* [23] confirmed that the chemical composition of pyrolysis residue depends on characteristics of the raw SS and the pyrolysis conditions. He *et al.* [24] determined the chemical composition and thermal stability of solid residues, as well as migration and transformation of HMs during SS pyrolysis. Hwang *et al.* [25–26] found that most HMs was completely retained by solid residue after SS pyrolysis treatment and the composition of raw SS had a significant influence on the quality of the resulting residue and thus, the mobility of HMs. Lu *et al.* [27] also studied the influence of pyrolysis temperature on physical and chemical properties of pyrolysis residue. It was observed that the total concentration of Cu, Zn, Cd and Pb in the residues increased with increasing pyrolysis temperature from 300–500°C. Marrero *et al.*. [28] reported that the HMs, such as Cu, Zn and Cd, were mainly retained in the residue after SS gasification treatment, of which are only partially leachable. Li *et al.* [29] proved that bioavailability and eco-toxicity of HMs in solid residue decreased after super-critical water gasification of SS, particularly for Cu in the bioavailable fraction of which decreased nearly 97%. To obtain a more comprehensive understanding, it is therefore necessary to conduct a quantitative assessment of HMs contamination hazards for pyrolysis and gasification residues, which will be discussed in depth in the present paper.

This study was aimed to (1) investigate quantitative assessment of HMs distribution in the various solid residues from SS pyrolysis and gasification treatment processes, (2) to provide significant information about the differentiation of the relative bonding strength of metal on various solid phases and their potential reactivity, (3) and to investigate the contamination levels of HMs in solid residues and potential ecological risk to the environments regarding their reutilization. For comparative purposes, the same assessment were employed for analyzing contamination level/risk of HMs in SS. In addition, the influences of pyrolysis temperature and moisture content of raw SS on the contamination level/risk of HMs in solid residues were also discussed.

2. EXPERIMENTAL

2.1. Materials Preparation

The dewatered SS in this study was sampled in a municipal wastewater treatment plant, located in Hangzhou of Zhejiang Province, China. In order to study the influence of moisture content of SS on the transformation behavior of HMs during gasification and pyrolysis of SS, some experiments were carried out for the following samples: (1) a totally dried aliquot of the sludge; (2) a partially dried fraction of this sewage sludge, with a moisture content of 55 wt%. Raw wet sludge was initially dried in open air for 2 days to remove the majority of the moisture content and obtain 55% of the sludge sample. In order to obtain dry sludge sample, the sludge was further dried in a lab-scale air convection oven at 105°C for 10 hours to obtain. The dry sludge was grounded and screened into fractions of particle diameter smaller than 0.25 mm. These sludge fractions were then kept in airtight containers in an ice box to prevent re-absorption of moisture or re-dewatering before experimentation. The proximate of the sludge (dry basis), including volatile matter content (46.3%), the amount of ash (48.2%) and the moisture content (3.8%), was analyzed according to the National Testing Standard of Proximate Analysis of Coal [30]. The fixed carbon content (1.7%) of the sludge was calculated on the basis of the mass balance. The ultimate analysis of the sludge was conducted by LECO CHN 600 element analyzer and the National Testing Standard of Ultimate analysis of Coal [31], including carbon (36.5%), hydrogen (5.3%), nitrogen (3.5%), sulfur (1.1%), and oxygen (52.6%).

2.2. Pyrolysis and Gasification Procedures to Collect Solid Residues

The schematic diagram of SS pyrolysis and gasification is shown in Figure 1. A lab-scale cylindrical quartz reactor with a heating area of 40 mm in diameter and 600 mm in length was used to carry out sludge pyrolysis and gasification tests. The reactor is heated by a programmable temperature control, and can be adjusted from room temperature to 1200°C. The SS pyrolysis tests were operated at atmospheric pressure and a nitrogen atmosphere. A nitrogen flow rate of 80 mL/min was passed through the whole system for 20 min prior to the commencement of the pyrolysis testing. The nitrogen flow was shut down during the sludge pyrolysis, which is good for high residence time of volatiles derived from sludge in the furnace and their secondary reactions. When the chosen ending temperature was reached, it was maintained for a pre-determined length of residence time (20 min). The gasification test of SS was operated under a high temperature steam atmosphere and at atmospheric pressure. The steam with

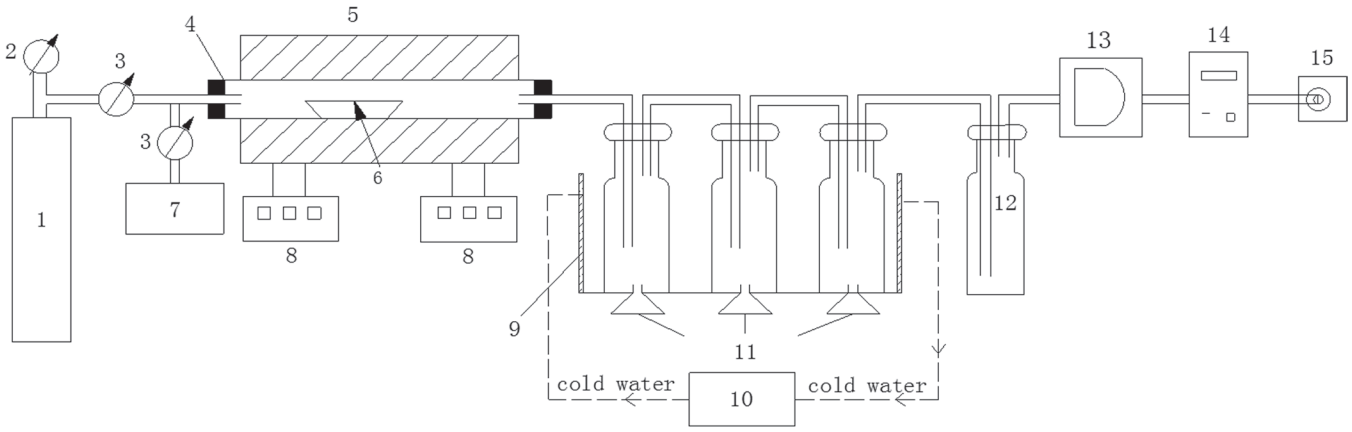

Figure 1. *The schematic presentation of the experimental apparatus. 1-nitrogen or air; 2-pressure gauge; 3-gas flow meter; 4-quartz tube; 5-reactor; 6-SS sample; 7-high temperature steam production; 8-programmable temperature controller; 9-gas condenser; 10-pump; 11-condensed oil fraction; 12-moisture absorber (anhydrous calcium sulfate); 13-filter; 14-gas flow meter; 15-Tedlar sampling bag.*

the mass flow rate of 2.5 g/min was fed into the reactor throughout the entire gasification process. A sample of sludge around 35 g in weight was placed in the center of the hot zone of the reactor for each pyrolysis and gasification treatment. With the chosen amount of sludge and the fed steam, the corresponding mass ratio of steam to the used SS was about 2.3 during the SS gasification. The resulting gaseous, aqueous and solid products from SS pyrolysis and gasification processes were carefully and separately collected. The volatiles evolved from the SS sample passed through three consecutive gas condensers which were placed in an ice-water bath. The condensed oil fraction recovered in the condensers showed a dark color with about pH 9. This fraction was separated from the organic fraction by decantation, while the organic fraction dissolved in the dichloromethane was obtained by evaporating the solvent at 45°C. The non-condensable gases were collected in Tedlar sample bags of 5 L with a polypropylene fitting for sampling. Upon the completion of the reaction, heating was suspended, the electric reactor was cooled down using fans, and the resulting solid residue was taken out and collected in sample bag for further weight and chemical analyses. The experimental conditions, by-product yields of SS pyrolysis and gasification and moisture contents of the used sludge are described in Table 1.

2.3. HMs Analysis

Six targeted elements to define environmental quality include Cu, Cr, Pb, Zn, Ni and Cd. They are selected because these elements are relatively high concentrations in the local SS, and are readily migrated from SS into pyrolysis and gasification residues, and hold a specific risk to the environment. In order to more accurately measure the total concentration of individual HM, replicate samples of the dried SS (approximately 0.2 g) and the collected residues samples (approximately 0.2 g) were digested in a microwave with an acid mixture composed of 9 mL of concentrated HNO_3 and 3 mL of concentrated HF [32]. Then the concentrations of the targeted HMs were measured using inductively coupled plasma-mass spectrometry (ICP-MS, Elan DRC-e).

Table 1. Operation Conditions and Products Yields of SS Pyrolysis and Gasification, the Moisture Content of the Used Sludge.

Experimental	Gangue (%)	Residue Sample Code			
		PR-1	**PR-2**	**PR-3**	**GR**
Operation Conditions	Average Heating rate (°C/min)	80	80	80	80
	Ending temperature (°C)	650	950	950	950
	Agent flow rate	80 ml/min	80 ml/min	80 ml/min	2.5 g/min
	Reaction agent	N_2	N_2	N_2	Steam
Yields of solid residue (g/g SS)[a]		0.59	0.56	0.54	0.48
Moisture content of SS (%)		0	0	55%	0

[a]Expressed on a SS dry basis.

The chemical forms of HMs were determined through an established BCR multi-step sequential extraction method [33]. Four fractions were collected during each extraction and grouped according to the metal species as follows: exchangeable, water and acid-soluble species (F1); reducible, iron and manganese oxides (F2); oxidizable, species bound to organic matter (F3); and residual, associated with mineral matter (F4). Multi-step sequential extractions were carried out for each fraction with different chemical forms of association and mechanisms of availability. Table 2 summarized the details of BCR extraction procedure. Sequential extractions were carried out in duplicate, using 1 g dry SS and various reagents. Solid samples were placed in polypropylene centrifuge tubes (30 mL with cap) and mixed in a stepwise fashion with different reagents to conduct the extractions. The suspensions were equilibrated as introduced in Table 2. In order to minimize loss of solid residues, between all successive extractions, the solid residues was suspended in 5 ml of 0.1M NaCl and centrifuged at 3000 rpm for 20 min to displace the extraction solution remaining from the previous step. The above step was aimed to reduce sample dispersion and to minimize the re-adsorption of the metal. The obtained supernatant was added to the former extractant. Afterwards, the supernatants was filtered through a 0.45 um membrane filter, and the residues were washed and shaken with 8 mL of deionized water for 25 min, and then centrifuged, making it ready for the subsequent extractions. The concentrations of HMs in different fractions were measured by ICP-MS.

2.4. Risk Assessment Methodology

In the past years, various assessment indices and methods, such as the geo-accumulation index (Igeo) and potential ecological risk index (RI), the analyses of risk assessment code (RAC) and bioavailability and eco-toxicity of HMs have been employed to assess the pollution levels of HMs in solid materials, such as some sediments, sewage sludge and its thermal treatment residues [29,33–39]. According to the total content or speciation characteristics of HMs, the index of I_{geo} and RI were categorized into all total content indices, and RAC was a speciation index [40].

Table 2. Sequential Extraction Procedures.

Fraction	Solution	Equilibrium Conditions
F1	40 ml 0.11M CH_3COOH	16 h, room temperature
F2	40 ml 0.5 M NH_2OH-HCL (pH 1.5)	16 h, room temperature
F3	10 ml 8.8M H_2O_2	1 h, room temperature 1 h, 85
F4	10 ml 8.8M H_2O_2 40 ml 1M NH_4OA_c (pH 2) HNO_3-HCl digestion	1 h, 85 16 h, room temperature

I_{geo} index can be obtained by the following Equation (1), where C_n is the measured concentration of bioavailable HMs in SS and solid residue (PR-1, 2, 3 and GR); B_n is the background values of individual HMs. It has been proved that the total content of HMs must be substituted with the content of bioavailable HMs. Otherwise, the assessed ecological risk and contamination degree of HMs in SS and its resulting residues after thermal treatment will be increased and overestimated [29]. Soil background values in Zhejiang Province were selected as reference values to evaluate toxic HMs contamination, which were from the statistical parameter of top soil environmental background in the plain regions of Zhejiang [41].

$$I_{geo} = \log_2 \frac{C_n}{1.5B_n} \tag{1}$$

Calculation of Potential ecological (RI) was employed to quantitatively assess the ecological risk of HMs. It was denoted to characterize the environmental ecological risk resulting from the distribution of HMs, which was obtained by the following Equations (2), (3) and (4) [28,33,34,36]. Where, C_f^i is the pollution index of each HM; C_d^i is the measured concentration of bioavailable HMs in SS and PR1, 2, 3 and GR; C_R^i is the reference value of individual HMs defined as B_n; E_R^i is the monomial potential ecological risk factor; T_R^i is the toxic response factor of each HM, and the value is in the order of Zn = 1 < Cr = 2 < Cu = Ni = Pb = 5 < Cd = 30 [44].

$$C_f^i = \frac{C_d^i}{C_R^i} \tag{2}$$

$$E_R^i = T_R^i \times C_f^i \tag{3}$$

$$RI = \Sigma_{i-1}^n E_R^i \tag{4}$$

Analysis of RAC index has been employed by several authors to assess the environmental risk associated with HMs pollution in some sediments or solid residues [28,34]. In this study, it was used to estimate HMs

contamination in SS and PRs and GR. The RAC assessment was carried out through comparing the mass percentages of HMs in the carbonate and exchangeable fraction with the classification of risk categorized in terms of RAC tabulated by Sundaray *et al.* [42].

3. RESULTS AND DISCUSSIONS

3.1. Total Concentration of HMs

The total concentrations of the six targeted HMs in SS, PR-1, 2 3 and GR are listed in Table 2. For comparative purposes, the discharge standards of pollutants for municipal wastewater treatment plant in China are also presented in Table 3. It can be seen that the concentration of each HM in the PR1, 2, 3 and GR is all higher than those in SS, except for Cd. The content of Cd in PR-1, 2 and 3 is slightly lowered than that in SS. One of the reasons may be that Cd is expected to partition in higher concentration in gaseous and liquid phases by-products (gas or bio-oil) due to its physical-chemical properties such as low vapor pressure and high volatility under the condition of high temperature. In addition, as a result of the trace concentration of Cd in the residue samples, an unavoidable sampling and measurement error of about 9% from three replicated samples could slightly influence the average contents of Cd in PR-1, 2, and 3. For all of the targeted elements, the content of Zn in various residues and SS samples is highest. Moreover, the concentration of the individual HM was all below the discharge standards of pollutants for municipal wastewater treatment plant before the pyrolysis and gasification treatment of SS. However, Cu in PR-2, PR-3 and GR, and Zn and Ni in all the tested residues exceeded the acid soil standards after pyrolysis and gasification treatment, but still were within the basic soil control range. The increase of the total concentration of individual HM in PRs and GR potentially means the contamination risk of HMs to environment increased. As discussed in previous investigations, the bioavailability and eco-toxicity of HMs in solid materials are strongly associated with their specific chemical forms and their binding state [6,25–26]. Therefore, whether the HMs in PRs and GR pose an eco-toxicity risk on the environment depends on further sequential extraction results.

3.2. Residual Rate of HMs

Among the targeted HMs, Cd held a relatively lower residual rate of below 55%. For the other HMs, their residual rates were all over 70%, which indicated that most of the HMs remained in the solid residues after pyrolysis and gasification treatment. The obtained results are similar to other research findings showing that HMs in SS are concentrated in residue fractions following pyrolysis [25–26,44]. It is also observed that the operation temperature influenced the residual rate of HMs to a different extent. As the pyrolysis temperature increased, Cu, Zn, Ni and Cr became increasingly trapped in the resulting solid residues. However, as the temperature increased from 650–950°C, the residual rate of Pb and Cd during SS pyrolysis decreased by 16.7% and 12%, respectively. In addition, the change of moisture content in the raw SS from 0–55% only showed a slight impact on the residual rates of the tested HMs. This may mean that a low water mass contained in SS was not a dominant factor influencing the partition of HMs. If enough water was involved in the SS pyrolysis process, it could promote the chemical reaction among mineral matters, metals, and water, and increase the residual rates of HMs in solid residues. This was confirmed by Verhulst *et al.* [45] that some HMs with high volatility could be easily converted to oxides, and a certain level of water in the system could decrease the metal volatilization by shifting the equi-

Table 3. The Total Concentration of HMs in SS, PRs and GR and Permitted Values in Discharge Standards (mg/kg)[a].

Sample Codes		Cu	Zn	Pb	Cr	Ni	Cd
SS		557	1860	114	335	81	1.92
PR-1		774.3	2570.1	161.6	408.3	115.5	1.8
PR-2		874.5	2846.1	129.5	413.1	129.7	1.41
PR-3		883.6	2829.6	141.7	414.3	117.4	1.7
GR		882.7	2941.4	174.2	470.0	140.3	2.3
Discharge standards values [45]	pH < 6.5	800	2000	300	600	100	5
	pH > 6.5	1500	3000	1000	1000	200	20

[a]The results are expressed as the average values, and the experimental errors of the replicated tests are less than 10%.

librium based on the chemical formula (1) towards the left, which improved their fixation rates to the resulting solid residue. The SS steam gasification in this study similarly proved the result. The residual rates of Zn, Cr, Ni, Pd, and Cd in GR were observed to be significantly lower than those in PR2 and PR3. The residual rates of Cu and Ni in GR were rarely varied though steam was fed into SS gasification reactor.

$$MO+2HCl(gaseous)=MCl_2(gaseous)+H_2O(gaseous) \quad (5)$$

3.3. Bioavailability of HMs

The bioavailability and eco-toxicity of HMs in the environment is dependent not only on their concentrations, but also on their chemical speciation [40]. It is widely recognized that the acid soluble/exchangeable fraction (F1) and the reducible fraction (F2) with a thermodynamically unstable characteristic are the direct toxicity fractions. The oxidizable fraction (F3) in oxidizing condition and the residual fraction (F4) are identified as a stable fraction, because they mainly contains primary and secondary minerals holding metals within their crystal structure and these metals are not expected to be leached into solution under normal condition in nature [46] . Hence, in this study, the bioavailable fraction was defined as the sum of F1 and F2 in order to accurately assess contamination levels and potential ecological risk of the HMs in SS, PRs and GR. The non-bioavailable fraction consisted of F3 and F4. Table 4 shows the statistical results of the average concentration of each HM in the bioavailable (C_{Bio}) and non-bioavailable (C_{nbio}) fractions. It can be found that the bioavailable fractions of HMs in PRs and GR notably decreased compared with those in SS. In particular, the amount of HMs in the bioavailable fraction most notably decreased for GR. The result is consistent with a previous study by Marrero [28], which reported that metals retained in the solid product of SS gasification could be expected to be much less mobile than those in SS. However, the amount of Pb in the bioavailable fraction of PRs showed a relatively small variation. Pb is preferentially bound to residual fractions (F4) and is almost undetectable in its conveniently mobile form [47].

Table 4. Statistical Results of Bioavailable Fractions of Heavy Metals in PRs and GR (mg/kg)[a].

Sample	Specification	Cu	Zn	Pb	Cr	Ni	Cd
SS	C_{Bio}	222.8	1209	42.2	184.25	56.7	0.86
	C_{nbio}	334.2	651	71.82	150.75	24.3	1.05
PR-1	C_{Bio}	25.5	682.8	25.9	7.4	12.0	0.2
	C_{nbio}	748.9	1870.6	135.7	401.0	98.5	1.6
PR-2	C_{Bio}	23.9	617.7	24.6	6.2	4.5	0.1
	C_{nbio}	850.6	2228.4	104.9	406.9	125.2	1.3
PR-3	C_{Bio}	2.6	761.8	32.6	8.1	3.4	0.1
	C_{nbio}	881.0	2067.8	109.1	396.2	114.0	1.6
GR	C_{Bio}	4.4	235.3	8.7	0.0	3.7	0.1
	C_{nbio}	842.1	2694.3	141.1	390.7	118.7	2.2

[a]The results are expressed as the average values, and the experimental errors of the replicated tests are less than 10%.

3.4. Contamination Assessment

3.4.1. Geo-accumulation Index (I_{geo})

Figure 2 shows the I_{geo} index of the six HMs in SS, PRs and GR. For SS, the I_{geo} values of Zn and Cu were above 2, meaning a heavy contamination in SS; Pb showed no contamination; Cr, Ni and Cd showed a moderate contamination. Compared with the I_{geo} values for SS, the values for PRs and GR were decreased to different extents. The I_{geo} values of Cu, Cr, Ni, Pb and Cd in all the residues samples were below zero, implying an uncontaminated level. Zn levels in all residues could be classified as heavy contamination except for GR showing a moderately contaminated level. On the whole, the contamination levels of the six HMs after pyrolysis and gasification processes were all evidently reduced, except for Zn. In particular, the contamination levels of Cu, Cr, Ni and Cd were ceased from a contaminated level to an uncontaminated level after pyrolysis and gasification treatment of SS.

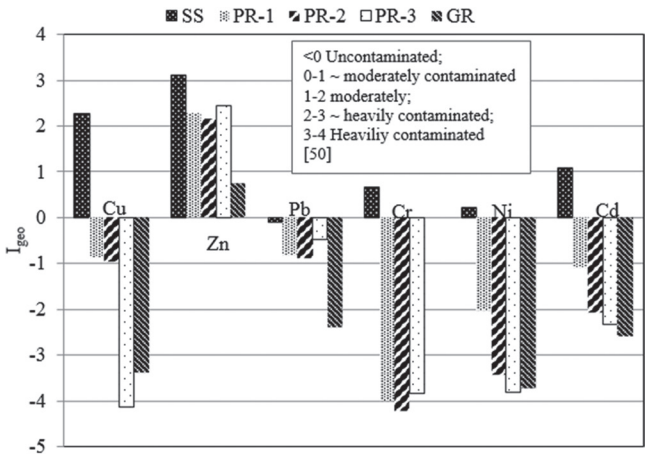

Figure 2. *I_{geo} index of HMs in SS, PRs and GR.*

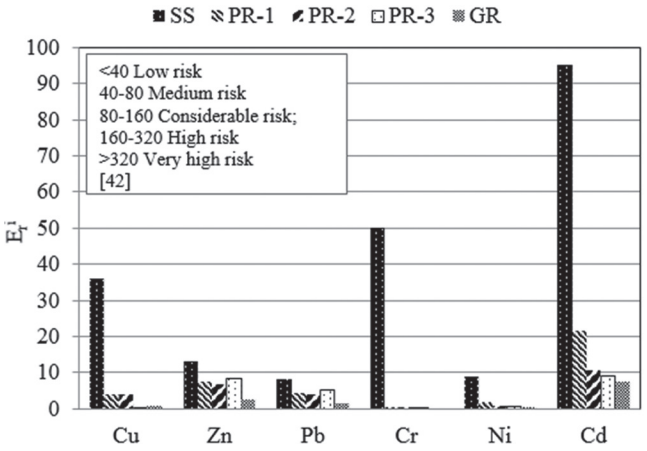

Figure 3. *Potentially ecological risk indices of HM in SS, PRs and GR.*

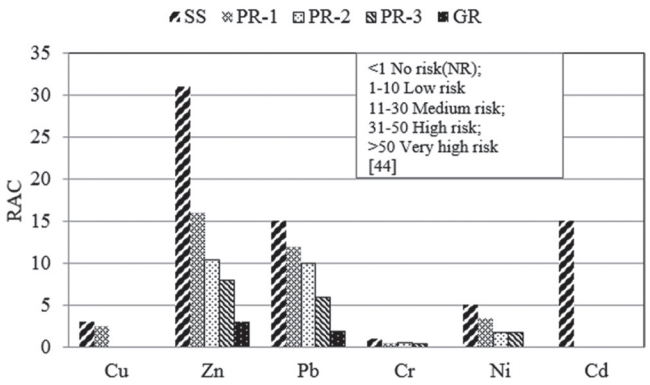

Figure 4. *The RAC index of HMs in SS, PRs and GR.*

3.4.2. Potentially Ecological Risk Index (RI)

Figure 3 shows the ecological risk assessment results of six targeted HMs. All of the risk indices (E_R^i) of the HMs in SS were higher than those in PRs and GR. It was observed that Cd polluted SS considerably, with a high E_R^i value of 95, and Cr polluted SS moderately, with an E_R^i value of 50. The two targeted HMs in SS were deemed a very high risk to the environments, and should give rise to wide-spread concerns. In regards to Zn, Pb, Cr and Ni in SS, the E_R^i values were below 40, therefore they can be classified as very low risk to the enviroment. However, for all the studied residues, the E_R^i values of Cu, Zn, Pb, Cr, Ni and Cd were all below 40, suggesting no or low risk to the local environment.

RI was employed to further evaluate the overall potential ecological risk of HMs. The RI method covers a variety of research domains i.e., biological toxicology, environmental chemistry, and ecology [40]. The RI of six targeted HMs for SS was as high as 211.2, representing a high risk to the environment. However, the solid residues PR-1, PR-2, PR-3 and GR showed much lower RI values (39.2, 26.2, 23.7 and12.8, respectively) presenting low risk or no risk to the environments. It can be concluded that the low ecological risk of residues resulted from the metal, Cd.

3.4.3. Analysis of Risk Assessment Code (RAC)

RAC can be characterized as the environmental risk due to the presence of HMs in the exchangeable and carbonate-bound fraction (F1). Figure 4 shows the results of the environmental risk assessment based on RAC index. The mass ratios of F1 in SS varied in decreasing order of Zn, Cd, Pb, Ni, Cu, and Cr. In particular, Zn posed a high risk to the ecosystem and Cd and Pd could be categorized as medium risk. It can be observed that the RACs of the HMs in SS were higher than those of PRs and GR. The RAC values for Zn and Pd in PR-1 and PR-2 were higher than 11, indicating a medium risk to the environment. The RAC indices for Cu, Cr and Ni in SS, PRs and GR were all below 10, and could be classified as low risk or no risk. Cr, Ni, Cu, Pd and Cd in GR could be classified as no risk, which was consistent with the results from their E_R^i, and RI values.

3.5. Comparisons of Different Assessment Methods

The comparison of the assessment results among the I_{geo}, E_R^i, RI and RAC indices consistently indicated that HMs contamination level were significantly decreased after SS pyrolysis and gasification. I_{geo}, and E_R^i indices showed uncontaminated and low risk of Cu, Pb, Cr, Ni, and Cd in the pyrolysis and gasification residues. The assessment results of the HMs in PRs and GR showed good agreement, implying negligible or very low risk to the environments. RAC index for most of HMs in residues also gave consistent results with I_{geo}, and E_R^i. The three assessment indices all showed a medium risk or moderate contamination for Cr in SS

However, there were some disagreements among the risk ranks of the HMs. The major disagreement existed for the risk assessment of Cu, Zn, Pd and Ni in SS and Zn in PRs. The assessment results based on I_{geo} index indicated that the levels of Zn and Cu pollution in SS were classified as heavy contamination risk, and the levels of Zn in PR-1, 2 and 3 were classified as moderate contamination or heavy contamination. However, based on E_R^i assessment results, Cu, Zn, Pd and Ni in SS and Zn in PRs presented a low risk. Based on RAC

index, Zn in PR-1 presented a medium risk because of its high percentage of F1 fraction and Cu in PR-3 and GR showed low risk to no risk. In particular, based on the I_{geo} and E_R^i indices, the level of Cr contamination in SS ranked as moderately contaminated, whereas a negative result was obtained from RAC indicating that Cr pollution in the SS presented a low risk to the environment. Similar contradictions were also observed for Pb. For instance, the risk classification of Pd in the SS and PR-1 based on RAC was medium rank, but they presented no pollution risk based on E_R^i and I_{geo}.

The three risk assessment methods possess distinctive characteristics, despite some disagreements existing among the risk ranks of the six targeted HMs. The I_{geo} method focuses primarily on the accumulation levels of the individual HM. RI can describe both ecological risk caused by a single pollutant and the overall risk or contamination from various pollutants. During the calculation of I_{geo} and RI, the concentration of the individual HM distributed in the F1 and F2 fractions is adopted as the measured parameters, instead of the total content of each HM. The RAC classification considers only F1 values, ignoring the F2, F3 and F4 proportions of each HM. For RI index, the total concentration and different fraction of individual HM were taken account while neglecting the difference of each HM in terms of their bioavailability and eco-toxicity.

3.6. Comparisons Between PRs and GR

Through assessing the risk contamination based on I_{geo}, and RAC, it was observed that PRs were polluted by some of the targeted HMs more heavily than GR by some HMs. Zn, for example, was considered to be heavy contamination classification based on I_{geo}, and to be under the medium risk categories to the environment based on the RAC value. In addition, the environmental risk assessment value of each HM in GR decreased or showed no risk to the environments, reflecting minimal contamination of the HMs and environmental risk to the ecosystem. Though the total concentration of HMs in GR increased, its bioavailable fractions of HMs decreased. According to the RI values, the potential ecological risk of GR is much lower than those of PRs.

The comparison among the obtained risk assessment results indicates that pyrolysis temperature has a significant impact on the ecological risk and pollution level. As pyrolysis temperature increased the I_{geo} values of the HMs decreased. A higher temperature could potentially contribute to a lower environmental risk of HMs in solid residues. With respect to Cd, for example, the rank of risk significantly decreased from medium risk to no risk when the reaction temperature increased from 650–950 °C. With the Cu and Ni, the rank of risk decreased from low risk to no risk. However, the moisture content of SS had little influence on the ecological risk and intensities of HMs pollution. The total concentration and bioavailability of HMs were only slightly influenced as the moisture content increased from 0–55%.

4. CONCLUSIONS

Most of HMs in SS was still retained by solid residues after gasification and pyrolysis treatment. The potential eco-toxicity and bioavailability of the targeted HMs were ceased, but their total concentrations increased compared with them in SS. According to I_{geo}, and E_R^i indices, the contamination levels of Cu, Pb, Cr, Ni and Cd in pyrolysis and gasification residues are uncontaminated or low risk to the environment, but as regards HMs in SS, their contamination levels and eco-toxicity risk to the environment maybe have an overestimated. On the whole, the pyrolysis and gasification treatment effectively reduced the bioavailability of HMs by chemical modification of their chemical speciation into less available forms. In addition, the modification of pyrolysis temperature could pose a significant reduction on contamination level and environmental risk of HMs. Meanwhile, the steam fed into reactor during SS gasification imposed a more active effect on reduction of the environmental risk caused by HMs in the resulting solid residue. Attention should also be paid to the fact that the three risk assessment methods, I_{geo}, RI (E_R^i) and RAC, possess distinctive characteristics.

5. ACKNOWLEDGEMENT

The authors want to appreciate the projects of National Natural Science Foundation (Grant No.51576178) for providing financial support of this work.

6. REFERENCES

1. Report of in-depth research and investment strategy planning on china sludge treatment industry (2013–2017), 2013, China.
2. Bramryd, T., "Long-term effects of sewage sludge application on the heavy metal concentrations in acid pine (*Pinus sylvestris* L.) forests in a climatic gradient in Sweden", *Forest Ecol. and Manage. 289*, 2013, pp. 434–444. http://dx.doi.org/10.1016/j.foreco.2012.08.045
3. Metcalfeddy, I., Tchobanoglous, G., Chow, V.T., Insley, R.K., 2003.

Wastewater Engineering: Treatment, Disposal and Reuse, fourth ed. McGraw-Hill Publishing Company Ltd, New York.

4. Pepper, I.L., Brooks, J.P., Gerba, C.P., "Pathogens in biosolids", *Adv. Agron 90*, 2006, pp. 1–41. http://dx.doi.org/10.1016/S0065-2113(06)90001-7
5. Dai, J., Xu, M., Chen, J., Yang, X., Ke, Z., "PCDD/F, PAH and heavy metals in the sewage sludge from six wastewater treatment plants in Beijing, China", *Chemosphere. 66*, 2007, pp. 353–361. http://dx.doi.org/10.1016/j.chemosphere.2006.04.072
6. Cai, Q.Y., Mo, C.H., Wu, Q.T., Zeng, Q. T., Katsoyiannis, A., "Concentration and speciation of heavy metals in six different sewage sludge-composts", *J Hazard. Mater, 147*, 2007, pp. 1063–1072. http://dx.doi.org/10.1016/j.jhazmat.2007.01.142
7. Delgado, G.M., Rodríguez, M.S., Lorenzo, L.F., Arienzo, M., Sánchez-Martín, M.J., "Seasonal and time variability of heavy metal content and of its chemical forms in sewage sludge from different wastewater treatment plants", *Sci Total Environ, 382*, 2007, pp. 82–92. http://dx.doi.org/10.1016/j.scitotenv.2007.04.009
8. Karvelas, M., Katsoyiannis, A., Samara, C., "Occurrence and fate of heavy metals in the wastewater treatment process". *Chemosphere, 53*, 2003, pp. 1201–1210. http://dx.doi.org/10.1016/S0045-6535(03)00591-5
9. Hopes, M.H., Abelha, P., Lapa, N., Oliveira, J.S., Cabrita, I., Gulyurthu, U., "The behaviour of ashes and heavy metals during the co-combustion of sewage sludges in a fluidized bed". *Waste Manage, 23*, 2003, pp. 859–870. http://dx.doi.org/10.1016/S0956-053X(03)00025-4
10. Samolada, M.C., Zabaniotou, A.A., "Comparative assessment of municipal sewage sludge incineration, gasification and pyrolysis for a sustainable sludge-to-energy management in Greece", *Waste Manage, 34*, 2014, pp. 411–420. http://dx.doi.org/10.1016/j.wasman.2013.11.003
11. Kim, Y., Parker, W., "A technical and economic evaluation of the pyrolysis of sewage sludge for the production of bio-oil", *Bioresour. Technol, 99*, 2008, pp. 1409–1416. http://dx.doi.org/10.1016/j.biortech.2007.01.056
12. Lumley, N.P.G., Ramey, D.F., Prieto, A.L., Braun, R.J., Cath, T.Y., Porter, J.M., "Techno-economic analysis of wastewater sludge gasification: A decentralized urban perspective", *Bioresour. Technol*, 2014, http://dx.doi.org/10.1016/j.biortech.2014.03.040
13. Manara, P., Zabaniotou, A., "Towards sewage sludge based biofuels via thermochemical conversion—A review", *Renew. Sust. Energy Rev, 116*, 2012, 2566–2582. http://dx.doi.org/10.1016/j.rser.2012.01.074
14. McKendry, P., "Energy production from biomass (part 3): gasification technologies", *Bioresour. Technol, 83*, 2002, pp. 55–63. http://dx.doi.org/10.1016/S0960-8524(01)00120-1
15. Fonts, I., Azuara, M., Gea, G., Murillo, M.B., "Study of the pyrolysis liquids obtained from different sewage sludge", *J. Anal. Appl. Pyrol, 85*, 2009, pp. 184–191. http://dx.doi.org/10.1016/j.jaap.2008.11.003
16. Gil-Lalaguna, N., Sánchez, J.L., Murillo, M.B. Rodríguez, Gea, E., G., "Air-steam gasification of sewage sludge in a fluidized bed. Influence of some operating conditions", *J. Chemical Eng. 248*, 2014, pp. 373–382. http://dx.doi.org/10.1016/j.cej.2014.03.055
17. Nipattummakul, N., Ahmed, I., Kerdsuwan, S., Gupta, A.K., "High temperature steam gasification of wastewater sludge", *Appl. Energy, 87*, 2010, pp. 3729–3734. http://dx.doi.org/10.1016/j.apenergy.2010.07.001
18. Xiong, S.J, Zhuo, J.K., Zhang, B.P., Yao, Q., "Effect of moisture content on the characterization of products from the pyrolysis of sewage sludge", *J. Anal. Appl. Pyrol, 104*, 2013, pp. 632–639. http://dx.doi.org/10.1016/j.jaap.2013.05.003
19. Song, X.D., Xue, X.Y., Chen, D.Z., He, P.J., Dai, X.H., "Application of biochar from sewage sludge to plant cultivation: Influence of pyrolysis temperature and biochar-to-soil ratio on yield and heavy metal accumulation", *Chemosphere, 109*, 2014, pp. 213–220. http://dx.doi.org/10.1016/j.chemosphere.2014.01.070
20. Beesley, L., Moreno-Jiménez, E., Gomez-Eyles, J.L., "Effects of biochar and green waste compost amendments on mobility, bioavailability and toxicity of inorganic and organic contaminants in a multi-element polluted soil", *J. Environ. Pollut. 158*, 2010, pp. 2282–2287. http://dx.doi.org/10.1016/j.envpol.2010.02.003
21. Jindarom, C., Meeyoo, V., Kitiyanan, B., "Surface characterization and dye adsorptive capacities of char obtained from pyrolysis/gasification of sewage sludge", *J. Chem. Eng, 133*, 2007, pp. 239–246. http://dx.doi.org/10.1016/j.cej.2007.02.002
22. Huang, H.J., Yuan, X.Z., "The migration and transformation behaviors of heavy metals during the hydrothermal treatment of sewage sludge", Bioresource Technology, 200, 2016, pp. 991–998. http://dx.doi.org/10.1016/j.biortech.2015.10.099
23. Agrafioti, E., Bouras, G., Kalderis D., Diamadopoulos, E., "Biochar production by sewage sludge pyrolysis", *J. Anal. Appl. Pyrol*, 2013, 101, pp. 72–78. http://dx.doi.org/10.1016/j.jaap.2013.02.010
24. He, Y.D., Zhai, Y.B., Li, C.T., Yang F., Chen, L., Fan, X.P., Peng, W.F., Fu, Z.M., "The fate of Cu, Zn, Pb and Cd during the pyrolysis of sewage sludge at different temperatures", *Environ. Technol, 35*, 2010, pp. 567–574. http://dx.doi.org/10.1080/09593330903514466
25. Hwang, I.H., Ouchi, Y., Matsuto, T., "Characteristics of leachate from pyrolysis residue of sewage sludge", *Chemosphere, 68*, 2007a, pp. 1913–1919. http://dx.doi.org/10.1016/j.chemosphere.2007.02.060
26. Hwang, I. H., Matsuto, T., Tanaka, N., Sasaki, Y., Tanaami, K., "Characterization of char derived from various types of solid wastes from the standpoint of fuel recovery and pretreatment before landfilling", Waste Manage, 27, 2007b, pp. 1155–1166. http://dx.doi.org/10.1016/j.wasman.2006.05.013
27. Lu, H. L., Zhang, W. H., Wang, S. Z., Zhuang, L.W., Yang, Y.X., Qiu, R. L., "Characterization of sewage sludge-derived biochars from different feed stocks and pyrolysis temperatures", *J. Anal. Appl. Pyrol, 102*, 2013, pp.137–143. http://dx.doi.org/10.1016/j.jaap.2013.03.004
28. Marrero, T.W., McAuley, B.P., Sutterlin, W.R., Morris, J. S., "Fate of heavy metals and radioactive metals in gasification of sewage sludge", *Waste Manage, 24*, 2004, pp. 193–198. http://dx.doi.org/10.1016/S0956-053X(03)00127-2
29. Li, L., Xu, Z.R., Zhang, C.L., "Quantitative evaluation of heavy metals in solid residues from sub- and super-critical water gasification of sewage sludge", *Bioresour. Technol., 121*, 2012, pp. 169–175. http://dx.doi.org/10.1016/j.biortech.2012.06.084
30. GB/T 212-2008, 2008. The National Testing Standard of Proximate Analysis of Coal of China.
31. GB476-91, 1991, the National Testing Standard of ultimate Analysis of Coal of China.
32. USEPA, Method 3052: Microwave assisted and digestion of siliceous and organically based matrices. 1996, Washington DC, USA.
33. Nemati K., Abu Bakar N.K., Radzi A. M., Sobhanzadeh E., "Speciation of heavy metals by modified BCR sequential extraction procedure in different depths of sediments from Sungai Buloh, Selangor, Malaysia", *J Hazard Mater, 192*(1), 2011, pp. 402–410. http://dx.doi.org/10.1016/j.jhazmat.2011.05.039
34. Abrahim, G., Parker, R., "Assessment of heavy metal enrichment factors and the degree of contamination in marine sediments from Tamaki Estuary, Auckland, New Zealand", *Environ. Monit. Assess, 136*, 2008, pp. 227–238. http://dx.doi.org/10.1007/s10661-007-9678-2
35. Huang, H.J., Yuan, X. Z., Zeng, G.M., Zhu, H.N., Li, H., Liu, Z.F., Jiang, H.W., Leng, L.J., Bi, W.K., "Quantitative evaluation of heavy metals' pollution hazards in liquefaction residues of sewage sludge", *Bioresour. Technol., 102*, 2011, pp. 10346–10351. http://dx.doi.org/10.1016/j.biortech.2011.08.117
36. Liu, H., Li, L., Yin, C., Shan, B., "Fraction distribution and risk assessment of heavy metals in sediments of Moshui Lake", *J. Environ. Sci, 20*, 2008, 390–397. http://dx.doi.org/10.1016/S1001-0742(08)62069-0
37. Liu, J.Y., Sun, S.Y., Xu, Y.B., Xie, W.M., Chen, T., Chen, M.T., "Heavy metal characteristics sewage sludge and its potential ecological risk assessment for agriculture use in Guangzhou (in Chinese)", *Acte Scientiae Circumstantiae, 29*, 2009, pp. 2545–2556.
38. Méndez, A., Gómez, A., Paz-Ferreiro, J., Gascó, G., "Effects of sewage sludge biochar on plant metal availability after application to a Mediterranean soil", *Chemosphere, 89*, 2012, pp. 1354–1359. http://dx.doi.org/10.1016/j.chemosphere.2012.05.092
39. Shi, G., Chen, Z., Bi, C., Li, Y., Teng, J., Wang, L., Xu, S., "Comprehensive assessment of toxic metals in urban and suburban street de-

posited sediments (SDSs) in the biggest metropolitan area of China", *Environ. Pollut, 158*, 2010, pp. 694–703. http://dx.doi.org/10.1016/j.envpol.2009.10.020

40. Hakanson, L., "Ecological risk index for aquatic pollution control. A sedimentological approach", *Water Res., 14*, 1980, pp. 975–1001. http://dx.doi.org/10.1016/0043-1354(80)90143-8
41. Wang, Q.H., Dong, Y.X., Zhou, G.H., Zheng, W., "Soil Geochemical Baseline and Environmental Background Values of Agricultural Regions in Zhejiang Province", *J. Ecolo. and Rural Environ, 23*, 2007, pp. 81–88.
42. Sundaray, S.K., Nayak, B.B., Lin, S., Bhatta, D., "Geochemical speciation and risk assessment of heavy metals in the river estuarine sediments—A case study: Mahanadi basin. Indian", *J. Hazard. Mater, 186*, 2011, pp.1837–1846. http://dx.doi.org/10.1016/j.jhazmat.2010.12.081
43. GB18918-2002, 2002 Discharge standard of pollutants for municipal wastewater treatment plant, China.
44. Yuan, H., Lu, T., Zhao, D., Huang, H., Noriyuki, K., Chen, Y., "Influence of temperature on product distribution and biochar properties by municipal sludge pyrolysis", *J. Mater. Cycles Waste Manage, 15*, 2013, pp. 357–361. http://dx.doi.org/10.1007/s10163-013-0126-9
45. Verhulst, D., Buekens, A., Spencer, P., Eriksson, G., "Thermodynamic behavior of metal chlorides and sulfates under the conditions of incineration furnaces", *Environ. Sci. Technol., 30*, 1996, pp. 50–56. http://dx.doi.org/10.1021/es940780+
46. Lasheen, M. R., Ammar, N.S., "Assessment of metals speciation in sewage sludge and stabilized sludge from different wastewater treatment plants, greater cairo. Egypt", *J. Hazard. Mater., 164*, 2009, pp. 740–749. http://dx.doi.org/10.1016/j.jhazmat.2008.08.068
47. He, M.M., Li, W.H., Liang, X.Q., Wu, D.L., Tian, G.M., "Effect of composting process on phytotoxicity and speciation of copper, zinc and lead in sewage sludge and swine manure", *Waste Manage, 29*, 2009, pp. 590–597. http://dx.doi.org/10.1016/j.wasman.2008.07.005

Dissipation and Residue of Azoxystrobin in Tomatoes and Soil Using Gas Chromatography with Tandem Mass Spectrometry

YANBING WU*, JUNJUN ZHAO, ZHENMIN YAN* and YINGHUI ZHU
Henan Institute of Science and Technology, Xinxiang, 453003, China

ABSTRACT: The analytical technique for the determination of azoxystrobin in tomato and soil was obtained by gas chromatography with tandem mass spectrometry (GC-MS/MS), and its dissipation fate was also investigated under field conditions. Azoxystrobin residues in tomato and soil were extracted with ethylacetate+cyclohexane extraction and followed by the dispersive-SPE purification. The average recoveries in tomatoes and soils at different spiked concentrations (0.1, 0.5 and 1.0 mg/kg) ranged from 86.16% to 105.47% with RSDs from 6.8% to 12.3%. The LOD ranged from 0.003 µg/kg to 0.004 µg/kg, and LOQ ranged from 0.009 µg/kg to 0.012 µg/kg. This developed methodology was also used to investigate the residues and dissipation of azoxystrobin in tomatoes and soil under the field conditions. The initial azoxystrobin concentrations in tomato fruits in Henan province and in Zhejiang province were 0.494 mg/kg and 0.638 mg/kg with half-lives of 9.9 days and 11.5 days, respectively. Concentrations were reduced by more than 50% at 10 days after application for both sample sets. Initial azoxystrobin concentrations in soil were 1.747 mg/kg and 1.845 mg/kg in Henan province and in Zhejiang province with half-lives of 8.6 days and 7.7 days, respectively.

INTRODUCTION

THERE being a world gross production of nearly 100 million tonnes in 2010 and an enhancement of 45% from 2000 to 2010, tomatoes are one of the main food crops according to human diets, as wells as 16 essential nutrients and many other chemical elements that are beneficial to human health. Today tomato is cultivated almost everywhere all over the world, among which, China, India, and Egypt were the three biggest producing countries. China is generally suitable for tomato growing, however, diseases are key factors threatening the tomato production [1]. Therefore, the pesticides involving a shorter preharvest interval (PHI) of seven days or less are needed to protect tomato from plant pathogens, for instance, gray mildew (*Phytophtora infestans*) and gray mold (*Botrytis cinerea*) [2,3].

Aazoxystrobin, belonging to a systemic *β*-methacrylate strobilurin fungicide, and it is effective to control the fungal diseases caused by four main groups of plant pathogenes including Basidiomycota, Ascomycota, Oomycota and Deuteromycota [4,5]. Its main action mode is the inhibition of electronic transport between cytochrome b and cytochrome c1 [5,6]. In terms of toxicity, it is low chronic to an adult man [2]. Its brand name is Amistar and first launched in 1996 by Syngenta company, and now became the world's biggest selling fungicide. Nowadays, there are several formulations of single and azoxystrobin mixtures in china, such as water dispersible granule (WG), aqueous suspension concentrate (SC), and aqueous suspo-emulsion (SE). Azoxystrobin mixtures can save the dosage and the costs, and also reduce the resistance development of single fungicide formulations.

In term of consumers' food safety and international import and export trade, maximum residue limit (MRL) in foods had been established from different governments [7]. The MRLs for azoxystrobin in tomatoes are 2, 0.2, 1, 1, 0.5 mg/kg in EU, U.S., Japan, Korean and Australia, respectively. However, there has been no MRLs for azoxystrobin in tomato in China. Therefore, the determination of azoxystrobin residues is important for the human exposure assessment to azoxystrobin in foods.

Solid phase extraction (SPE) and solid phase microextraction (SPME) followed by multiple operation steps have become regular sample preparation techniques for azoxystrobin analysis [8,9]. However, in these methods, time consuming and a great number of organic solvents are often required. The QuECh-

*Authors to whom correspondence should be addressed.
E-mail: (Yanbing Wu) wybhist@126.com; (Zhenmin Yan) yanzhenmin1978@163.com

1544-8053/16/03 269-06

doi:10.12783/issn.1544-8053/13/4/4

ERS method is a newly developed sample preparation technique for pesticide residue analysis. Compared to traditional and regular extraction methods, the method was recently selected as an alternative technique for sample extraction and cleanup due to its many advantages [7,10]. However, to our knowledge, there is no previous report based on the use of the QuEChERS extraction technique for determining azoxystrobin residue in tomatoes. And the dissipation of azoxystrobin in tomatoes and soil under field conditions has not been studied.

A larger amount of analytical methods had been used for determining and monitoring azoxystrobin residues in biological and environmental matrices. These methods included high performance liquid chromatography (HPLC) with diode array detector (DAD) [11], massspectrometry (MS) detector [12] and tandem mass spectrometry (MS/MS) [13,14], gas chromatography (GC) with electron capture detector (ECD) [6,15], NPD detector [16], and MS detector [8,17]. Furthermore, enzyme-linked immunosorbent assay (ELISA) [4, 18], the chemiluminescence (CL) method [19], and fluorescence methods [20] have been investigated for the determination of azoxystrobin. In tandem mass spectrometry, there is a significant increase in the precision and reproducibility of the target compounds [7,10].

In this paper, we developed a fast, simple and effective extraction procedure and GC-MS/MS technique to determine the residue and dissipation of azoxystrobin in tomato and soil.

MATERIAL AND METHOD

Chemical and Reagent

An azoxystrobin standard (purity ≥ 99.7%) and 30% azoxystrobin·propamocarb hydrochloride suspension concentrate were obtained from Li'er (China) Co., Ltd. Analytical grade Ethylacetate, cyclohexane, NaCl and MgSO4 were obtained from Beijing Chemical and Reagent Co. Graphitized carbon (GCB) and primary secondary amine(PSA) were get from Agela Tecnology Co.. Ultra-pure water was prepared from a Milli-Q purification system from America Bedford Co.

The standard stock solution of azoxystrobin (100 mg/L) was prepared in acetone; standard curve analysis (0.05–2.0 mg/L) were obtained in acetone by serial dilution to 0.05, 0.1, 0.5, 1.0 and 2.0 mg/L. All the above standard solutions were stored at –20°C prior to use.

Extraction and Purification Procedure

Samples extraction. The blank samples (tomatoes and soils) were gathered from Henan province of China and did not contain the target analyte(azoxystrobin). The above samples were extracted based on a modified QuEChERS method; 10 g of representative portion of homogenized samples (tomatoes and soils) were weighed and put in a 50 mL poly-tetrafluoroethylene (PTFE) centrifuge screw-capped tubes. In the recovery experiment, the tomato and soil samples were fortified with different concentrations of standard azoxystrobin solution, well agitated and stood for 1h at room temperature. Next, 10 mL of extraction solvent (ethylacetate + cyclohexane) (1 + 1, v/v) was added and the cap was closed. The above samples were immediately vortexed vigorously for 5 min. After 4g of $MgSO_4$ and 2g of NaCl were added into the tubes, the above tubes were agitated for 2 min and then centrifuged for 10min at a speed of 2077 g (4000 rpm).

Cleanup. In each case, above upper layer of 1.5 mL solvent (ethylacetate + cyclohexane) was added into the dispersive solid-phase extraction (SPE) tubes containing 15 mg GCB, 20 mg PSA and 100 mg anhydrous $MgSO_4$ for purification. Afterward, the tubes agitated for 1 min and centrifuged for 5 min at a speed of 2077 g. The supernatant solution was filtered through a 0.22 μm polypropylene filter prior to GC-MS/MS analysis.

GC-MS/MS Analysis

The concentrations of azoxystrobin were investigated by a Varian 4500 GC equipped with a 300 module triple quadrupole mass spectromete, a 1177 Series split/splitless auto-injector and a Capillary Column VF-5 (30 m × 0.25 mm × 0.25 μm). The high pure helium of 99.999% was employed as the carrier gas with a constant flow rate of 1.0 mL/min. The column temperature was programmed as follows: initially at 150°C holding for 1 min and directly increased to 280°C at the rate of 40°C/min and holding for 20 min. The temperature of the injector port was set at 250°C and a volume of 2 μL supernatant solution was injected into the column with the splitless mode. The MS spectrometer was manipulated at the positive electron ionization (EI+) mode, with 250°C of ion source temperature and 280°C of transfer-line temperature, as well as 70 eV of electron ionization energy, and 7.0 min for solvent delay time. The scan mode was selected in the MRM. The parent ion of azoxystrobin was m/z 344, as well as its daugh-

ter quantitative ion and qualitative ion were m/z 329 and m/z 273, respectively.

Method Performance

Matrix effect assessment, precision, accuracy, LOD and LOQ were carried out to develop analytical methodology for azoxystrobin detection. As for recovery experiment, it was evaluated by extraction and analysis of five replicates at three different spiked concentrations (0.1, 0.5, and 1.0 mg/kg) by adding known volume of azoxystrobin standard solutions into different matrices (tomatoes and soils).

Field Application

In the field trials, the dissipation experiment in tomato and soil was carried out from Henan province and Zhejiang province of China in 2012. The different treatments and controls plots were divided into 15 m^2 sized blocks with three replicates. The application of 30% azoxystrobin · propamocarb hydrochloride suspension concentrate in dissipation experiments was in the dosage of 526.5 g (a.i.)/ha with using a single spray. Representative tomato and soil samples were picked up after 2 h, 1, 2, 3, 5, 7, 10d and 14d when azoxystrobin spraying. All of the above tomato and soil matrices were immediately put into polyethylene bags and kept in a deep freeze (–20°C) prior to analysis.

RESULTS AND DISCUSSION

Extraction Solvents

Acetone and petroleum ether are the solvents involved in the published journal references [2,3]. And subsequently it was cleaned up using mini chromatographic columns. It required a lot of time and organic solvents that are harmful to environment. In our study, fungicide azoxystrobin residues were extracted by the solvents according to the solvent system recommended by Bo *et al.* (2007) [17]. The extraction effects for three kinds of solvent systems are compared in this experiment. The results are as follows: the emulsion phenomenon is serious and not easily layered in the solvent system of acetonitrile/water (9 + 1, v/v), and there are a large amount of impurity peaks in the solvent system of methylene chloride/acetone (7 + 3, v/v), and there is a good recovery and selectivity in the solvent system of ethyl acetate/cyclohexane, so ethyl acetate/cyclohexane (1 + 1, v/v) solution is chosen as extraction solvent.

Cleanup Method

In the quantitative determination of the pesticide residue in foods by GC, due to the complexity of matrix, without purification treatment after extraction, the content of total flow will affect the target ion, and reduce the sensitivity of the detector. SPE is the commonly used approach for the pesticide preconcentration. In order to select suitable sorbents for cleanup, we firstly checked the cleanup effect of silica column and C18 column. And it was found that azoxystrobin was cleaned up on a silica SPE column to obtain an extract suitable for analysis. Compared to the SPE, dispersive SPE cleanup is easier and faster. These cleanup sorbents include GCB, PSA, florisil, C18, and so on. And they can fastly remove the impurities and colorings such as chlorophyll, carotene. In our study, we found that the combination of GCB with PSA can effectively remove the visible pigments.

MS/MS Parameters

The pure standard solution of azoxystrobin at 1 mg/L was infused into the tandem mass spectrometer with continuous flow injection. In this study, we evaluated ESI+ and ESI- ion modes, and it was proven that the ESI+ mode could get higher precursor ion and daughter ions signal intensities and good fragmentation patterns than the ESI- mode; so the ESI+ mode was selected for the analysis. The azoxystrobin was monitorized with scanning mode in the range of m/z 50–600. The parent ion of azoxystrobin was selected as m/z 344, as well as its daughter quantitative ion and qualitative ion selected were m/z 329 and m/z 273, respectively.

Matrix Effect

As we know, the electrospray ionization of the target analytes may be influenced by the existence of matrices compounds, and they also have been co-extracted from the samples when electrospray ionization (ESI) is used [7,10]. The matrix effects may affect the repeatability and accuracy of the developed method. Therefore, in order to decrease the matrix effect and get much better results, a calibration was carried out for azoxystrobin analysis by adding the external azoxystrobin standards into tomato and soil samples in the current study. A zero value denotes that there is no matrix effect, a positive value means that the compound response is strengthened by the different matrixes, and a negative value shows that the compound response is inhibited by the

Table 1. Standard Curve Data, LODs and LOQs for Azoxystrobin in Tomato and Soil.

Matrixes	Standard Curve	Relative Coefficient (R^2)	LODs (μg/kg)	LOQs (μg/kg)
Tomato	$y = 37595x - 689.3$	0.995	0.003	0.009
Soil	$y = 24588x + 1235.8$	0.994	0.004	0.012

different matrixes. In the present study, the matrix effect value is 2.5%, it showed that the azoxystrobin response was enhanced by the matrixes of tomatoes and soil.

Linearity, LODs and LOQs

The calibration curves of azoxystrobin were obtained at five different concentrations (between 0.05 mg/kg and 2 mg/kg) in different tomato and soil matrix (Table 1). The linearity was good with a coefficient of determination (R^2) higher than 0.99 in two matrixes standards solutions for azoxystrobin. LODs and LOQs were calculated at spiked level (0.1 mg/kg) according to an signal/noise (S/N) of 3:1 and 10:1, respectively. The results showed that the LODs of azoxystrobin ranged from 0.003 μg/kg to 0.004 μg/kg, and LOQs ranged from 0.009 μg/kg to 0.012 μg/kg in tomatoes and soils. In this developed method, the LOQs for azoxystrobin in toamto and soil samples were much below than the MRL (0.2–2 mg/kg) set by different government agencies.

Recovery, Precision and Accuracy

As shown in Table 2, the recoveries of azoxystrobin obtained with this method at different spiked concentrations for 0.1 mg/kg, 0.5 mg/kg and 1.0 mg/kg in tomatoes and soil samples. The mean recoveries ranged from 86.16% to 105.47%, and the relative standard deviations (RSDs) of repeatability of the azoxystrobin ranged from 6.8% to 12.3%. They may provide authoritative reference for azoxystrobin residue analysis.

Validation in Tomato and Soil Samples under Field Conditions

The method application was carried out to detect azoxystrobin residue in tomato and soil dissipation rate experiment both in Zhejiang province and Henan province in 2012. The curves for azoxystrobin dissipation in field treated tomato and soil samples were shown in Figure 1. The $t_{1/2}$ of azoxystrobin was obtained using the first-order kinetics equations as follows, $C_t = C_0 e^{-kt}$ and $t_{1/2} = (\ln 2)/k$. C_t is the concentration of the azoxystrobin at specific time, C_0 is the initial concentration after the azoxystrobin applicaton, k is the constant of dissipation rate, and $t_{1/2}$ denotes the half-life. The $t_{1/2}$ and other parameters of azoxystrobin residue dissipation were summarized in Table 3. The initial concentrations in the tomato samples from Henan province and Zhejiang province were 0.494 mg/kg and 0.638 mg/kg, respectively. It was found that the decline in azoxystrobin concentration was gradual when azoxystrobin spraying. Azoxystrobin residue concentrations were decreased by more than 50% at 10 days after application both in Henan province and in Zhejiang province. Initial concentrations in soil were 1.747 mg/kg and 1.845 mg/kg in Henan province and in Zhejiang province with half-lives of 8.6 days and 7.7 days, respectively.

Previous studies showed that the dissipation rates of azoxystrobin changed from different matrixes. Because of the systemic activity of azoxystrobin, it was stable in tomato fruits and there is no any decrease under greenhouse conditions. But it is sensible to sunlight, the photodegradation test showed that the waxes had a stronger screen effect compared to the glass, and its $t_{1/2}$ is 9.6 h and 0.9 h, respectively[3]. In a greenhouse study, when the tomato leaves was sprayed with homogenous 0.1% aqueous solution of Amistar 250 SC, it was found that the $t_{1/2}$ of azoxystrobin was on the average within 13 days [2]. Huan *et al.* found that the half-lives of the azoxystrobin in banana soil in Yunan province were shorter than in Hainan province, and the half-lives were 11.9–13.9 days and 16.0–16.1 days,

Table 2. Average Recoveries (%) and RSDs (%) of Azoxystrobin at Various Spiked Concentrations (n = 5).

	Spiked, 0.1 mg/kg		Spiked, 0.5 mg/kg		Spiked, 1.0 mg/kg	
Matrixes	Average (%)	RSD (%)	Average (%)	RSD (%)	Average (%)	RSD (%)
Tomato	105.47	10.3	98.13	9.7	86.30	12.3
Soil	89.89	8.5	89.05	6.8	86.16	9.6

Table 3. Half-lives and Other Parameters for Azoxystrobin Dissipation in Tomato and Soil.

Sample	Site	Dissipation Curve	Determination Coefficient (R^2)	Half Life $t_{1/2}$ (days)
Tomato	Henan	$y = 0.440e^{-0.07t}$	0.990	9.9
	Zhejiang	$y = 0.495e^{-0.06t}$	0.937	11.5
Soil	Henan	$y = 1.623e^{-0.08t}$	0.990	8.6
	Zhejiang	$y = 1.731e^{-0.09t}$	0.990	7.7

respectively [21]. In the current study, the concentration of residues and the dissipation rate were analyzed under field conditions. And the decline in azoxystrobin concentration was fast and continous. The possible reasons are as follows: on the one hand, it was due to the existence of sunlight under the field condition, and it accelerated the dissipation of the azoxystrobin; on the other hand, the above-mentioned results suggest that it was also associated with the samples from different sites and at different collection times, and the temperature, solar radiation level, rainfall and soil physicochemical properties play a vital part in the dissipation of the azoxystrobin.

CONCLUSION

A very simple residue analytical technique had been set up and investigated for the dissipation of azoxystrobin in tomato and soil based on QuEChERS and GC-MS/MS. This developed method obtained satisfactory validation parameters, e.g., linearity, accuracy and precision, LOD and LOQ. In addition, it is cheap and simple to enforce. Therefore, the method can be used for the routine determination of azoxystrobin residues in tomato and soil samples. This study also provided basic data for azoxystrobin registration and MRL establishment in China.

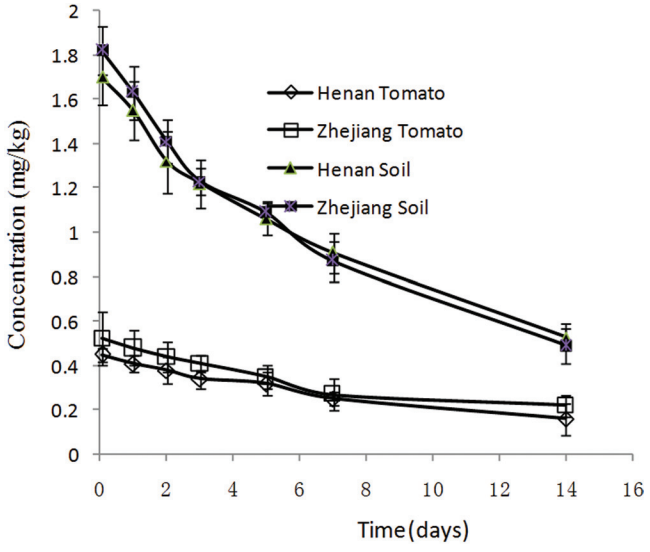

Figure 1. *Dissipation curves of azoxystrobin in two different sites under field conditions.*

ACKNOWLEDGEMENT

This work was funded by the National Nature Science Foundation of China (Grant no. 31201528) and Aid Project for the Leading Young Teachers in Henan Provincial Institutions of Higher Education of China(Grant no.2013GGJS-135).

REFERENCES

1. Kong, Z., Dong, F, Xu, J., Liu, X., Zhang, C., Li, J., Li, Y., Chen, X., Shan, W., and Zheng, Y., "Determination of difenoconazole residue in tomato during home canning by UPLC-MS/MS", *Food Control*, Vol. 23, No. 2, 2012, pp. 542–546. http://dx.doi.org/10.1016/j.foodcont.2011.08.028
2. Szpyrka, E., and Sadło, S., "Disappearance of azoxystrobin, cyprodinil, and fludioxonil residues on tomato leaves in a greenhouse", *Journal of Plant Protection Research*, Vol. 49, No. 2, 2009, pp. 204–208. http://dx.doi.org/10.2478/v10045-009-0030-4
3. Garau, V. L., Angioni, A., Del Real, A. A., Russo, M., and Cabras, P., "Disappearance of azoxystrobin, pyrimethanil, cyprodinil, and fludioxonil on tomatoes in a greenhouse", *J. Agric. Food. Chem.*, Vol. 50, No. 7, 2002, pp. 1929–1932. http://dx.doi.org/10.1021/jf011219f
4. Kondo, M., Tsuzuki, K., Hamada, H., Yamaguchi, Y., Uchigashima, M.,Saka, M., Watanabe, E., Iwasa, S., Narita, H., and Miyake, S., "Development of an Enzyme-Linked Immunosorbent Assay (ELISA) for Residue Analysis of the Fungicide Azoxystrobin in Agricultural Products", *J. Agric. Food. Chem.*, Vol. 60, No. 4, 2012, pp. 904–911. http://dx.doi.org/10.1021/jf203534n
5. Bartlett, D. W., Clough, J. M., Godwin, J. R., Hall, A. A., Hamer, M., and Parr?Dobrzanski, B., "The strobilurin fungicides", Pest Manage. Sci., Vol.58, No. 7, 2002, pp. 649–662. http://dx.doi.org/10.1002/ps.520
6. Gajbhiye, V. T., Gupta, S., Mukherjee, I., Singh, S. B., Singh, N., Dureja, P., and Kumar, Y., "Persistence of Azoxystrobin in/on Grapes and Soil in Different Grapes Growing Areas of India", *Bulletin of Environmental Contamination and Toxicology*, Vol. 86, No. 1,2011, pp. 90–94. http://dx.doi.org/10.1007/s00128-010-0170-2
7. Xu, J., Doug, F., Liu, X., Li, J., Li, Y., Shan, W.,and Zheng, Y., "Rapid Analysis of Tetraconazole Residues in Fruits and Vegetables using Ethyl Acetate Extraction and Gas Chromatography-tandem Mass Spectrometry", *Bull. Korean Chem. Soc.*, Vol. 32, No. 12, 2011, pp. 4265–4269. http://dx.doi.org/10.5012/bkcs.2011.32.12.4265
8. Vi-as, P.,; Martínez-Castillo, N., Campillo, N., and Hernández-Córdoba, M., "Liquid-liquid microextraction methods based on ultrasound-assisted emulsification and single-drop coupled to gas chromatography–mass spectrometry for determining strobilurin and oxazole fungicides in juices and fruits", *J. Chromatogr. A*, Vol. 1217, No. 42, 2010, pp. 6569–6577. http://dx.doi.org/10.1016/j.chroma.2010.08.046
9. Christensen, H. B., and Granby, K., "Method validation for strobilurin

fungicides in cereals and fruit", *Food Addit. Contam.*, Vol. 18, No. 10, 2001, pp. 866-874. http://dx.doi.org/10.1080/02652030121435

10. Wu, X., Xu, J., Liu, X., Dong, F., Wu, Y., Zhang, Y., and Zheng, Y., "Determination of Herbicide Propisochlor in Soil, Water and Rice by Quick, Easy, Cheap, Effective, Rugged and Safe (QuEChERS) Method Using by UPLC-ESI-MS/MS", *Bull. Korean Chem. Soc.*, Vol. 34, No. 3, 2013, pp. 917–921. http://dx.doi.org/10.5012/bkcs.2013.34.3.917
11. Polati, S., Bottaro, M., Frascarolo, P., Gosetti, F., Gianotti, V., and Gennaro, M., "HPLC-UV and HPLC-MS n multiresidue determination of amidosulfuron, azimsulfuron, nicosulfuron, rimsulfuron, thifensulfuron methyl, tribenuron methyl and azoxystrobin in surface waters", *Anal. Chim. Acta*, Vol. 579, No. 2,2006, pp. 146–151. http://dx.doi.org/10.1016/j.aca.2006.07.034
12. Jørgensen, L. F., Kjær, J., Olsen, P., and Rosenbom, A. E., "Leaching of azoxystrobin and its degradation product R234886 from Danish agricultural field sites", *Chemosphere,* Vol. 88, No. 5, 2012, pp. 554–562. http://dx.doi.org/10.1016/j.chemosphere.2012.03.027
13. Sevigne-Itoiz, E., Fantke, P., Juraske, R., Kounina, A., and Anton-Vallejo, A., "Deposition and residues of azoxystrobin and imidacloprid on greenhouse lettuce with implications for human consumption", *Chemosphere,* Vol. 89, No. 9, 2012, pp. 1034–1041. http://dx.doi.org/10.1016/j.chemosphere.2012.05.066
14. Utture, S. C., Banerjee, K., Dasgupta, S., Patil, S. H., Jadhav, M. R., Wagh, S. S., Kolekar, S. S., Anuse, M. A., and Adsule, P. G., "Dissipation and Distribution Behavior of Azoxystrobin, Carbendazim, and Difenoconazole in Pomegranate Fruits", *J. Agric. Food. Chem.*, Vol. 59, No. 14, 2011, pp. 7866–7873. http://dx.doi.org/10.1021/jf200525d
15. Aguilera, A., Valverde, A., Camacho, F., Boulaid, M., and Garcia-Fuentes, L., "Effect of household processing and unit to unit variability of azoxystrobin, acrinathrin and kresoxim methyl residues in zucchini", *Food Control*, Vol.25, No. 2, 2012, pp. 594–600. http://dx.doi.org/10.1016/j.foodcont.2011.11.038
16. Schirra, M., Palma, A., Barberis, A., Angioni, A., Garau, V. L., Cabras, P., and D'Aquino, S., "Postinfection Activity, Residue Levels, and Persistence of Azoxystrobin, Fludioxonil, and Pyrimethanil Applied Alone or in Combination with Heat and Imazalil for Green Mold Control on Inoculated Oranges", *J. Agric. Food. Chem.*, Vol. 58, No. 6, 2010, pp. 3661–3666. http://dx.doi.org/10.1021/jf904521f
17. Bo, H., "Determination of azoxystrobin residues in fruits and vegetables by gas chromatography/mass spectrometry with solid-phase extraction", *Chi J.Chromatogr*, Vol. 25, No. 6,2007, pp. 898–901.
18. Watanabe, E., and Miyake, S., "Quantitative analysis of fungicide azoxystrobin in agricultural samples with rapid, simple and reliable monoclonal immunoassay", *Food Chem.*, Vol. 136, No. 2, 2013, pp. 695–702. http://dx.doi.org/10.1016/j.foodchem.2012.09.001
19. Yang, X.A., and Zhang, W.B., "A novel green analytical procedure for monitoring of azoxystrobin in water samples by a flow injection chemiluminescence method with off-line ultrasonic treatment", *Luminescence*, Vol. 28, No. 5, 2013, pp. 641–647. http://dx.doi.org/10.1002/bio.2409
20. Flores, J. L., Díaz, A. M., and de Córdova, M. L. F., "Determination of azoxystrobin residues in grapes, musts and wines with a multicommuted flow-through optosensor implemented with photochemically induced fluorescence", *Anal. Chim. Acta*, Vol. 585, No. 1, 2007, pp. 185–191. http://dx.doi.org/10.1016/j.aca.2006.11.076
21. Huan, Z.B., Xu, Z., Lv, D.Z., Xie, D.F., and Luo, J.H., "Dissipation and Residues of Difenoconazole and Azoxystrobin in Bananas and Soil in Two Agro-Climatic Zones of China", *Bull Environ Contam Toxicol*, vol. 91, 2013, pp.734–738. http://dx.doi.org/10.1007/s00128-013-1128-y

A Method for Determining *Ascaris* Viability Based on Early-to-Late Stage In-Vitro Ova Development

BRADLEY W. SCHMITZ*, JENNIFER PEARCE-WALKER, CHARLES P. GERBA and IAN L. PEPPER
Water and Energy Sustainable Technology (WEST) Center, The University of Arizona, 2959 West Calle Agua Nueva, Tucson, Arizona 85745, USA

ABSTRACT: This study suggests a new method for determining the viability of *Ascaris* spp. ova, based on in-vitro early-to-late stage development of ova. This method includes stages prior to larval development, providing an estimation of potential viability. After application of biosolids onto soil and exposure to 7°C, 22°C, or 37°C for 45 days, ova were microscopically distinguished as viable or non-viable according to progression through development categories. Results were compared to viability estimates from current methods that distinguish viable ova as motile larva. Results suggest conventional techniques underestimate viability, whereas the new method provides a more conservative approach.

INTRODUCTION

ASCARIS LUMBRICOIDES is the most common roundworm infecting humans, causing 1.3 billion illnesses worldwide [1–2]. Ascariasis is endemic in areas of Africa, Latin America, and the Far East suffering from poverty and poor sanitation [1,3–4]. Particularly, wherever people defecate around settlements and in geographical regions where night soil (human faeces) is applied as an agricultural fertilizer [1,5]. Female worms produce 240,000 ova per day, all of which are passed by the infected host via faeces [1,5–8]. Soil and fecal-oral transmissions are routine as ova are deposited in high abundances, then ingested via hand-to-mouth contact from contaminated objects, or consumed with polluted crops, meat, or water [1,3,5,9–10].

Survival of *Ascaris* spp. ova after land application of biosolids can be highly variable, depending on soil composition and climate, as well as, other abiotic and biotic factors. Williams *et al.*, indicated that exposure to different soil types and temperatures influenced *A. suum* ova inactivation [11]. *Ascaris* spp. are most prevalent in tropical and sub-tropical regions, but occur worldwide in various climates [12–13]. Yet, even though developmental time depends on geographic area and climate, there is a lack of understanding of *Ascaris* spp. survival and inactivation in arid and semi-arid climates [14–15]. One objective of this study is to determine the survivability of *A. suum* ova in arid biosolid-amended soils.

Methods to extract and concentrate *Ascaris* spp. ova from biosolids via flotation and sedimentation have proven to be adequate [16–19]. However, there is not an universally accepted assay for determining viability of ova [16]. Staining techniques are rapid, as viable ova contain multiple layers that are impermeable, whereas ova that are permeable are assumed to be non-viable [20–22]. Potential infectivity is assumed at the moment ova remain impermeable. However, some slightly permeable ova are stained with a light appearance and are assumed to be non-viable [20]. Without monitoring embryo development it is unknown whether slightly stained ova were actually viable, or if some non-viable ova remained impermeable.

Real-time PCR (qPCR) may suggest viability, as signals drastically increase throughout the progression of ova development. In principle, viable ova will grow into infective larval stages that contain approximately 600 cells, with qPCR signals increasing as more cells are produced [23]. Whereas non-viable ova will remain single-celled and provide a low signal [23]. However, this method may be subjective as it incorporates total nucleic acid, without any discrepancy for infectious and non-infectious ova.

Current microscopy methods dictate viable ova as those containing motile distinguishable larvae, but all others are non-viable [16,24–27]. The Environmental Protection Agency (EPA) method classifies *Ascaris*

*Author to whom correspondence should be addressed.
Department of Civil & Environmental Engineering, National University of Singapore, Block E1A, #07-03, No. 1 Engineering Drive 2, Singapore, 117576; Phone : +65 9899 5150; Fax: +65 6779 1635; Email: bschmitz@nus.edu.sg

1544-8053/16/03 275-12

doi:10.12783/issn.1544-8053/13/4/5

spp. ova into six stages of a life cycle, labeling unembryonated ova as non-viable [17]. Yet, these methods are subject to major constraint, as they do not monitor embryo development, and/or consider all ova displaying early-stages of embryonation, prior to motile larvae, to be non-viable.

The sequential development of *A. suum* ova outside of a host has been documented into 12 stages; 1-cell, 2-cell, 3-cell, 4-cell, early-morula, late-morula, blastula, gastrula, pre-larva 1, pre-larva 2, first-stage larva (L_1), and second stage larva (L_2) [28]. Current microscopy techniques do not include these stages in the determination of viability and are underestimating the development of ova [28–29]. Cruz *et al.* suggest that early developmental stages, prior to larvae, are capable of developing into infectious stages and must be considered when determining viability [28].

The goal of the present study was to develop a methodology for enumerating the viability of *Ascaris* spp. ova with consideration to all development stages. Therefore, a new method would not assume that ova prior to containing distinguishable larvae are non-viable. Also, the requirement for motility of cell structures and/or larvae inside the ova would be disregarded, as ova that are stationary during microscopy are often viable. Such a method would provide enumeration of potential viability, revising the viewpoint of possible infection and human health risks associated with *A. lumbricoides* ova in biosolids, wastewater, compost, and soils.

In the present study, the viability of *A. suum* ova was compared utilizing the current microscopy methods and a new development-stage enumeration technique created by the authors. *A. suum* ova were used as a model for *A. lumbricoides*, as the two are morphologically and genetically similar, yet the swine type is less infectious, easier to acquire, and more resistant to environmental stresses [10,12,30–31]. Results obtained by both methods were compared to determine any significant differences between the methods.

2. MATERIALS AND METHODS

2.1. Viable and Non-Viable Ova Controls

Concentrated *A. suum* ova were purchased from Excelsior Sentinel, Inc. (Trumansburg, NY, USA), and were initially tested by both enumeration methods to ensure viability. Briefly, a suspension containing ova was serially diluted directly from the packaging to a concentration of approximately 100 ova/ml, aliquoted into 250 µl triplicates in 24-well culture plates containing equal amounts of 0.2 N H_2SO_4 (to prevent the growth of fungi), counted for total number, and examined via light microscopy for ova development throughout a 30-day incubation at ambient temperature (22°C). Viability was determined by the criteria for each enumeration technique, as described in Section 2.6.

Briefly, 227 ova were placed into a 15 ml conical tube and submerged in a water bath at 52°C for 24 hours. Then, ova were aliquoted into designated 24-well culture plates containing equal amounts of 0.2 N H_2SO_4 and observed via microscopy. The total number of viable-intact ova were examined via microscopy prior to heat exposure. The same ova were examined via microscopy post-thermal inactivation to observe non-viable morphology. Inactive ova appeared as dark-oval shapes, often containing bubbles, and did not progress in development over the incubation period (Figure 1). The resulting heat inactivation provided a control to visualize dead (non-viable) ova.

Death (D) by heat inactivation was calculated as follows:

$$D = \frac{N_d}{N_i} \times 100 \quad (1)$$

where N_d represents the number of non-viable ova after thermal inactivation, and N_i represents the number of viable ova prior to thermal inactivation. Non-viable ova were examined over 30 days at ambient temperature (22°C) to ensure no further embryonation or development.

2.2. Microcosm Preparation

Microcosms were created to simulate the decay of *A. suum* ova in arid soil amended with biosolids incubated at 7°C, 22°C, and 37°C for up to 45 days. Class B biosolids (anaerobic digestion followed by dewatering) were obtained from a local wastewater treatment plant. The mean total solids content was determined to be 6.2 ± 0.1%, (Standard Method 2540 G) [32]. The pH of the biosolid was adjusted to 7 by the addition of 1 N NaOH.

Brazito sandy loam soil was collected from the University of Arizona Agricultural Center in Tucson, AZ using a shovel down to a 6-inch depth. Soil was mixed in a capped bucket, and then large matter was separated and removed by passage through a 2 mm sieve. The mean soil moisture content was determined to be 8.4 ± 0.1 (Standard Method D2216) [33].

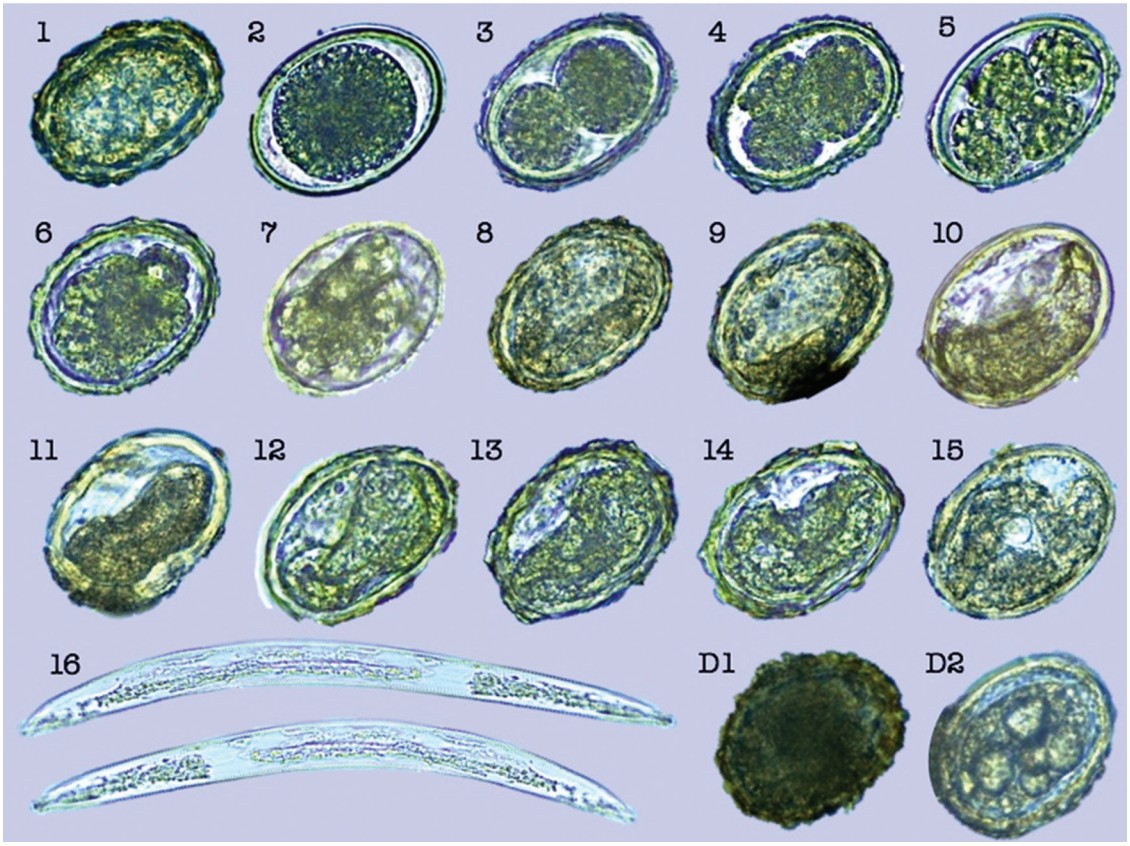

Figure 1. *A. suum ova development-stage chart for classifying ova. Unembryonated; stage 1; Embryonated, stages 2 – 7; Well-developed, stages 8 – 15; Excystation, stage 16. Dead/non-viable A. suum ova; stage D1 (disfigured dark-oval structure) and/or D2 (bubbled yolk from heat inactivation).*

Briefly, 50 µl of *A. suum* ova (3.0×10^5 ova/ml; >90% viability) was added directly to 1.5 g of Class B biosolids and mixed vigorously for several minutes in an aluminum dish to obtain a homogenous mixture of approximately 10,000 ova/g of total solids, which is the same mean concentration of night soil [5]. Using a flat spatula, the entire 1.5 g of ova-biosolid mixture was transferred to the surface of 50 g of Brazito sandy loam soil in an uncovered 50 ml beaker. The aluminum dish was rinsed with DI water to ensure the entire mixture was transferred. Then, the spatula was used to till the top few cm of the soil surface to blend in the ova-biosolid mixture. Additional deionized (DI) water was added to the biosolid-amended soil to increase the moisture content of each microcosm to approximately 22.25% (less than 25% suggested for pathogen destruction) [12,34]. A total of 48 microcosms were prepared.

2.3. Microcosm Exposure to Experimental Conditions

Triplicate microcosms were held at 7°C (refrigerator), 22°C (ambient temperature), or 37°C (incubator), and processed at time intervals of 0 (control), 5, 15, 30, and 45 days. Microcosms were not exposed to light and temperature was held constant throughout the time intervals. Ambient temperature was held constant at 22°C in a laboratory room that received pre-set automatic air conditioning without any windows or air ventilation obstructions. Temperatures were monitored via thermometers (cat no. S01639; Fisher Scientific, Waltham, MA, USA) placed alongside the microcosms. Greater than 90% moisture loss was achieved within 24 hours of incubation for samples held at 37°C, and within 48 hours for samples held at 7°C and 22°C.

2.4. Extraction of Ova from Biosolid-Amended Soil

A. suum ova were extracted from biosolid-amended soil microcosms according to a combination of modified Wisconsin and Tulane flotation methods, previously described [16,18]. The total material in each microcosm was transferred into a 250 ml polypropylene bottle, suspended in 125 ml of DI water, and agitated for 30 seconds. Then, additional DI water was added to

the bottle to create a solution volume of approximately 250 ml, and agitated for one minute. The bottle was centrifuged (Allegra® X-15R; Beckman Coulter, Inc., Brea, CA, USA) at 2383 × g for 15 minutes and the resulting supernatant was poured into a bucket containing pure bleach. The process was repeated three times, until the supernatant was clear and solids aggregated at the bottom of the bottle, to ensure sedimentation of *A. suum* ova into the pellet.

The process was repeated a fourth time with Sheather's sucrose solution (1420 ml DI water, 1.81 kg white granulated sugar, 24 ml Formalin) instead of DI water. Specific gravity of the solution was tested to be approximately 1.27 using a hydrometer. The bottle was centrifuged at 2690 × g for 30 seconds and one minute. The upper portion of the resulting supernatant, containing a Sheather's sucrose solution and *A. suum* ova mixture, was poured into stacked 63 µm (top) and 38 µm (bottom) sieves (Erie Scientific, Portsmouth, NH, USA). Large particles collected on the 63 µm sieve were rinsed with DI water into the bucket containing bleach. *A. suum* ova and other contents collected on the 38 µm sieve were rinsed with 15 ml of DI water into a 15 ml conical tube (Falcon® 352097; Becton Dickinson, Franklin Lakes, NJ, USA). The tube was centrifuged at 2690 × g for 5 minutes and the resulting supernatant was aspirated down to a 5 ml volume with a small pellet (0.1 to 0.3 ml) at the bottom. The supernatant was vortexed to dismantle the pellet and create a homogenous solution. If necessary, the solution was serially diluted with 0.2 N H_2SO_4.

To ensure the extraction process was not detrimental to ova viability, triplicate microcosms were created and inoculated with ova directly to obtain a concentration of 10,000 ova per/g. Then, the ova were extracted and viability was determined via both enumeration techniques throughout a 30-day incubation at ambient temperature in culture plates, as described below.

2.5. 30-Day Incubation and Microscopy Observations

Following extraction, 250 µl volume of concentrated ova and 250 µl of 0.2 N H_2SO_4 were added into designated 24-well culture plates (ref. no. 3526, Corning Inc., Corning, NY, USA). Each well was incubated at ambient temperature (22°C) and counted for the total number of ova after 0, 12, 15, and 30 days. Ova observations and total counts from days 0 and 30 were used to enumerate viability, as described in Section 2.6. Brief observations at days 12 and 15 were made to ensure ova remained intact, the total number of ova was consistent over time (check for human error), and there were no fungi growing in the wells. Ova were counted by scanning each well left-to-right under light microscopy (model no. 82026-630; VWR VistaVision, Radnor, PA, USA). Ova development was examined with a 100× magnification lens via light microscopy (model no. 82026-630; VWR VistaVision, Radnor, PA, USA) and confirmed with a 60× magnification image projected onto a screen via digital microscopy (EVOS XL Cell Imaging System; Advanced Microscopy Group, Bothell, WA, USA). Approximately 200 ova were collected into each well and multiplied by the appropriate serial dilution to determine the actual amount of ova contained in the original samples.

2.6. Enumeration of *A. suum* Ova Viability

Figure 2 displays how viability is determined via the conventional microscopy observations. Figure 1 displays the development stages for designating ova into categories based on the in-vitro development-stage. These techniques are described below.

2.6.1. Conventional Microscopy Technique

After the 30-day incubation in culture plates at ambient temperature (22°C), ova from each well were observed via microscopy. Ova suspected of containing a larva (Figure 2) were examined for 5–10 minutes and categorized as viable if motility was observed. Motile larvae that were currently exiting from ova (excystation) were also considered viable. All other ova, regardless of development or motility, were considered inactive and non-viable (Figure 2). Viability (V_c) was calculated as follows:

$$V_c = \frac{(N_w + N_e)}{N_t} \times 100 \qquad (2)$$

where N_w indicates the number of ova containing larvae, N_e indicates the number of motile larva with current excystation, and N_t indicates the total number of viable and non-viable ova observed.

2.6.2. In-Vitro Development-Stage Enumeration Technique

Ova observed via microscopy were distinguished based on development stages, and grouped into cat-

egories, as visually represented (Figure 1): unembryonated, cortication intact with indistinguishable cells inside (stage 1); embryonated, containing one to several individual cells (stages 2–7); well-developed, containing a distinguishable structure comprised of conglomerated cells (stages 8–15); or excystation, containing larva that was currently or had recently exited from an ovum (stage 16). These categories are based upon the 12 stages of development, previously described [28]. Ova that did not progress in development, had a dark-oval disfigured structure (Figure 1, D1), and/or contained bubbled yolk (Figure 1, D2) similar to those seen in the thermal inactivation-exposure control were considered dead/non-viable. Several visual examples of ova designated into each category are provided in the supplementary material (Figure S1 – S7).

Total counts of ova designated into each category were used to calculate the total number of ova that had progressed in development and could be considered viable. In brief, total counts of ova designated into each category via microscopy were collected during days 0 and 30 of incubation in culture plates at ambient temperature. The differences in ova assigned to each category before and after incubation were used to estimate viability. As the total number of ova increased for categories describing further development stages, the approximate number of ova capable of progressing to infectious stages could be determined. Since ova were grouped into categories, motility and development of individual ovum was not monitored. Therefore, Viability (V_d) was calculated as follows:

$$V_d = \frac{(N_{md} + N_{wd} + N_{zd}) - (N_{ui} + N_{mi} + N_{wi})}{N_t} \quad (2)$$

where N_{md} indicates the number of embryonated ova after the 30-day incubation, N_{wd} indicates the number

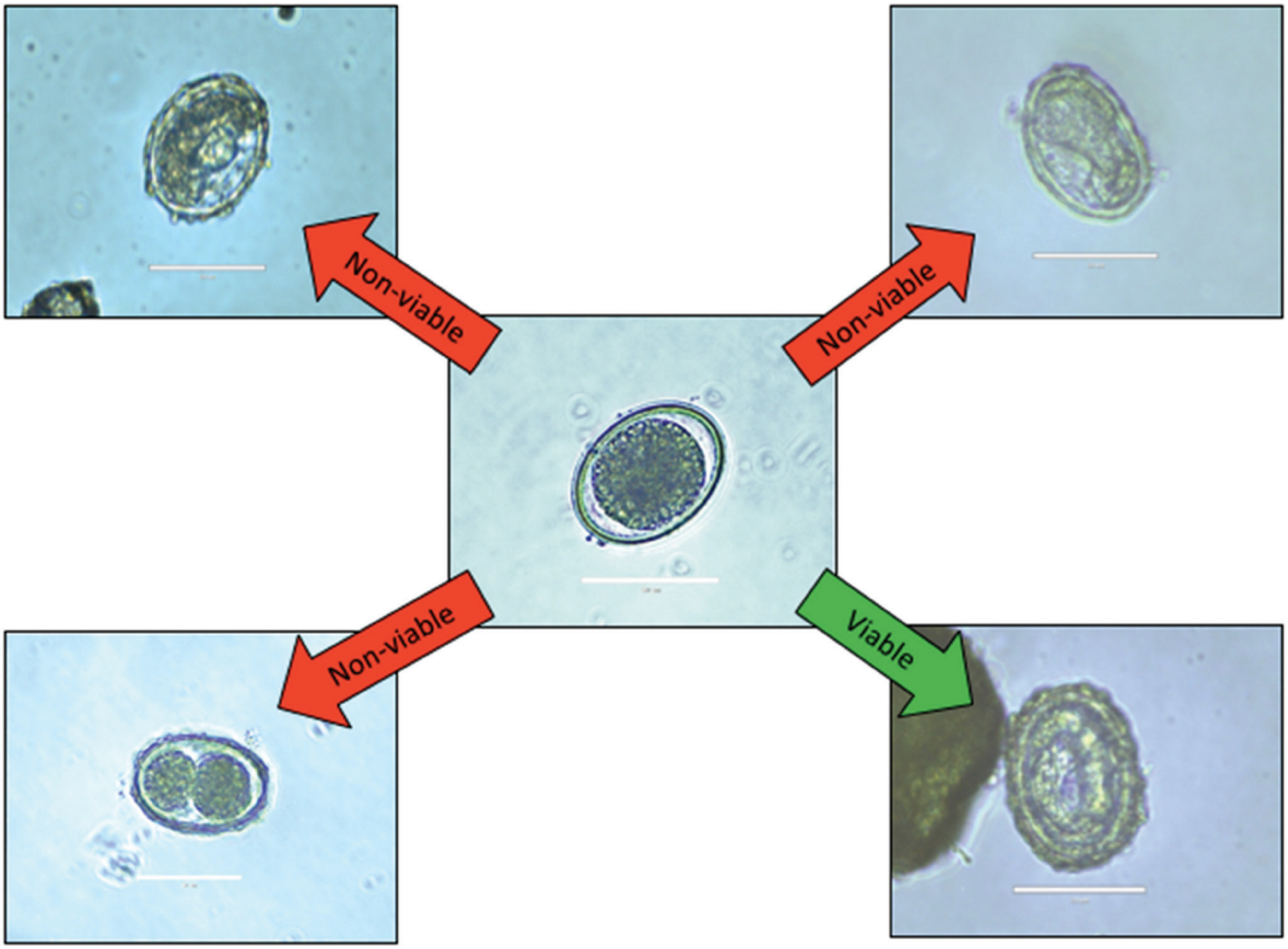

Figure 2. *Viable and non-viable ova observations determined via the conventional microscopy method. Arrows represents time elapsed between day 0 and 30 observation periods, and distinguish viable and non-viable ova based on development characteristics. Green arrows, viable; Red arrows, non-viable.*

of well-developed ova after the 30-day incubation, N_{zd} indicates the number of excyst ova after the 30-day incubation, N_{ui} indicates the number of unembryonated ova prior to incubation, N_{mi} indicates the number of embryonated ova prior to incubation, N_{wi} indicates the number of well-developed prior to incubation, and N_t indicates the total number of viable and non-viable ova.

2.7. Statistical Analysis

The number of viable ova per gram of biosolid-amended soil (V_g) was calculated as follows:

$$V_g = \frac{\left[\frac{(V_c \text{ or } V_d) \times N_i}{100}\right]}{W} \quad (4)$$

where V_c indicates the percent viability determined via the conventional enumeration method, V_d indicates the percent viability determined via the development-stage enumeration method, N_i indicates the number of ova inoculated into each microcosm, and W indicates the initial wet weight of the microcosm (soil + biosolid + *A. suum* ova + DI water).

The inactivation of viable ova per gram of biosolid-amended soil (I) was calculated as follows:

$$I = \frac{N}{N_o} \times 100 \quad (5)$$

where N is the number of viable ova after incubation, and N_o is the number of viable ova at time zero (Day 0 control).

Student's *t*-tests were performed with Microsoft Excel for Mac 2015 (Microsoft Corp., Redmond, WA, USA) to determine whether the conventional and development-stage enumeration methods resulted in significantly different numbers of viable ova per gram of biosolid-amended soil (P value was ≤ 0.05).

3. RESULTS

3.1. Viable and Non-Viable Ova Confirmations

Ova from each control were examined utilizing the conventional and development-stage enumeration techniques. Both methods verified *A. suum* purchased from Excelsior Sentinel, Inc. (Trumansburg, NY, USA), contained 98% viability (Table 1). Prior to incubation in culture plates, all ova were unembryonated. After incubation, 159 out of 162 ova developed into motile larvae and were considered viable according to the conventional method. Since these ova exhibited progression throughout the 30-day period, they were also considered viable according to the in-vitro development-stage method. Only a single ovum remained unembryonated and did not show any progression in development, so it was considered non-viable according to both methods.

Heat-exposure at 52°C for 24 hours in a water bath resulted in 226 out of 227 ova without observable viability before and after a 30-day incubation at ambient temperature. All of these ova appeared dark and often contained bubbles. Disfigured morphology and the absence of development confirmed greater than 95% inactivation (Table 1). One ovum appeared normal and was able to develop into a motile larva, so was designated as viable by both methods.

The extraction-control microcosm showed viability greater than 97% via both enumeration methods (Table 1), indicating the extraction process was not detrimental to ova that were recovered. Examinations of developmental stages and inactivated ova (Figure 1) from control samples provided visual confirmations for comparison when observing microcosm samples.

3.2. Comparison of Viability Methods

The conventional and development-stage enumera-

Table 1. Viable, Non-Viable, and Extraction Controls.

	Enumeration Technique— Mean Viability and Death	
Control	**Conventional (%)**	**Development-Stage (%)**
Prior to Exposure (Viability confirmation)	**98 ± 0.03** (159/162)	**98 ± 0.03** (159/162)
Heat Inactivation (Non-viable confirmation)	*99.5* (226/227)	*99.5* (226/227)
Extraction (Process confirmation)	**97.2 ± 0.03** (375/387)	**97.2 ± 0.03** (375/387)

Bold numbers indicate the mean viability and standard deviation of ova from triplicate control samples. Italicized numbers indicate the mean death rate of ova exposed to 52°C for 24 hours in a water bath. Numerator; total number of viable ova in the viability/process confirmation tests, or the number of non-viable ova after the heat exposure tests. Denominator; total number of ova in the control tests.

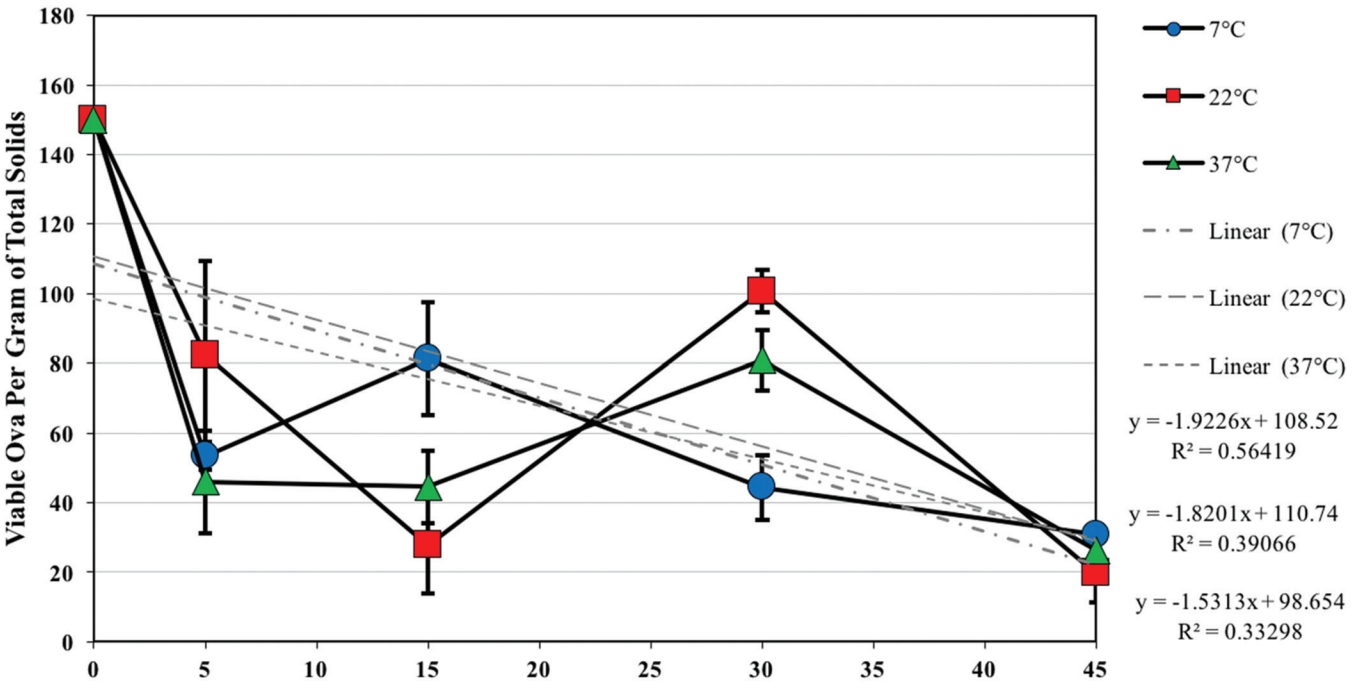

Figure 3. *Number of viable ova per gram of biosolid-amended soil enumerated via the conventional method. Viability at different temperatures (●, 7°C; ■, 22°C; ▲ 37°C). Inactivation rate determined via the slope of the best fit lines. Duration; number of days in the microcosms.*

tion methods resulted in significantly different numbers of viable ova per gram of biosolid-amended soil from the same microcosms incubated at 7°C, 22°C, or 37°C for 5 or 15 days, or 7°C for 30 days, as determined via Student's *t*-tests (*P* value ≤ 0.05) (Table 2; Figures 3 and 4). The two methods did not result in significantly different numbers of viable ova from samples that were incubated at 22°C and 37°C for 30 days, or any microcosm incubated for 45 days, regardless of temperature (Table 2; Figures 3 and 4). Enumeration via the conventional method resulted in greater inactivation and log10 reduction of viable ova in the biosolid-amended soil than the development-stage enumeration (Figures 5 and 6).

Table 2. Viability and Inactivation Based on Enumeration Methods.

		Conventional			Development-Stage			
Temperature (°C)	Time (Days)	Viable (ova/g)	Inactivation (%)	Reduction Viable (log_{10})	Viable (ova/g)	Inactivation (%)	Reduction Viable (log_{10})	*P* value
	0	150 ± 0	—	—	150 ± 0	—	—	—
7	*5*	53 ± 4	64 ± 3	1.81	111 ± 13	26 ± 8	1.40	0.002
	15	81 ± 16	46 ± 11	1.65	125 ±18	17 ± 12	1.15	0.033
	30	44 ± 9	70 ± 6	1.85	63 ± 4	58 ± 3	1.76	0.032
	45	31 ± 0	80 ± 0	1.90	39 ± 0	74 ± 0.0	1.87	—
22 (Ambient)	5	83 ± 27	45 ± 18	1.63	142 ± 20	6 ± 13	1.32	0.037
	15	28 ± 14	82 ± 9	1.91	99 ± 26	34 ± 17	1.49	0.014
	30	101 ± 6	33 ± 4	1.51	113 ± 13	25 ± 9	1.38	0.229
	45	20 ± 8	87 ± 6	1.94	22 ± 8	86 ± 5	1.93	0.771
37	5	46 ± 15	69 ± 10	1.84	130 ± 14	13 ± 9	0.99	0.002
	15	45 ± 10	70 ± 7	1.85	125 ± 23	17 ± 15	1.01	0.005
	30	81 ± 9	46 ± 6	1.66	86 ± 4	42 ± 3	1.63	0.372
	45	26 ± 7	82 ± 5	1.92	42 ± 13	72 ± 8	1.86	0.269

Mean and standard deviation viability, inactivation, and log_{10} reduction determined via the conventional and development-based enumeration methods. Temperature; indicates the degrees Celsius at which the microcosm was incubated. Time; indicates the number of days at which the microcosm was incubated. *P* value of Student's *t*-tests comparing viability (ova/g) determined via the conventional and development-stage enumeration techniques (*P* value was ≤ 0.05).

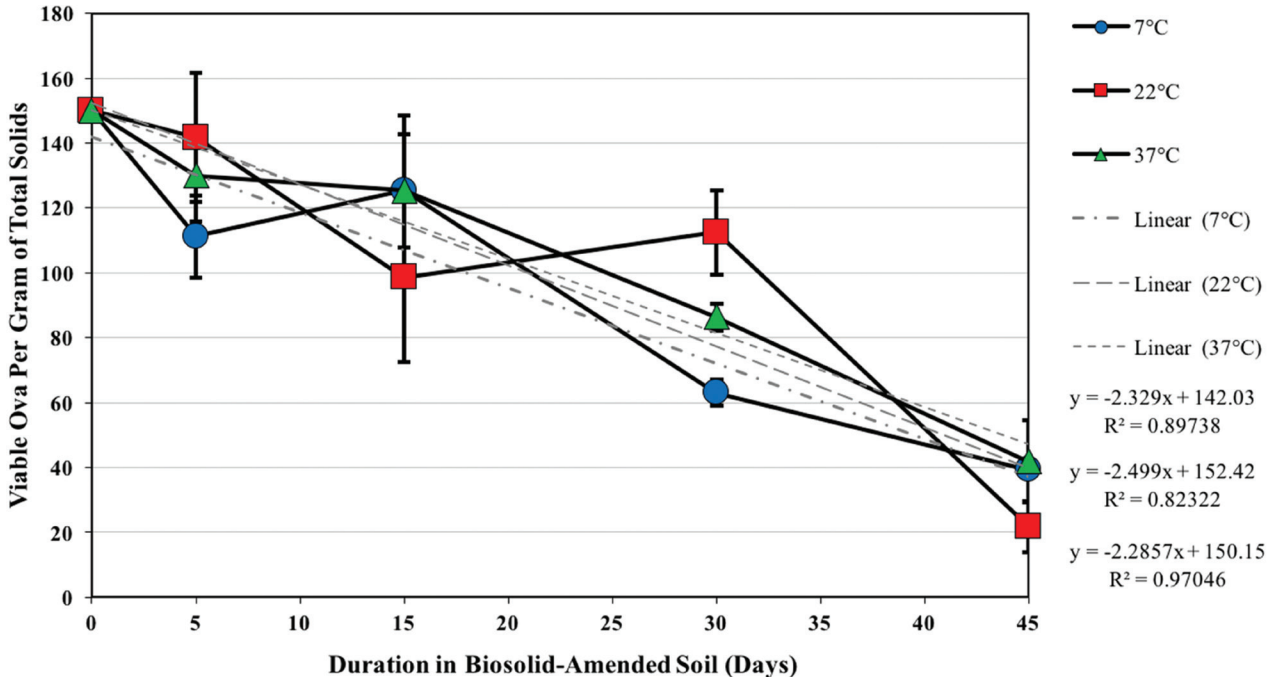

Figure 4. *Number of viable ova per gram of biosolid-amended soil enumerated via the development-stage method. Viability at different temperatures (●, 7°C; ■, 22°C; ▲ 37°C). Inactivation rate determined via the slope of the best fit lines. Duration; number of days in the microcosms.*

3.3. Temperature Effects on *A. suum* Ova Inactivation

The rate of ova inactivation was determined by the slope of the best fit line and linear regression (Figures 5 and 6). The rate of inactivation was similar at all temperatures, but was slightly greater for the development-stage method than the conventional method (Figures 5 and 6). The conventional method assumed rapid inactivation and decrease in viable ova five days after biosolids were applied onto soil (Figures 3 and 5).

4. DISCUSSION

This study created a new microscopy method that considers ova as viable, regardless of development stage, based on observations of in-vitro characteristics before and after a 30-day incubation at ambient temperature. This study also determined the survival of *A. suum*. ova in biosolids applied to arid soils. *A. suum* was used as a model organism for the development, survival, and inactivation of *A. lumbricoides*, as it is much easier to handle in the laboratory [30–31].

The new microscopy method tallies counts of ova into groups based on attributes observed via microscopy. Then, viability is enumerated based on the total number of ova that proceeded into a further development category after a 30-day incubation at ambient temperature. These ova are assumed to be capable of continuing development into infectious stages and are considered viable. This method is simple, as microscopy observations and ova counts are only needed before (day 0) and after (day 30) incubation, without the need to monitor the development of individual ova. This method is often less time consuming than the conventional microscopy method, as observing motility is not required to designate viability, which can take 5–10 minutes per ovum [28]. However, differentiating characteristics throughout ova development may be subjective and requires experience observing *Ascaris* spp. via microscopy. Results from this method were compared to the conventional microscopy technique that bases viability on motile larvae within the ova, and determined a significant difference in the assessment of viability (Student's *t*-tests P value was ≤ 0.05).

Our results suggest that the conventional method underestimates the number of potentially viable *A. suum* ova by not considering early-stages and the capability to progress into infectious stages. Microcosms containing arid soil amended with biosolids (*A. suum* inoculated) were subjected to different temperatures for 45 days. Within the first 15 days, the conventional method suggested significantly lower viability of *A. suum* ova than the development-stage method (P value was < 0.05). This was expected, as many ova in samples processed within two weeks of application onto soil

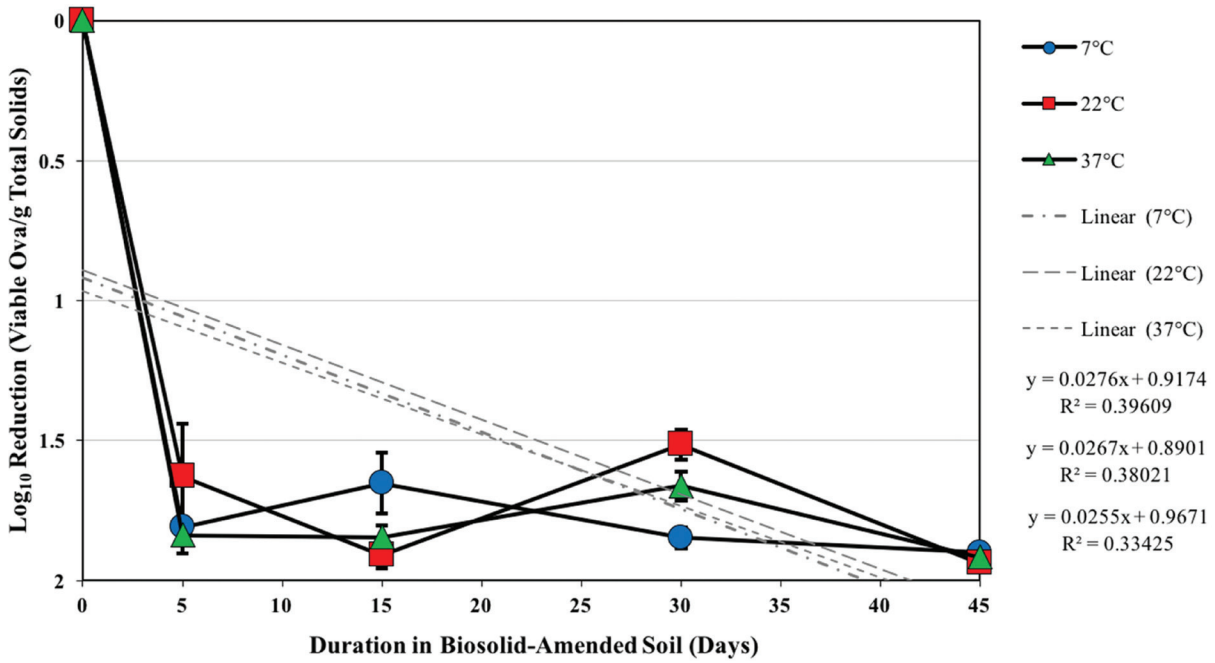

Figure 5. *Log_{10} reduction enumerated via the conventional method. Reduction at different temperatures (●, 7°C; ■, 22°C; ▲ 37°C). Inactivation rate determine via the slope of the fit lines provided in the legend. Duration; number of days in the microcosms.*

were not given enough time to form larvae, so were considered non-viable via the conventional method. Yet, the development-stage method enumerated higher viability of the same ova, by estimating the total number of ova that progressed in development, including those prior to larval stages. This enabled the assessment of viability in recently applied human fecal material, as viable and non-viable ova could be differentiated prior to the formation of larvae which usually requires more time. Consequently, the development-stage method provides a more conservative approach and is more suitable for assessing ova viability in soils recently (within 15 days) amended with biosolids and/or night soil.

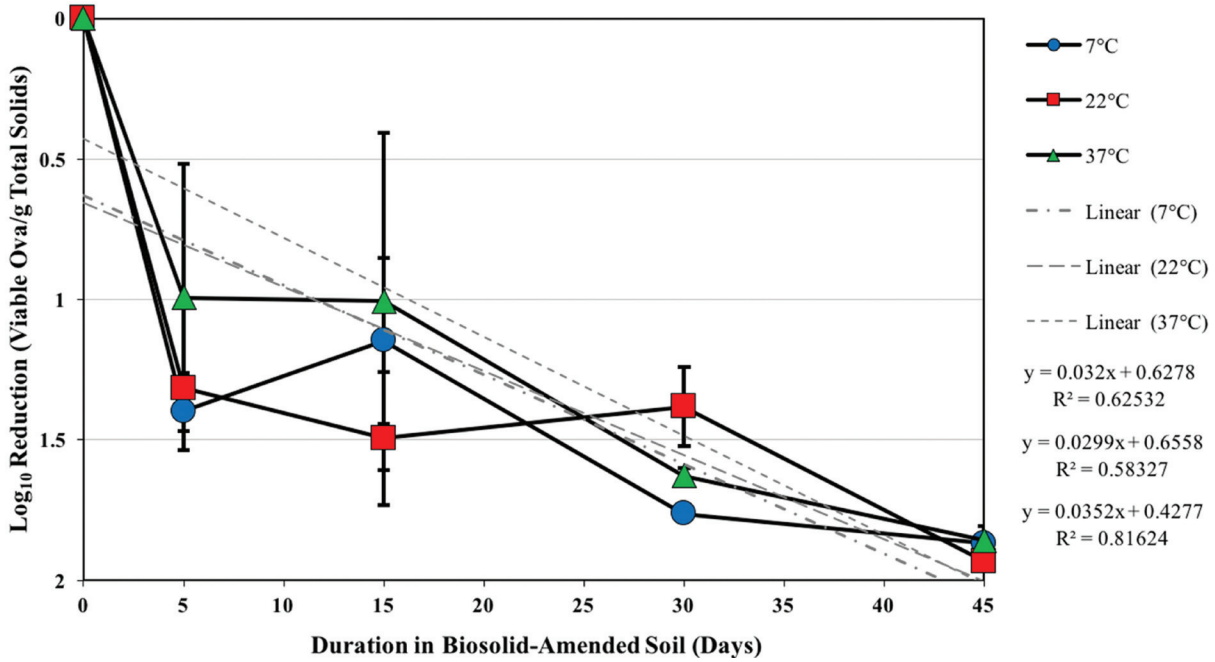

Figure 6. *Log_{10} reduction enumerated via the development-based method. Reduction at different temperatures (●, 7°C; ■, 22°C; ▲ 37°C). Inactivation rate determine via the slope of the fit lines provided in the legend. Duration; number of days in the microcosms.*

The conventional method estimated a lower number of viable ova/g of total solids in microcosms incubated longer than 15 days, except at 7°C for 30 days. However, viability assessments were not significantly different from those enumerated via the development-stage method. This was a result of environmental stresses causing increased inactivation, while slowing and/or halting development. Therefore, fewer ova were potentially viable, leading to similar assessments between the two enumeration methods. This indicates that either method may be suitable for determining ova viability in soils impacted by fecal material for more than 30 days. Yet, the development-stage technique may provide a more conservative approach, as our results indicated slightly higher numbers of viable ova/g total solids.

Practical applications for utilizing the in-vitro development-stage method are relatively unknown as this study only analyzed ova viability in arid soils amended with biosolids. We expect this method to be more applicable in tropical and sub-tropical regions where *A. lumbricoides* is prevalent and environmental conditions are favorable for ova development [12–13]. Further research is needed to determine the usefulness of this method for determining ova viability in applications other than human fecal materials applied onto agricultural soils, such as sewage sludge treatment processes.

Previous research suggests that high temperature, low moisture content, and biotic factors influence *A. suum* ova inactivation [5,15,35]. *A. lumbricoides* ova may be diminished under these conditions in the arid Southwest region of the United States. Ova have previously been reported to only survive for 2–4 weeks under dry and sunny conditions [35]. Williams *et al.*, suggested that survival within soil types is influenced by soil holding moisture ability [11]. The present study utilized the same sandy loam soil as Williams *et al.*, adjusted the moisture content to 22.25%, and created microcosms to determine *A. suum* inactivation at different temperatures. The greatest period of ova inactivation coincided with >90% moisture loss achieved within 24–48 hours, suggesting low moisture content was a major cause of ova death.

Whereas, the rate of ova inactivation seemed to be independent of temperature conditions. *Ascaris* spp. ova are typically inactivated when held at temperatures greater than 45°C (lethal temperature) for long periods of time [7]. This study exposed *A. suum* ova to conditions lower than the lethal temperature for 45 days. Accordingly, the rate of inactivation was similar for all microcosms held at 7°C, 22°C, and 37°C (Figures 5 and 6). However, our results suggest that inactivation fluctuated over time, as the number of viable ova increased in samples held at constant 22°C between 15 and 30 days, and 7°C between 5 and 15 days (Figures 5 and 6). This was most likely due to separate microcosms being processed for each time point, causing ova to be exposed to unknown inconsistencies between samples and/or extraction procedures. Nonetheless, all microcosms had similar numbers of viable ova after 45 days in land applied biosolids, suggesting that inactivation was not influenced by temperature over long periods of time.

Biotic factors that occur naturally in soil may have influenced *A. suum* ova in the microcosms. In particular, fungi may have interfered with ova development [35]. Ova extracted from microcosms were incubated in 0.2 N H_2SO_4 to prevent the growth of fungi in culture plates. However, soil was not autoclaved prior to creating the microcosms. Thus, fungi may have affected the survival and inactivation of *A. suum* ova during the simulation of contaminated land applied fecal material, especially over time. Since we did not incorporate a sterilize-soil control, we are not able to disclose the influence that biotic factors had on ova development. Therefore, we suggest that in arid soils with temperatures below 40°C, ova inactivation primarily results from low moisture content and/or biotic factors.

In conclusion, this study details a new method for assessing the viability of *Ascaris* spp. in biosolid-amended soils. This method incorporates the potential for early-stage ova to develop into infectious stages. Whereas, conventional microscopy methods underestimate viability by disregarding ova that do not contain motile larvae. When comparing the two enumeration techniques, the in-vitro development-stage method suggested significantly higher viability of ova in recently amended soils. Therefore, the in-vitro development-stage method provides a more conservative estimation of potential viability that agencies can consider when creating regulations and guidelines intended to minimize human health risks associated with *A. lumbricoides* ova in soils amended with human fecal materials. Also, this study demonstrates that ova inactivation in arid soils is primarily due to biotic factors and/or low moisture conditions.

ACKNOWLEDGEMENTS

The authors would like to thank Ms. Maria Campillo and Ms. Emily Wall for their laboratory contribution

and technical assistance. We would like to thank an anonymous wastewater treatment facility in southern Arizona for supplying biosolids and materials.

This study was supported by the National Science Foundation (NSF) Water and Environmental Technology (WET) Center, The University of Arizona. We would also like to acknowledge the NSF-WET Center for providing support to Bradley Schmitz and Jennifer Pearce-Walker during this project.

REFERENCES

1. WHO, "Prevention and control of intestinal parasitic infections", Technical report series No. 749, Geneva, Switzerland: World Health Organization, 1987.
2. de Silva, N. R., Chan, M. S., Bundy, D. A. P., "Morbidity and mortality due to ascariasis: re-estimation and sensitivity analysis of global numbers at risk", *Tropical Medicine and International Health*, Vol. 2, No. 6, 1997, pp. 519–528. http://dx.doi.org/10.1046/j.1365-3156.1997.d01-320.x
3. Jimenez, B., "Helminth ova removal from wastewater for agriculture and aquaculture reuse", *Water Science and Technology*, Vol. 55, No. 1–2, 2007, pp. 485–493. http://dx.doi.org/10.2166/wst.2007.046
4. Pecson, B. M., Nelson, K. L., "Inactivation of *Ascaris* suum eggs by ammonia", *Environmental Science and Technology*, Vol. 39, No. 20, 2005, pp. 7909–7914. http://dx.doi.org/10.1021/es050659a
5. Feachem, R. G., Bradley, D. J., Garelick, H., and Mara, D. D. 1983. *Sanitation and Disease: Health Aspects of Excreta and Wastewater Management*, New York, NY: John Wiley & Sons.
6. WHO, "Health and guidelines for the use of wastewater in agriculture and aquaculture", Technical Report Series No. 778, Geneva, Switzerland: World Health Organization, 1989.
7. Koné, D., Cofie, O., Zurbrügg, C., Gallizzi, K., Moser, D., Drescher, S., Strauss, M., "Helminth eggs inactivation efficiency by faecal sludge dewatering and co-composting in tropical climates", *Water Research*, Vol. 41, No. 19, 2007, pp. 4397–4402. http://dx.doi.org/10.1016/j.watres.2007.06.024
8. Yanko, W., "Occurrence of pathogens in distribution and marketing municipal sludges", U.S. Environmental Protection Agency, Health Effects Research Laboratory, 1988, EPA/600/S1-87/014.
9. Morales-Espinoza, E. M., Sánchez-Pérez, H. J., del Mar Garcia-Gil, M., Vargas-Morales, G., Méndez-Sánchez, J. D., Pérez-Ramirez, M., "Intestinal parasites in children, in highly deprived areas in the border region of Chiapas, Mexico", *Salud Pública de México*, Vol. 45, No. 5, 2003, pp. 379–388. http://dx.doi.org/10.1590/S0036-36342003000500008
10. Bethony, J., Brooker, S., Albonico, M., Geiger, S. M., Loukas, A., Diemert, D., Hotez, P. J., "Soil-transmitted helminth infections: ascariasis, trichuriasis and hookworm", *Lancet*, Vol. 367, 2006, pp. 1521–1532. http://dx.doi.org/10.1016/S0140-6736(06)68653-4
11. Williams, D. L., Pepper, I. L., Gerba, C. P., "Survival of *Ascaris* ova in desert soils: a risk assessment", *Journal of Residual Science and Technology*, Vol. 9, No. 4, 2012, pp. 151–157.
12. Mehl, J., Kaiser, J., Hurtado, D., Gibson, D. A., Izurieta, R., Mihelcic, J. R., "Pathogen destruction and solids decomposition in composting latrines: study of fundamental mechanisms and user operation in rural panama", *Journal of Water and Health*, Vol. 9, No. 1, 2011, pp. 187–199. http://dx.doi.org/10.2166/wh.2010.138
13. Pullan, R. L., Smith, J. L., Jasrasaria, R., Brooker, S. J., "Global numbers of infection and disease burden of soil transmitted helminth infections in 2010", *Parasites and Vectors*, Vol. 7, No. 1, 2014, pp. 1–37. http://dx.doi.org/10.1186/1756-3305-7-37
14. Darimani, H. S., Ito, R., Maiga, Y., Sou, M., Funamizu, N., Maiga, A., "Effect of post-treatment conditions on the inactivation of helminth eggs (*Ascaris* suum) after the composting process", *Environmental Technology*, Vol. 37, No. 8, 2015, pp. 920–928. http://dx.doi.org/10.1080/09593330.2015.1092587
15. Stromberg, B. E., "Environmental factors influencing transmission", *Veterinary Parasitology,* Vol. 72, No. 3-4, 1997, pp. 247–256. http://dx.doi.org/10.1016/S0304-4017(97)00100-3
16. Bowman, D. D., Little, M. D., Reimers, R. S., "Precision and accuracy of an assay for detecting *Ascaris* eggs in various biosolid matrices", *Water Research*, Vol. 37, No. 9, 2003, pp. 2063–2072. http://dx.doi.org/10.1016/S0043-1354(02)00597-3
17. U.S. EPA, "The test method for detecting, enumerating, and determining the viability of *Ascaris* ova in sludge", Environmental Regulation and Technology: Control of Pathogens and Vector Attraction in Sewage sludge. Washington, DC.: Office of Research and Development, 2003, pp. 166–172.
18. Cox, D. D., Todd, A. C., "Survey of gastrointestinal parasitism in Wisconsin dairy cattle", *Journal of American Veterinary Medical Association*, Vol. 141, No. 6, 1962, pp. 706–709.
19. Goodman, D., Haji, H. J., Bickle, Q. D., Stoltzfus, R. J., Tielsch, J. M., Ramsan, M., Savioli, L., Albonico, M., "A comparison of methods for detecting the eggs of *Ascaris*, *Trichuris*, and hookworm in infant stool, and the epidemiology of infection in Zanzibari infants", *The American Journal of Tropical Medicine and Hygiene*, Vol. 76, No. 4, 2007, pp. 725–731.
20. de Victoria, J., Galván, M., "Preliminary testing of a rapid coupled methodology for quantitation/viability determination of helminth eggs in raw and treated wastewater", *Water Research*, Vol. 37, No. 6, 2003, pp. 1278–1287. http://dx.doi.org/10.1016/S0043-1354(02)00477-3
21. Zhou, B., Li, F., Liang, J., "The use of methylene blue-eosin-borax stain in determining the viability of *Ascaris* ova", *Journal of Parasitology and Parasitic Diseases*, Vol. 3, No. 1, 1984, pp. 48–49.
22. Meyer, K. B., Miller, K. D., Kaneshiro, E. S., "Recovery of *Ascaris* eggs from sludge", *Journal of Parasitology*, Vol. 64, No. 2, 1978, pp. 380–383. http://dx.doi.org/10.2307/3279701
23. Raynal, M., Villegas, E. N., Nelson, K. L., "Enumeration of viable and non-viable larvated *Ascaris* eggs with quantitative PCR", *Journal of Water and Health*, Vol. 10, No. 4, 2012, pp. 594–604. http://dx.doi.org/10.2166/wh.2012.101
24. Pecson, B. M., Barrios, J. A., Jiménez, B. E., Nelson, K. L., "The effects of temperature, pH, and ammonia concentration on the inactivation of *Ascaris* eggs in sewage sludge", *Water Research*, Vol. 41, No. 13, 2007, pp. 2893–2902. http://dx.doi.org/10.1016/j.watres.2007.03.040
25. Manser, N. D., Wald, I., Ergas, S. J., Izurieta, R., Mihelcic, J. R., "Assessing the fate of *Ascaris* suum ova during mesophilic anaerobic digestion", *Environmental Science and Technology*, Vol. 49, No. 5, 2015, pp. 3128–3135. http://dx.doi.org/10.1021/es505807a
26. McKinley, J. W., Parzen, R. E., Álvaro, M. G., "Ammonia inactivation of *Ascaris* ova in ecological compost by using urine and ash", *Applied and Environmental Microbiology*, Vol. 78, No. 15, 2012, pp. 5133–5137. http://dx.doi.org/10.1128/AEM.00631-12
27. Nordin, A., Nyberg, K., Vinnerås, B., "Inactivation of *Ascaris* eggs in source-separated urine and feces by ammonia at ambient temperatures", *Applied and Environmental Microbiology*, Vol. 75, No. 3, 2009, pp. 662–667. http://dx.doi.org/10.1128/AEM.01250-08
28. Cruz, L. M., Allanson, M., Kwa, B., Azizan, A., Izurieta, R., "Morphological changes of *Ascaris* spp. eggs during their development outside the host", *Journal of Parasitology*, Vol. 98, No. 1, 2012, pp. 63–68. http://dx.doi.org/10.1645/GE-2821.1
29. O'Lorcain, P. O., Holland, C. V., "The public health importance of *Ascaris* lumbricoides", *Parasitology*, Vol. 121, 2000, pp. S51–S71. http://dx.doi.org/10.1017/S0031182000006442
30. Johnson, P. W., Dixon, R., Ross, A. D., "An in-vitro test for assessing the viability of *Ascaris* suum eggs exposed to various sewage treatment processes", *International Journal of Parasitology*, Vol. 28, 1998, pp. 627–633. http://dx.doi.org/10.1016/S0020-7519(97)00210-5
31. Leles, D., Gardner, S. L., Reinhard, K., I-iguez, A., Araujo, A., "Are *Ascaris lumbricoides* and *Ascaris* suum a single species", *Parasites and Vectors*, Vol. 5, No. 1, 2012, pp. 1–7. http://dx.doi.org/10.1186/1756-3305-5-42
32. Water Environment Federation. 1999. Standard methods for the examination of water and wastewater: part 1000.

33. ASTM, "Standard test methods for laboratory determination of water (moisture) content of soil and rock by mass", West Conshohocken, PA: American Society for Testing and Materials International, 1988, pp. 1–7.

34. Capizzi-Banas, S., Deloge, M., Remy, M., Schwartzbrod, J., "Liming as an advanced treatment for sludge sanitization: Helminth eggs elimination—*Ascaris* eggs as model", *Water Research*, Vol. 38, No. 14–15, 2004, pp. 3251–3258. http://dx.doi.org/10.1016/j.watres.2004.04.015

35. Nelson, K. L., Darby, J. L., "Inactivation of Viable *Ascaris* Eggs by Reagents during Enumeration", *Applied and Environmental Microbiology*, Vol. 67, No. 12, 2001, pp. 5453–5459. http://dx.doi.org/10.1128/AEM.67.12.5453-5459.2001

36. Gaasenbeek, C. P. H., Borgsteede, F. H. M., "Studies on the survival of *Ascaris* suum eggs under laboratory and simulated field conditions", *Veterinary Parasitology*, Vol. 75, No. 2–3, 1998, pp. 227–234. http://dx.doi.org/10.1016/S0304-4017(97)00198-2

Effect of Drying Method of Corn Stover on Sugar Recovery during Dilute Sulfuric Acid Pretreatment

YAN YAO[1,2], YOUSHAN SUN[3], JIAYING YU[1] and SHUTING ZHANG[1,*]

[1]*School of Environment Science and Technology, Tianjin University, Tianjin 300072, China*

[2]*School of Resources Environmental Science and Engineering, Hubei University of Science and Technology, Xianning 437100, Hubei, China*

[3]*School of Energy and Environment Science Engineering, Hebei University of Technology, Tianjin 300401, China*

ABSTRACT: The effects of drying method on the sugar conversion of corn stover during dilute sulfuric acid pretreatment were studied. Oven-dried corn stover (ODCS) was more sensitive to temperature and time during dilute sulfuric acid pretreatment than air-dried corn stover (ADCS). The yield of the total reducing sugar reached 43.9% when ODCS was pretreated for 50 min at 120°C, which was even higher than the value of the ADCS treated for 90 min. The glucose yield of ODCS was 1.6- to 1.9-fold higher than ADCS. These results indicate that rapidly losing water is a better drying method compared to air drying.

INTRODUCTION

BIOFUELS such as bioethanol and biogas are recognized as a renewable and environmentally friendly energy sources to supplement the urgent shortage of petroleum fuels [1]. Corn stover is widely used to produce biogas because of high content of carbohydrate, low cost, and abundant source. However, the binding of the main components of corn stover, namely, lignin, cellulose, and hemicellulose to each other as well as their high degree of polymerization cause barriers for the utilization [2]. Pretreatment is vital to disrupt the structures and improve the rate of production by converting biomass to fermentable sugars.

Numerous different pretreatments have been studied, such as acid, alkali, hydro-thermal, steam explosion, and enzymatic pretreatment [3]. Among them, dilute sulfuric acid pretreatment appears as the most favourable process for corn stover biomass [4]. It can give over 90% recovery of hemicellulose sugars, and accelerate the rate of subsequent cellulose hydrolysis [5]. Nevertheless, the hydrolysis efficiency of cellulose is limited during this process. Stronger reaction conditions such as higher temperature or acid concentration are required to attain more cellulose sugar recovery, thus greatly increasing the energy consumption and process investment [6]. A low-cost approach that can enhance the hydrolysis was investigated.

*Author to whom correspondence should be addressed.
E-mail: zhangst@tju.edu.cn ; Tel: +86 22 87402148

As agricultural residue, corn stover has a short annual harvest window and needs storage for sustainable utilization. Efficient storage can significantly improve the efficiency of pretreatment by influencing the character of the feedstocks [1]. To date, various storage methods have been developed based on aerobic methods as dry bales or anaerobic methods as silage [7]. Former studies denoted that wet stored corn stover could be hydrolyzed more easily than dried corn stover [8]. However, silage requests to maintain a strict anaerobic condition and takes a large land-use, which restricts its large scale applications. Dry storage is most commonly used in traditional agriculture for its facility [9]. The agricultural residues are collected and weathered at natural ambience for several days before baling. The biological activities gradually declined with the decrease of moisture, and the process lasts for a long time. These activities induce fibrosis and consumption of carbohydrate, and thereby inhibit hydrolysis in pretreatment. In view of this phenomenon, a method which can quickly volatilize the moisture is introduced in our study. Fresh corn stover is dried in an oven at moderate temperature before storage. It improves the harvest efficiency and saves the field of natural drying process. Although the method is used in lab scale sometimes, the fundamental and systematic research on evaluating the effects of drying processes on pretreatment is lacking.

Our study focused on the effects of the drying process on dilute sulfuric acid pretreatment of corn stover. Sugar recovery during pretreatment was investigated

1544-8053/16/03 287-07

doi:10.12783/issn.1544-8053/13/4/6

to estimate the effect, and physicochemical properties were discussed to ascertain the reasons. Microstructure characterizations of corn stover before and after pretreatment were measured through X-ray diffraction (XRD), Brunauer-Emmett-Teller (BET) specific surface area, Fourier transform infrared (FTIR) spectroscopy, and scanning electron microscopy (SEM).

MATERIALS AND METHODS

Materials

The corn stover, collected immediately after harvest from suburban Tianjin, China in late September 2013, was cut into approximately 2 cm pieces. The shredded corn stover was dried in a fan-assisted oven for 48 h at 60°C with the moisture of 3.27% and named oven dried corn stover (ODCS). The control group was air dried for three months at room atmosphere with 3.37% moisture and denoted ADCS. Both samples were milled with ball mill pulverizer and screened into fractions (10 to 20 mesh), then stored in zip-locked plastic bags at room temperature in preparation for analysis and pretreatment.

Methods

Dilute Sulfuric Acid Pretreatment

The raw material was pretreated with 1.0% (w/v) dilute sulfuric acid. First, 15.0 g of dry corn stover and 135.0 g of an acid solution were put into 250-mL reagent bottles, which were sealed and heated in a water bath at 80°C and autoclaved at 100°C and 120°C for 10, 30, 50, 70, and 90 min, respectively. To reduce the sugar degradation, formation of inhibitors like furfural and HMF, and operating costs in scaled up operation, pretreatment intensity was maintained at low levels. After pretreatment, the mixtures were cooled and then filtered to separate the filtrate and solid fractions. The liquid fraction was collected for carbohydrate analysis and the solid residues were thoroughly washed with deionized water and dried at 60°C to estimate the chemical compositions and microstructures. All these experiments and the following tests were performed in triplicate.

Chemical Analysis

The chemical compositions of raw and pretreated corn stover were measured by a standard analysis procedure according to the Laboratory Analytical Procedure [10]. Sugars (glucose, xylose, and arabinose) were analyzed by high performance liquid chromatography (LabAlliance WA2002SF, USA) with a refractive index detector by using a column (BioRad Aminex HPX-87H, 300 × 7.8 mm, Hercules, CA) at 65°C with 5 mM H_2SO_4 as the eluent at a flow rate of 0.6 ml/min. All liquid samples were previously autoclaved with 4 mM H_2SO_4 at 121°C for 1 h to convert solubilized sugars from oligomeric to monomeric form. The amount of total reducing sugar in liquid samples was determined by adding up the values of glucose, xylose, and arabinose. Sugar yields were calculated as follows:

$$\text{Sugar yield (\%)} = \frac{\text{Released sugar amount} \times 100}{\text{Theoretic sugar amount in native biomass}}$$

Characteristics Analysis

The BET specific surface area (SSA) and pore volume of the raw materials and pretreated solid residues were determined by N_2 adsorption isotherm applying an Autosorb-1 Volumetric System (Quantachrome Instruments, Inc. USA). The crystallinity index (*CrI*) was measured by diffracted intensity of Cu radiation (1.54 Å, 40 kV, and 200 mA) using an X-ray diffractometer (D/max 2500 XRD system, Math Co, Japan). The samples were scanned in 2θ range from 10° to 30° with a step size of 0.02°. The *CrI* was calculated by the following equation [11].

$$CrI = \frac{I_{002} - I_{am}}{I_{002}} \times 100 \quad (1)$$

where I_{002} is the intensity of the 002 peak at $2\theta \approx 22°$ and I_{am} is intensity of the background scatter measured at $2\theta \approx 18°$.

The FTIR spectra was obtained using a Nicolet 6700 FTIR (Thermo Fisher Scientific Co., USA) spectrometer with a spectral resolution of 1 cm^{-1} and over the wave length range of 600–4000 cm^{-1}. Micrographs were taken using a Philips XL-30TMP SEM (the Netherlands) using 20 KV accelerating voltage.

RESULTS AND DISCUSSION

Effect of Oven-dried Method on Dilute Sulfuric Acid Pretreatment

The total amount of sugar released can reflect the

effectiveness of acid pretreatment [12]. In this work, dilute sulfuric acid was chosen as the pretreatment catalyst, and the drying methods were evaluated by the acid pretreatment.

The yield of the total reducing sugar was shown in Figure 1(a) (varying temperature from 80–120°C at 70 min) and 1(b) (varying time from 10–90 min at 120°C). The yield of ODCS was much higher than ADCS. As shown in Figure 1(a), total sugar yield showed a significant increase with the raising temperature for both materials, which was consistent with previous result [13]. The maximum total reducing sugar yield reached 45.1% for the ODCS and 39.2% for the ADCS, respectively. This result implied that ODCS was a better raw material than ADCS for dilute sulfuric acid pretreatment. Figure 1(b) showed that the ODCS hydrolyzed more efficiently than ADCS, with higher sugar yields and shorter pretreated time, which coincided with Figure 1(a). When increasing the reaction time from 10–50 min, the reducing sugar increased evidently from 20.6–24.4 g/(100 g DM) for ODCS, and the increase became slighter after 50 min. When the residence time reached 70 min, sugar yield from the hemicellulose reached 78.6%, but the hydrolyzed cellulose did not show much change. Therefore, it seemed to be unnecessary to prolong pretreated time for ODCS after 70 min. The total reducing sugar yield of ADCS increased much more slightly than ODAS as time increased. It was 43.9% when ODCS was treated for 50 min, and it was even higher than the yield while ADCS was pretreated for 90 min. The same phenomenon was apparent when temperature was set at 80 and 100°C.

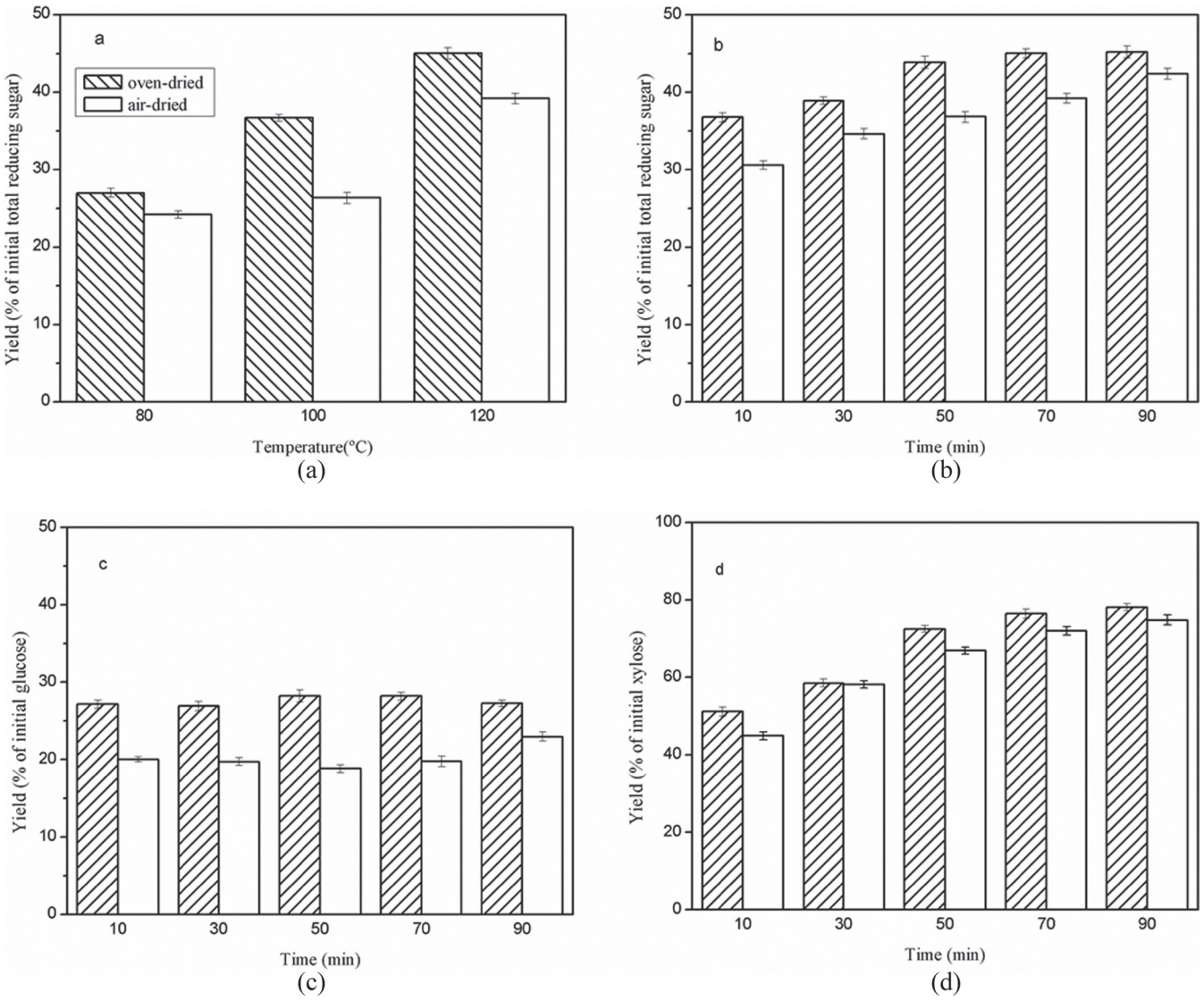

Figure 1. *Effect of (a) pretreatment temperature and (b) time on total reducing sugar yield. Effect of pretreated time on (c) glucose yield and (d) xylose yield. Data reported as average ± SD.*

In our experiment scale, nearly no furfural and HMF were detected in the hydrolysate except for being pretreated at 120°C for 90 min, with which the yield of furfural was 0.09 g/L.

According to previous literature [4], hemicellulose was one of the major solubilized components of biomass during dilute sulfuric acid pretreatment. The pretreated liquid consisted of initial water extractives and sugars hydrolyzed from the structural carbohydrate. Figures 1(c) and 1(d) exhibited the glucose and xylose yields in the pretreated liquid without original soluble sugars when reacted at 120°C. Residence time didn't have a visible effect on glucose yield because of the semicrystalline structure of cellulose. The glucose yield was 1.6- to 1.9-fold higher for ODCS than that of ADCS. Xylose yield exhibited similar trends with the total sugar yield, yet there was no significant difference between the two materials. Therefore, it could be concluded that the difference of total sugar yield between ODCS and ADCS was mainly responsible from the better cellulose hydrolysis. The physiochemical properties including chemical compositions and microstructures of the feedstock were investigated to account for the phenomenon.

Effect of Drying Process on Chemical Compositions

The chemical composition of ODCS compared with that of ADCS is listed in Table 1. The total carbohydrate contents of the two feedstocks were similar, with 64.9% for ODCS and 64.5% for ADCS in weight percent on dry basis. The glucan and lignin content were much higher than fresh corn stover (25.8% for glucan and 8.8% for lignin) for both materials, whereas the content of total nonstructural carbohydrate was obviously lower (23.9% for fresh corn stover, not shown in the table). This phenomenon could be due to the respiration of plant cells and microbial metabolism during storage [13]. Because the content of hemicellulose scarcely changed during dried procedure (13.9% for fresh corn stover), the diminished water-extractable sugars were mainly transformed into cellulose and lignin. The content of lignin for ODCS was lower than control group which indicated a lower lignified degree. The total soluble sugars in this study (17.7% for ODCS and 17.9% for ADCS) were much higher than those found in the literature (2.4–11.6%) due to the distinct climate, humidity, and breed [1,14]. It should be noted that there was little difference of glucan contents between ODCS and ADCS, the pretreatment results were mostly due to the different structures caused by the drying process.

Table 1. Chemical Composition of Oven-dried and Air-dried Corn Stover (Average ± SD).

	Content (% Dry matter)	
Component	**Oven Dried**	**Air Dried**
Glucan	31.2 ± 0.6	30.7 ± 0.3
Xylan	13.4 ± 0.3	14.0 ± 0.4
Arabinan	2.6 ± 0.1	1.9 ± 0.1
Soluble glucose	10.7 ± 0.2	9.6 ± 0.3
Soluble xylose	7.0 ± 0.2	8.3 ± 0.2
Lignin	16.3 ± 0.5	17.3 ± 0.4
Ash	5.9 ± 0.1	6.1 ± 0.2
Others	12.9 ± 0.5	12.1 ± 0.4

Effect of Drying Process on Physical Properties of Crystallinity

Crystallinity is believed to be an important feature affecting the efficiency of pretreatment [15], and it was distinctly changed during dried process. The *CrI* of ODCS before treatment was 47.97%, and it was much lower than ADCS (53.43%). Since the content of cellulose for ODCS was nearly the same with ADCS, it could be concluded that the content of no-crystalline cellulose for ODCS was higher than ADCS, and the amorphous cellulose could be easily broken down by dilute acid [15]. Which caused ODCS hydrolyzed more effectively than ADCS. The *CrI* was increased after pretreatment because of the solubilization of amorphous components, which was accordant with other authors [11]. The *CrI* of ODCS pretreated by dilute sulfuric acid at 120°C for 70 min was 61.9%, while it was 63.7% for ADCS under the same conditions. It indicated that although pretreatment raised the *CrI*, the trend of *CrI* was consistent before and after pretreatment.

BET Analysis

Surface properties and porous structures of lignocellulosic materials have some correlation with hydrolysis [17]. Table 2 showed that the SSA and pore volume of ODCS (1.79 ± 0.03 m^2/g for SSA and 0.57 ± 0.01 $c.c.10^{-2}/g$) were much smaller than ADCS (3.95 ± 0.11 m^2/g for SSA and 1.26 ± 0.04 $c.c.10^{-2}/g$). For ODCS, water was lost rapidly and resulted in capillary shrinkage and collapse of pores in the micro-structure. The hydrolysis with dilute acid pretreatment of ODCS was

Table 2. Specific Surface Area (SSA), Pore Volume, and Average Pore Size of Untreated and Pretreated Biomass (Average ± SD).

	SSA (m^2/g)	Pore Volume ($c.c.10^{-2}/g$)	Pore Size (102 Å)
UODCS	190	5.4	6.32
PODCS	210	4.9	9.1
UADCS	190	6.7	8.5
PADCS	170	5	6.87

UODCS: unpretreated oven dried corn stover
PODCS: pretreated by dilute sulfuric acid at 120°C for 70 min of oven dried corn stover
UADCS: unpretreated air dried corn stover
PADCS: pretreated by dilute sulfuric acid at 120°C for 70 min of air dried corn stover

better than ADCS, which implied that SSA and pore volume shouldn't be the only reason to influence hydrolysis. Average pore size should be brought into consideration. Sulfuric acid hydrolysis increased the SSA, pore volume, and pore size, except for SSA of ADCS. This was due to the hydrolysis of cellulose and hemicellulose and the removal of some lignin. The reduced SSA of pretreated ADCS might be due to broken capillaries. Partial capillaries were expanded or vanished during the pretreatment, which improved the average pore size but reduced the SSA. The SSA of ODCS is increased because of the formation of micropores during the pretreatment. The treatment can not only break some capillaries to make them expand or vanish, but also form some micropores in ODCS. The multiaperture structure made it more conductive for the following use such as enzymatic hydrolysis.

FTIR Analysis

The FTIR spectrum analysis was used to evaluate the structural constituents and was showed in Figure 2. The bands at 3340 and 2930 cm^{-1} were associated with hydrogen bonds and methylene of cellulose, which were related to typical cellulose [18]. The absorption peak of ODCS was weaker than ADCS, which implied that ODCS had less content of crystalline cellulose and explained the lower crystallinity. Furthermore, untreated ODCS represented a stronger adsorption peak at 900 cm^{-1} than ADCS, which related to amorphous cellulose [1]. The intensity showed a decrease after pretreatment for both materials at this peak, and the reduction was larger for ODCS than ADCS. It indicated that main cellulose reduction was attributed to amorphous cellulose and explained the better cellulose hydrolysis of ODCS. Peaks around 1200 to 1000 cm^{-1} demonstrated the linkages between lignin and hemicellulose [19]. The intensities of these peaks were also weaker for untreated ODCS. This suggested that hemicellulose of ODCS could hydrolyze quickly, which was in accordance with the experimental results.

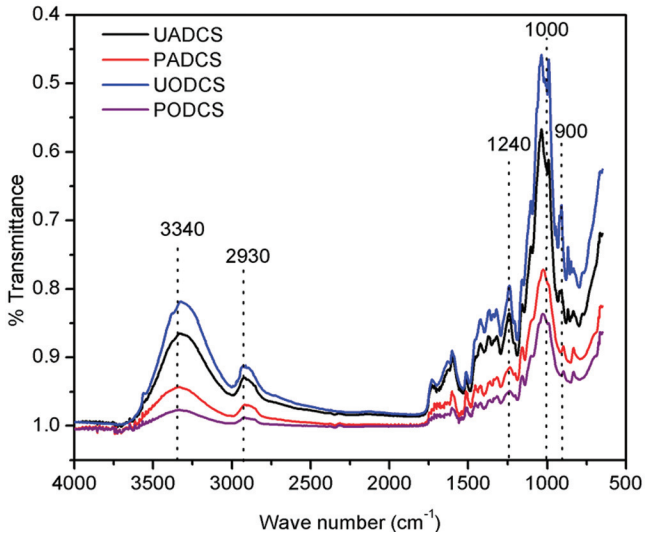

Figure 2. *FTIR spectra of two kinds of untreated corn stover and solid residues after pretreatment at 120°C for 70 min.*

Scanning Electron Microscopy Analysis

The SEM images are shown in Figure 3. Untreated corn stover had smooth surfaces and showed highly ordered fibrils. Few holes and cracks existed on the surface of ODCS due to the shrinkage, which resulted from the quick loss of water. Biomass after pretreatment revealed some holes on the surface and it denoted that hemicellose and lignin were removed during pretreatment [15]. There were more and larger holes for ODCS compared with ADCS, which proved that the hemicellose and lignin of ODCS could be removed effectively. The chemical composition of the pretreatment residuals was analyzed, and compared to raw materials, the lignin contents were decreased 28.96% and 20.4% for ODCS and ADCS respectively. Some droplets appeared on the surface of the pretreated biomass, illustrating that some lignin melted during pretreatment and agglomerated on the surface.

CONCLUSIONS

The drying process affects the hydrolysis efficiency of dilute acid pretreatment by influencing the characteristics of corn stover. Corn stover that rapidly lost water in the oven with moderate temperature was more

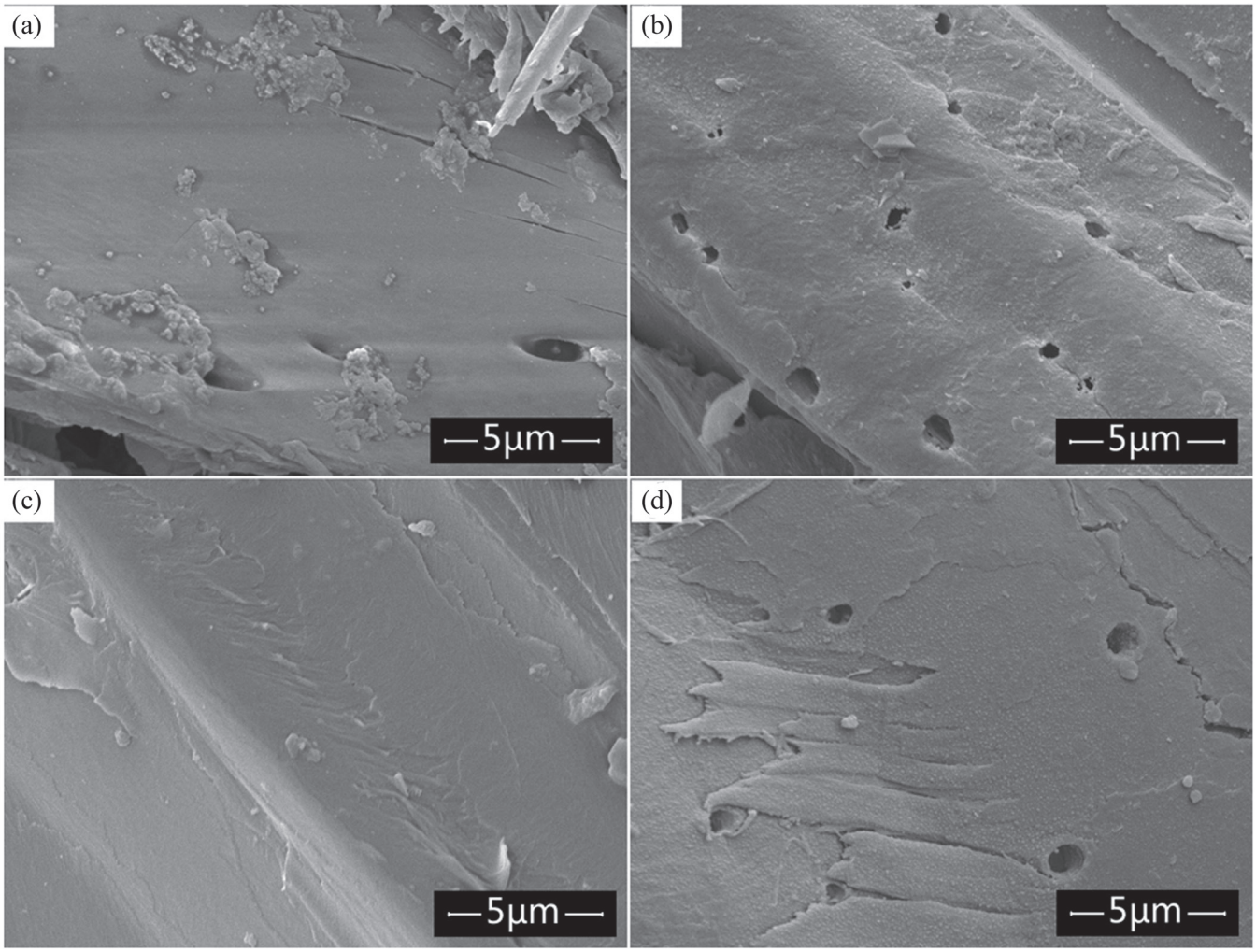

Figure 3. *SEM images for (a) untreated corn stover of ODCS, (b) ODCS pretreated at 120°C for 70 min, (c) untreated corn stover of ADCS, and (d) ADCS pretreatment at 120°C for 70 min.*

sensitive to temperature and time than natural air-dried stover when was pretreated with dilute sulfuric acid. The maximum yield of total reducing sugar reached 45.1% for oven-dried corn stover, and was 39.2% for air-dried corn stover. The glucose yield of ODCS was 1.6- to 1.9-fold higher than that of ADCS after pretreatment. The OCDS had lower crystallinity and relatively more amorphous cellulose structure. Therefore, the OCDS could be hydrolyzed by dilute sulfuric acid easily and effectively, which indicates that oven drying was more attractive than air drying for corn stover.

ACKNOWLEDGMENTS

We are grateful to Prof. Yimin Zhang for use of their HPLC facilities. Thanks to Dr. Yingte Li and Qian Li for helping prepare raw corn stover samples.

REFERENCES

1. Liu, Z. H., Qin, L., Jin, M. J., Pang, F., Li., B. Z., Kang, Y., Dale, B. E., and Yuan, Y. J., "Evaluation of storage methods for the conversion of corn stover biomass to sugars based on steam explosion pretreatment", *Bioresoure Technology*. Vol. 132, 2013, pp. 5–15. http://dx.doi.org/10.1016/j.biortech.2013.01.016
2. Wang, R. J., Sun, Y. S., Zhang, S. T., and Lu, X. B., "Two-step pretreatment of corn stalk silage for increasing sugars production and decreasing the amount of catalyst", *Bioresource Technology*, Vol. 120, 2012, pp. 290-294. http://dx.doi.org/10.1016/j.biortech.2012.06.025
3. Yang, Y., Ratna, S. S., Burns, J. C., and Cheng, J. J., "Dilute acid pretreatment of oven-dried switchgrass germplasms for bioethanol production", *Energy & Fuels*, Vol.23, No. 7, 2009, pp. 3759–3766.
4. Alvira, P., Tomás-Pejó, E., Ballesteros, M., and Negro, M. J., "Pretreatment technologies for an efficient bioethanol production process based on enzymatic hydrolysis: A review", *Bioresource Technology*, Vol. 101, No. 13, 2010, pp. 4851–4861. http://dx.doi.org/10.1016/j.biortech.2009.11.093
5. Avci, A., Saha, B. C., Kennedy, G. J., and Cotta, M. A., "Dilute sulfuric acid pretreatment of corn stover for enzymatic hydrolysis and efficient ethanol production by recombinant Escherichia coli FBR5 without detoxification", *Bioresource Technology*, Vol. 142, 2013, pp. 312–319. http://dx.doi.org/10.1016/j.biortech.2013.05.002

6. Talebnia, F., Karakashev, D., and Angelidaki, I., "Production of bioethanol from wheat straw: An overview on pretreatment, hydrolysis and fermentation", *Bioresource Technology*, Vol. 101, No.13, 2010, pp. 4744–4753. http://dx.doi.org/10.1016/j.biortech.2009.11.080
7. Pakarinen, A., Maijala, P., Jaakkola, S., Stoddard, F. L., Kymalainen, M., and Viikari, L., "Evaluation of preservation methods for improving biogas production and enzymatic conversion yields of annual crops", *Biotechnology for Biofuels*, Vol. 4, No. 20, 2011, pp. 1–13. http://dx.doi.org/10.1186/1754-6834-4-20
8. Tanjore, D., Richard, T. L., and Marshall, M. N., "Experimental methods for laboratory-scale ensilage of lignocellulosic biomass", *Biomass & Bioenergy*, Vol. 47, 2012, pp. 125–133. http://dx.doi.org/10.1016/j.biombioe.2012.09.050
9. Williams, S. D., and Shinners, K. J., "Farm-scale anaerobic storage and aerobic stability of high dry matter sorghum as a biomass feedstock", *Biomass and Bioenergy*, Vol. 46, 2012, pp. 309–316. http://dx.doi.org/10.1016/j.biombioe.2012.08.010
10. Sluiter, A., Hames, B., Ruiz, R., Scarlata, C., Sluiter, J., and Templeton, D., "Determination of sugars, byproducts, and degradation products in liquid fraction process samples", NREL/TP-510-42623, Laboratory Analytical Procedure (LAPs), National Renewable Energy Laboratory, Golden, CO. 2008, Issue Date: 12/08/2006
11. Hsu, T. C., Guo, G. L., Chen, W. H., and Hwang, W. S., "Effect of dilute acid pretreatment of rice straw on structural properties and enzymatic hydrolysis", *Bioresource Technology*, Vol. 101, No. 13, 2010, pp. 4907–4913. http://dx.doi.org/10.1016/j.biortech.2009.10.009
12. Jung, Y. H., I. J. Kim, H. K. Kim, and K. H. Kim., "Dilute acid pretreatment of lignocellulose for whole slurry ethanol fermentation", *Bioresource Technology*, Vol.132, 2013, pp.109–114. http://dx.doi.org/10.1016/j.biortech.2012.12.151
13. Luo, X., and Zhu, J. Y., "Effects of drying-induced fiber hornification on enzymatic saccharification of Lignocelluloses", *Enzyme and Microbial Technology*, Vol. 48, No. 1, 2011, pp.92–99. http://dx.doi.org/10.1016/j.enzmictec.2010.09.014
14. Yang, B., and Wyman, C. E., "Pretreatment: The key to unlocking low-cost cellulosic ethanol", *Biofuels Bioproducts & Biorefining*, Vol. 2, No.1, 2008, pp. 26–40. http://dx.doi.org/10.1002/bbb.49
15. Li, C. L., Knierim, B., Manisseri, C., Arora, R., Scheller, H. V., Auer, M., Vogel, K. P., Simmons, B. A., and Singh, S., "Comparison of dilute acid and ionic liquid pretreatment of switchgrass: Biomass recalcitrance, delignification and enzymatic saccharification", *Bioresource Technology*, Vol. 101, No. 13, 2010, pp. 4900–4906. http://dx.doi.org/10.1016/j.biortech.2009.10.066
16. Kumar, R., Mago, G., Balan, V., and Wyman, C. E., "Physical and chemical characterizations of corn stover and poplar solids resulting from leading pretreatment technologies", *Bioresource Technology*, Vol. 100, No. 7, 2009, pp. 3948–3962. http://dx.doi.org/10.1016/j.biortech.2009.01.075
17. Barakat, A., Vries, H. D., and Rouau, X., "Dry fractionation process as an important step in current and future lignocellulose biorefineries: A review", *Bioresource Technology*, Vol. 134, 2013, pp. 362–373. http://dx.doi.org/10.1016/j.biortech.2013.01.169
18. He, Y., Pang, Y., Liu, Y., Li, X., and Wang, K., "Physicochemical characterization of rice straw pretreated with sodium hydroxide in the solid state for enhancing biogas production", *Energy Fuels*, Vol. 22, No. 4, 2008, pp. 2775–2781. http://dx.doi.org/10.1021/ef8000967
19. Pang, F., Xue, S. L., Yu, S. S., Zhang, C., Li, B., and Kang, Y., "Effects of combination of steam explosion and microwave irradiation (SE-MI) pretreatment on enzymatic hydrolysis, sugar yields and structural properties of corn stover", *Industrial Crops and Products*, Vol. 42, 2013, pp. 402–408. http://dx.doi.org/10.1016/j.indcrop.2012.06.016

Analytical Pyrolysis Study of Peanut Shells using TG-MS Technique and Characterization for the Waste Peanut Shell Ash

XIWEN YAO[1], KAILI XU[1,*] and YU LIANG[2]
[1]*College of Resources and Civil Engineering, Northeastern University, Shenyang, Liaoning 110819, China*
[2]*College of Information Science and Engineering, Northeastern University, Shenyang, Liaoning 110819, China*

ABSTRACT: As an agricultural waste produced from the processing of peanut, the yield of peanut shells in China is quite abundant. Although numerous studies on the pyrolysis of peanut shells have been carried out, most of them were focused on the dynamics models for predicting kinetics parameter of biomass, and rarely on the evolution of gaseous products in pyrolysis. This study carried out a set of experiments on the pyrolysis of peanut shells under different heating rates in order to fill the knowledge gap. Besides, there is also a lack of information available concerning the characterization of resulting peanut shell ash. Thus, the aim of this study is to investigate the pyrolysis behaviors of peanut shells thoroughly and to characterize the properties of peanut shell ash that serves as predictors for its applications. The results show that the decomposition of peanut shells follows a stepwise mechanism, and the activation energy calculated by Flynn-Wall-Ozawa method varies from 58.3 to 88.6 kJ·mol^{-1}. Compared with low heating rate, fast heating rate at low temperatures is more suitable for biogas production. Chemical and phase analysis shows that peanut shell ash has a high SiO_2 content except for other oxides (K_2O, CaO, MgO, Al_2O_3, etc.) that quite suitable in glass production, implying its potential for glass production and as a mineral admixture in concrete. Released volatile matters in pyrolysis create many pores in carbonaceous materials, thus low-cost adsorbents can be produced from these carbon residues.

INTRODUCTION

FACING with the increasing energy needs, especially for the environmental benign energy, the biomass waste, as a renewable source of energy, is of great potentiality [1]. The amount of available biomass residues for conversion into renewable fuels and value-added products is quite immense. Finding an environmental and sustainable method for utilization of biomass waste has become a critical problem in many agricultural countries. The biomass waste can be considered as a zero net CO_2 energy source, because the CO_2 generated by biomass combustion can be absorbed and recycled from the atmosphere by replanting harvested biomass [2]. The use of biomass thus makes no contribution to the increase of CO_2 in the atmosphere [3]. During the past decade, harnessing energy from biomass has grown tremendously [4]. Converting biomass residues via thermo-chemical conversion to produce clean fuels is significant, especially in the agricultural countries [5].

Moreover, biomass consists of carbohydrates, lignin, proteins, fats, and other chemicals (such as vitamins, dyes, and flavors), so the integrated valorisation and exploitation of all biomass fractions in different applications within the biorefinery concept proposed by Femando *et al.* [6] is also of great importance. Until now, many researches have been suggesting that all biomass fractions can be isolated from biomass and utilized for synthesis of various useful chemicals. For example, Noor *et al.* [7] reported that the cellulose isolated from cotton gin waste can be used for the synthesis of carboxymethyl cellulose. Wang *et al.* [8] suggested that lignin can be used as a template for the synthesis of porous carbon-CeO_2 composites, and Vilela *et al.* [9] carried out the first investigation on the use of lipophilic extracts from the ripe pulp of ten banana cultivars. In addition, vegetable oils from biomass residues have been widely used as renewable raw materials in many applications, including adhesives, paints, coatings, plasticizer, detergents, and lubricants [10].

Energy production from biomass depends on the biomass biodegradability and conversion process. Currently, harnessing energy from biomass mainly focuses

*Author to whom correspondence should be addressed.
Email: kaili_xu@aliyun.com; Tel: +86-024-83678405

1544-8053/16/03 295-11

doi:10.12783/issn.1544-8053/13/4/7

on thermo-chemical conversion [11]. Among these processes, gasification can efficiently convert biomass to a variety of gaseous fuels [12]. As a sub-category of gasification, pyrolysis plays a key role in gasification [13]. For predicting the qualities of gaseous products released in gasification, mathematical model needs the knowledge of pyrolysis kinetics [4]. Thermogravimetry - mass spectroscopy (TG-MS) appears to be a promising solution to study biofuel pyrolysis [14,15]. In pyrolysis, heavier hydrocarbons can be cracked giving rise to lighter ones, which is the greatest interest as their heating values are high [16]. Here, it is important to note that for comparing their heating values, they are unified to present in the same unit (kJ/kg or kJ/Nm^3). The inorganic minerals left after thermo-chemical process are biomass ashes, which are often regarded as waste materials of little value. Thus, it is meaningful to study the ash characterization to offer a basic reference for transforming it into value-added goods.

Peanut is an important and common oil crop which is planted extensively in the world. During the processing of peanut, large volumes of peanut shells (PS) can be generated, requiring an economical and environmental disposal. Until now, several reports have been suggesting that the PS can be used as raw materials for activated carbons and can be used to absorb metal ions. For example, Wilson *et al.* [14] reported that adsorbents developed from PS can serve as a replacement for commercial carbons in the adsorption of selected metal ions, such as Cu^{2+}, Ni^{2+}, Pb^{2+}, etc. Wafwoyo *et al.* [17] studied the use of acid-modified PS as metal ion adsorbents from aqueous solutions. Furthermore, due to its high calorific value, the PS is suggested to be highly suitable for use as an alternative to fossil fuels [18]. Much research have been also addressed the combustion of PS [18-21]. Duan *et al.* [19] investigated the combustion characteristics of crushed and pelletized PS in a pilot-scale vortexing fluidized bed combustor with flue gas recirculation [19], while Arromdee and Kuprianov [20] characterized the combustion performance of PS in a conical fluidized-bed combustor, and they also compared the thermal and combustion reactivity of peanut and tamarind shells [21]. Recently, numerous studies on PS pyrolysis have been carried out, most of which were focused on dynamics models to predict the kinetics [12,13,15,17,22,23]. The research conducted by Zhu *et al.* [13] is related to hydrolysis and pyrolysis of PS. Ferreiro *et al.* [22] studied the impact of heating conditions on the kinetics parameter of PS. Braz *et al.* [24] studied the pyrolysis properties of six lignocellulosic biomass. Wang *et al.* [12] explored the impact of alkali metal compounds on PS pyrolysis. Chen *et al.* [25] suggested that the pyrolysis of PS are excellent due to its substantial volatile matter.

Although the variety of researches have focused on the pyrolysis of PS, and the impacts caused by various influencing factors such as atmosphere and heating rate are obtained, only few studies were focused on the emission of gaseous products during the pyrolysis of PS [26]. No researches were found in previous literature, which used mass spectroscopy (MS) to study the impacts of heating rates on gaseous products released during the pyrolysis. So, a series of experiments on PS pyrolysis under various heating rates were conducted to fill the knowledge gap. Thus, this work quantitatively studies the emission behaviors of some typical non-condensable gases (such as CO, CO_2, CH_4, and H_2), together with the thermo-physical properties in the pyrolysis of PS. Besides, the characterization of resultant PSA were also studied in detail using a series of qualitative and quantitative methods.

EXPERIMENTAL

Biomass Materials

Prior to experiments, the PS samples were collected from the countryside of Shenyang, northeast China. Firstly, the samples were dried at 105 ± 0.5°C for 24 h in an oven, then grinded and pulverized with a rotary cutting mill, finally sieved with a 100 mesh sieve. Those passed through the sieve (< 0.154 mm in size) were gathered in a closed container and kept for next analyses. Here, it should be noted that the influence of different collection periods on the primary characterization of PS samples can be negligible since the characterization of different biomass mainly depends on the variety and geographic location, and rarely on the collection periods. Besides, as mentioned before, all the PS samples used in this study have been pretreated in a unified procedure prior to experiments using a series of experimental methods. All experimental process presented in this study can be replicated, and the results shown can be largely reproducible.

The volatile matter, moisture and ash content in PS were measured by 5E-TG800 Rapid Proximate Analyzer of Kaiyuan Apparatus Company, China. The fixed carbon content in the proximate analysis was determined by subtracting the total sum of volatile matter, moisture and ash content from 100%. The biomass samples used for determining the content of volatile matter were about 0.5 g in each test while the samples

used for the moisture and ash content were about 1 g. Ultimate analysis was analyzed by Vario MACRO Elemental Analyzer of Elementar, Germany, and each test uses about 100 mg biomass samples. The low heating value of PS was measured by 5E-C5508 calorimeter of Kaiyuan Apparatus Company, China, and each test uses 1 ± 0.1 g samples.

Pyrolysis Experiments

The thermogravimetric analysis (TGA) of biomass was conducted in a sensitive thermal balance (NETZCH-STA449 F3, Germany) at the heating rates of 5, 10, 20°C/min up to a final temperature of 1200°C. During the pyrolysis, high purity helium (99.99%) at a flow velocity of 30 mL/min was utilized as the carrier gas. The sensitivity was 1 µg and 0.01°C, and about 5 mg PS samples were pyrolyzed for each test. A quadrupole mass spectrometer (QMS 403D, Pfeiffer Vacuum Technology, Germany) coupled to the thermal balance was employed for gas evolution analysis.

Kinetic Models

In this study, the kinetic analysis of the pyrolysis of PS samples is based on the rate equation of decomposition of solids [27]:

$$\frac{d\alpha}{dt} = A\exp\left[\frac{-E}{RT}\right] f(\alpha) \tag{1}$$

where $d\alpha/dt$ denotes the rate of the process, α is conversion rate, and it is defined as $(w_0 - w)/(w_0 - w_f)$, w_o, w_f and w are the biomass weight at the starting, end, and at a specific time t, respectively. A is the pre-exponential constant ($s - 1$), E stands for the activation energy (kJ·mol^{-1}), R is the universal gas constant (8.314 J·K^{-1}·mol^{-1}), $f(\alpha)$ represents the function of conversion, which is expressed by:

$$f(\alpha) = (1-\alpha)^n \tag{2}$$

where n is the reaction order.

Substituting Equation (2) into Equation (1), the expression of reaction rate is therefore transformed into the next equation:

$$\frac{d\alpha}{dt} = A\exp\left[\frac{-E}{RT}\right](1-\alpha)^n \tag{3}$$

For non-isothermal reactions, the linear heating rate $\beta = dT/dt$ is incorporated in Equation (3), and then Equation (4) can be derived:

$$\frac{d\alpha}{dT} = \frac{A}{\beta}\exp\left[\frac{-E}{RT}\right](1-\alpha)^n \tag{4}$$

In this study, an integral method of kinetic analysis, namely Flynn-Wall-Ozawa (FWO) method was used for calculating activation energy. FWO method is an integral iso-conversional technique, which involves taking logarithms of both sides of Equation (4), and integrating these with respect to α and T variables and using the approximation of Doyle the following expression is obtained [28]:

$$\ln\beta \cong \log\left[A\frac{E}{R_g(\alpha)}\right] - 2.315 - 0.4567\left[\frac{E}{RT}\right] \tag{5}$$

Thus, the plot of ln(β) *versus* 1/T for various heating rates allows to obtain parallel lines for a fixed degree of conversion, $g(\alpha)$ is the integral form of the $f(\alpha)$. The slopes of these lines are proportional to activation energy. The activation energy is determined by the slopes of such plots which give $-0.4567E/R$ at different heating rates, and the analysis was focused on the process with conversion ranging from 0.1 to 0.8.

Preparation of Biomass Ash

So far, there is no specified standards that are available for preparing biomass ashes in China. Through comparison of biomass ashes obtained at different temperatures, previous literature [29–31] suggested that 600°C was the optimal ashing temperature for determining the properties of biomass ash. Hence, in this experimental study, the ashing temperature of the PS materials was set at 600°C according to ASTM standards in America (ASTM E1755-01). The prepared PS samples (particle size < 0.154 mm) were first put in a Muffle furnace (SX2-15-12, Dongtai Shuangyu Instruments Co. Ltd., Jiangsu, China), and then they were kept for 2 hours at 600°C under free air.

Determination of Ash Characterization

The chemical composition of PSA was obtained using X-ray fluorescence (XRF) (ZSX100e. Rigaku Co., Japan). The main crystalline minerals present in the ash were determined by an X-ray diffractometer (XRD) (X'Pert PRO, PANalytical B.V., Netherlands). Scanning electron microscopy (SEM) (Ultra Plus, Carl

Zeiss Co. Ltd., Germany) and energy dispersive X-ray (EDX) (Genesis, Edax DX-4) at an accelerating voltage of 20-30 kV were used to obtain information of the morphological structure and the elemental composition of the surface of ash particles.

RESULTS AND DISCUSSION

Thermogravimetric Characterization of PS

Table 1 summarizes the results of PS, which is the average value of three tests. Here, it is worth of notice that the proximate analysis was done on received basis while the ultimate analysis was based on air dried basis. Figures 1(a) and 1(b) respectively shows the TG curves and the DTG curves obtained for PS under helium. The main characteristic parameters determined from TG and DTG profiles for various heating rates are listed in Table 2.

As observed from the TG curves in Figure 1(a), the thermal decomposition of PS follows a three-step stepwise mechanism. The first weight loss mainly occurs below about 220°C, and as seen from Figure 1(b), this initial weight loss is accompanied by a distinct shoulder peak at around 100°C standing for the weight loss rate. Analyzing these behaviors, the weight loss that occurs around 200°C is mostly related to the initial pyrolysis of hemicellulose and lignin [32]. Specifically, at temperatures below 200°C, the evaporation of unbound moisture in the PS also can make a great contribution to the weight loss variation within 70 to 140°C.

The second pyrolysis stage is located within 220 to 450°C, in which the maximum weight loss rate appears, as can be seen in Figure 1(b), and the high devolatilization of hemicellulose, cellulose, and lignin can be achieved in this temperature zone [33]. Furthermore, the largest weight loss of PS takes place in this pyrolysis stage [Figure 1(a)]. Besides, with the increment of heating rate, the temperature corresponding to the maximum decomposition rate shows a tendency to shift towards a higher temperature region, and this is in good agreement with Cao *et al.* [34], who reported that a shift on the DTG curves to higher temperature zones during the pyrolysis of corn cob could be clearly observed as the heating rate was increased.

Table 1. Primary Characterization of PS Materials.

Proximate Analysis (wt.%)		Ultimate Analysis (wt.%)	
Moisture	1.16	C	46.15
Volatile Matter	71.36	H	5.62
Ash	6.81	O	38.25
Fixed Carbon	20.67	N	1.89
Low Heating Value (MJ/kg)	16.52	S	0.12

When the temperature is higher than 450°C, it also can be found that the decomposition of the PS proceeds at a slow rate, which is associated to the pyrolysis of lignin at high temperatures. The slow pyrolytic process was almost complete after approximately 600°C, which is basically consistent with the pyrolysis mechanism of drying sewage sludge. As for DTG [Figure 1(b)], the weight loss rate above 450°C is close to zero, indicating the weight loss in the third stage can be neglected.

As shown in Table 2, the starting temperature (T_s) and the peak temperature (T_{max}) of the main weight loss, the temperature of full width at half maximum ($\Delta T_{1/2}$), the maximum weight loss rate $(dw/dt)_{max}$, and the mean weight loss rate $(dw/dt)_{mean}$ all increase with the increment of heating rate, and the total weight loss (W_t) arrives at 66.62%, 68.45%, and 69.37% when the heating rate is 5, 10, and 20°C/min, respectively. Thus, from the above analyses, it can be inferred that the pyrolysis with a fast heating rate at low temperatures is suitable for gasification in the actual production.

Activation Energy Analysis

The linear plot of $\ln(\beta)$ against $1/T$ is displayed in Figure 2. The calculated activation energies using Equation (5) for the FWO method are presented in Table 3.

As seen from Figure 2, the activation energy obviously increases with the increment of conversion rate. Moreover, the linear and parallel relationships can be

Table 2. Characteristic Parameters from the Thermal Degradation Curves of PS Biomass.

Heating Rate (β) (°C/min)	Starting Temperature (T_s) (°C)	Peak Temperature (T_{max}) (°C)	Temperature of Full Width at Half Maximum ($\Delta T_{1/2}$) (°C)	Maximum Weight Loss Rate $(dw/dt)_{max}$ (%/min)	Mean Weight Loss Rate $(dw/dt)_{mean}$ (%/min)	Total Weight Loss (W_t) (%)
5	153.8	332.4	69.6	–3.687	–0.0555	66.62
10	187.5	342.3	73.5	–6.454	–0.0570	68.45
20	216.4	352.8	76.7	–12.021	–0.0578	69.37

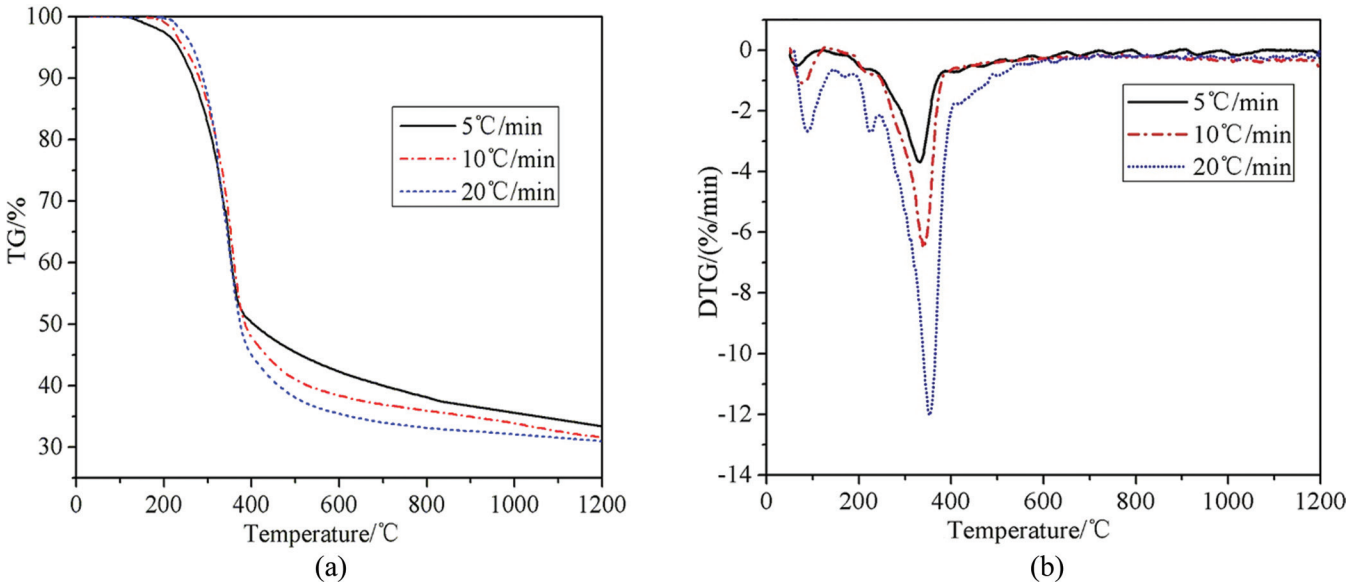

Figure 1. *Thermogram curves of the prepared PS samples (a) TG curves, (b) DTG curves.*

clearly seen, which indicates the activation energies at different conversion rates.

Besides, the results in Table 3 show that the values of activation energy of PS calculated from the FWO method are within the range of 58.3–88.6 kJ·mol^{-1}, and the average activation energy is approximately 65.61 kJ/mol. Because the active energy is a function of reaction mechanism rather than a function of heating rate and conversion rate, thus the increase of activation energy with conversion can be attributed to the shift in reaction mechanisms. In other words, the increase of activation energy with conversion increasing implies that the PS pyrolysis is a complex process consisting of some different reactions. The reaction mechanism varies greatly with conversion changing. A further study on what mechanism resulted in the change of activation energy will be conducted in the next work. The R^2 correspond to linear fittings are greater than 0.98, meaning a good linear dependence.

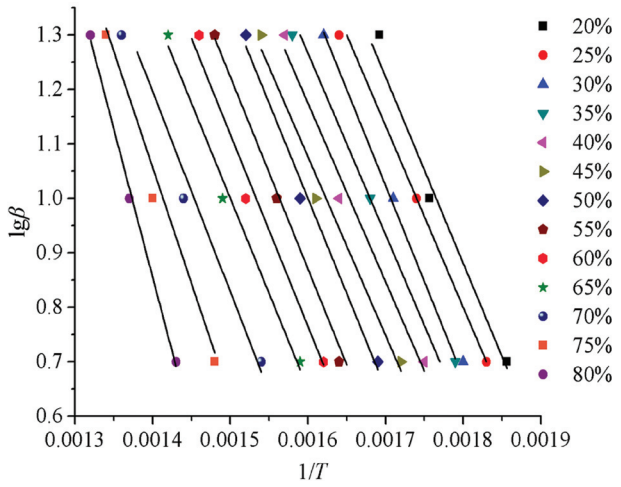

Figure 2. *Arrhenius plots at selected conversion rates by FWO method.*

Mass Spectroscopy Analysis

Here, taken pyrolysis under the heating rates of 10 and 20°C/min as examples, the emission concentration for typical non-condensable gases (mainly including CO, CO_2, CH_4, and H_2) in the pyrolysis of PS are described in Figure 3.

As seen from Figure 3(a), the emission of CO takes place with no distinct releasing peaks in the whole pyrolysis process. Specifically, as for the case of 20°C/min, the emission of CO is much higher than that of 10°C/min case, which indicates that higher heating rate is more suitable for CO releasing. According to literature [35], most of the CO is released from the cracking of carboxyl (C=O) and carbonyl (C–O–C)

Table 3. Activation Energy of PS (R^2, the Square of the Correlation Coefficient).

α/%	E/kJ·mol^{-1}	R^2	α/%	E/kJ·mol^{-1}	R^2
20	58.3098	0.9866	55	64.1773	0.9989
25	59.2739	0.9987	60	64.8709	0.9915
30	59.6990	0.9971	65	65.4076	0.9922
35	60.6815	0.9874	70	66.8652	0.9872
40	62.3070	0.9896	75	75.4784	0.9865
45	63.5843	0.9870	80	88.6143	0.9945
50	63.6066	0.9966	Mean	65.6058	0.9918

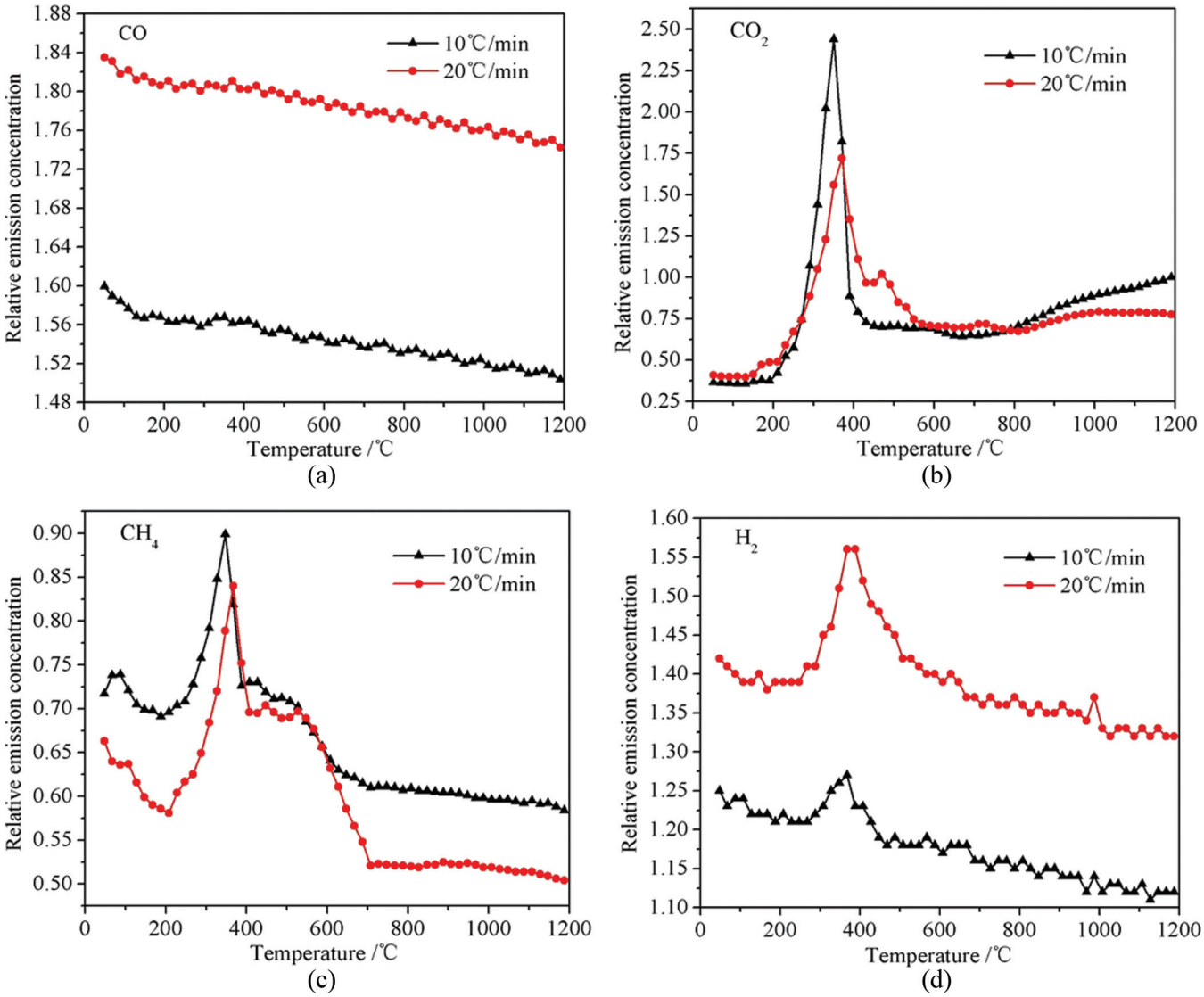

Figure 3. *Evolution of typical non-condensable gases with temperature rising during the pyrolysis of PS.*

during the pyrolysis of lignin and hemicellulose beyond 600°C.

As seen from Figure 3(b), the CO_2 emission under 10 and 20°C/min exhibits a conspicuous emission peak within 200–500°C. Besides, the CO_2 releasing profile in case of 10°C/min is similar to that case of 20°C/min, and the CO_2 evolution is concentrated beyond 200°C. At low temperatures (< 500°C) the abundant C=O chemical groups existing in hemicellulose was verified to favour CO_2 production while above 500°C the lignin pyrolysis made a little contribution for it [15].

According to Figure 3(c), the evolution of CH_4 during the pyrolysis of PS is mostly concentrated between 200 and 600°C, which corresponds well to the weight loss shown in Figure 1. Moreover, it needs to be noted that the CH_4 emission in the case of 10°C/min has two releasing peaks. The first peak with low concentration is at around 100°C while the second one with higher concentration shifts to higher temperatures (200–400°C). Liu *et al.* [36] demonstrated that lignin is rich in methoxyl-O-CH_3 chemical groups. Therefore, the CH_4 emission is most likely generated

Table 4. Chemical Composition of PSA Determined by XRF Analysis (wt.%).

SiO_2	K_2O	Na_2O	CaO	MgO	SO_3	P_2O_5	Fe_2O_3	Al_2O_3	TiO_2	Cl
56.38	10.40	0.67	8.26	4.92	3.42	2.46	3.87	8.73	0.51	0.24

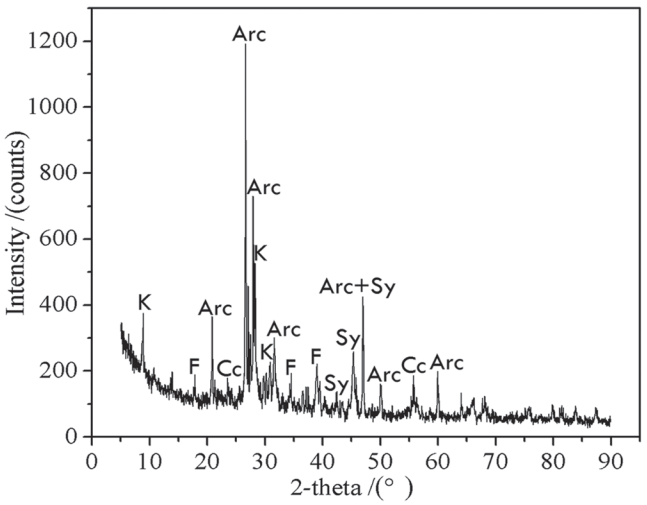

Figure 4. *XRD pattern of PSA. Arc, arcanite (K_2SO_4); Cc, calcite ($CaCO_3$); F, fairchildite ($K_2Ca(CO_3)_2$); K, kalicinite ($KHCO_3$); Sy, sylvite (KCl).*

through the cracking of methoxyl-O-CH_3 during the pyrolysis of lignin below 600°C.

With regards to H_2, its emission mainly focuses at low temperatures (around 50–600°C), as can be observed in Figure 3(d), and its emission concentration reaches the maximum peak at around 300–500°C. Similar to the CO emission, the emission concentration of H_2 under 20°C/min is also relatively higher with respect to the case of 10°C/min. After 600°C, the H_2 emission slightly decreases with the increment of temperature, indicating that the H_2 emission was mostly produced during the pyrolysis of cellulose and hemicellulose. This result is basically in agreement with Wu *et al.* [23], who suggested that the highest H_2 concentration was obtained for the thermal pyrolysis of cellulose and hemicellulose in the absence of the catalyst.

Chemical and Phase Analysis of PSA

The elemental oxides in PSA measured by XRF are listed in Table 4. The XRD results are shown in Figure 4. In this study, all elements (except Cl) were converted to oxides. The Cl was translated into equivalent oxygen, then all these constituents were normalized to 100%.

As can be observed from the results in Table 4, the PSA samples are mainly composed of SiO_2, K_2O, CaO, and Al_2O_3. Besides, lesser amounts of Na_2O, MgO, SO_3, P_2O_5, Fe_2O_3, TiO_2, and Cl were also detected. Specifically, the proportions of alkali metal oxide K_2O (10.40%) is much higher than that of other compounds except SiO_2 (56.38%), and it was verified by XRD results (see Figure 4), which displayed the presence of potassium in the predominant crystalline phases, such as arcanite (K_2SO_4), fairchildite ($K_2Ca(CO_3)_2$), kalicinite ($KHCO_3$), and sylvite (KCl). Furthermore, calcium was mainly identified in the crystalline form of calcite ($CaCO_3$). Additionally, the presence forms of alkali earth metals (such as Ca and Mg) with relatively high content are likely to be metal cation ions connected with oxygen functional groups [28].

Besides, the composition results indicate that the SiO_2 content occupies an absolutely dominant position in the composition. However, with regards to silica, it was not detected in any form of crystalline phases, as can be observed from Figure 4, which indicates that the silica is most likely present in the amorphous SiO_2.

SEM-EDX Analysis of PSA

Prior to SEM-EDX analysis, a metal spraying treatment of biomass ash is quite necessary since the electrical conductivity of fly ash is poor [38]. After that, the morphology and surface composition of the ash were obtained by SEM-EDX analysis. Figure 5 shows the SEM images of PSA at various magnifications. The EDX spectra in spots a-c in Figure 5 are shown in Figures 6(a), 6(b), and 6(c), respectively.

As seen from Figure 5(a), most of these obtained PSA particles are in irregular shapes, and their size ranges from approximately 1 to 150 μm. Figure 5(b) shows the details of the selected zones of some typical PSA particles at higher magnification. The EDX spectrum of spot a [Figure 6(a)] exhibits a high peak of carbon, which implies that there still exists unburned carbon residues in the PSA.

Figure 5(c) exhibits the original and fibrous texture of a piece of large ash particle with a particle size greater than 100 μm, which further indicates the inadequate combustion of PS at 600°C. In addition, many small pores can be found throughout this particle. As determined by EDX analysis, the spectrum of point b [Figure 6(b)] on the surface of the large ash particle presents a high content of elements C, Si, and O, and this result exactly consists with the composition results earlier, further verifying that amorphous SiO_2 is predominant in PSA.

Figure 5(d) shows details of the external surface of a typical PSA particle. At a closer examination of this image, many small granules can be observed. The EDX results of point c [Figure 6(c)] show that the surface of the granules is particularly rich in potassium and chlorine, indicating that these small granules are covered with KCl, and this is consistent with the earlier

XRD data, from which most of KCl present in the ash has been regarded as sylvite.

Potential Applications of PSA

Based on the composition results, it seems that the PSA is the combination of silica and metallic oxides, similar to the raw materials used for silicate ceramics production in the traditional ceramic industry. Moreover, considering that the PSA has a appreciable content of SiO_2 except for other oxides (such as K_2O, CaO, MgO, Al_2O_3, etc.) that quite suitable in glass production, we can conclude that the PSA can be potentially utilized as a silica source for producing high quality glasses. Also, the significant presence of high SiO_2 content can make the ash have a possibility to be used as a mineral admixture in concrete production and other applications.

Besides, a large quantity of nutrient elements (such as K, Ca, and P) indicates the potential of PSA to be used as a fertilizer or a soil amendment in agriculture. Specifically, the high proportion of CaO (8.26%, see Table 4) in PSA makes it possible for SO_2 capture, basically the same to ash residues generated from the oleoresin industries in India [37]. Furthermore, the released volatile matters during the pyrolysis of PS created a large amount of pores in the carbonaceous materials, thus some low-cost adsorbents can be produced from the carbon residues separated from PSA. Particularly, the suitability of PSA as a precursor for producing activated carbon has been justified by chemical activation with H_3PO_4 [38]. To clarify, as far as our literature survey could ascertain, no available studies about the percentage of the raw PSA material used in different industries per year have been published. Thus, it is hard to provide a believable estimation of the necessities

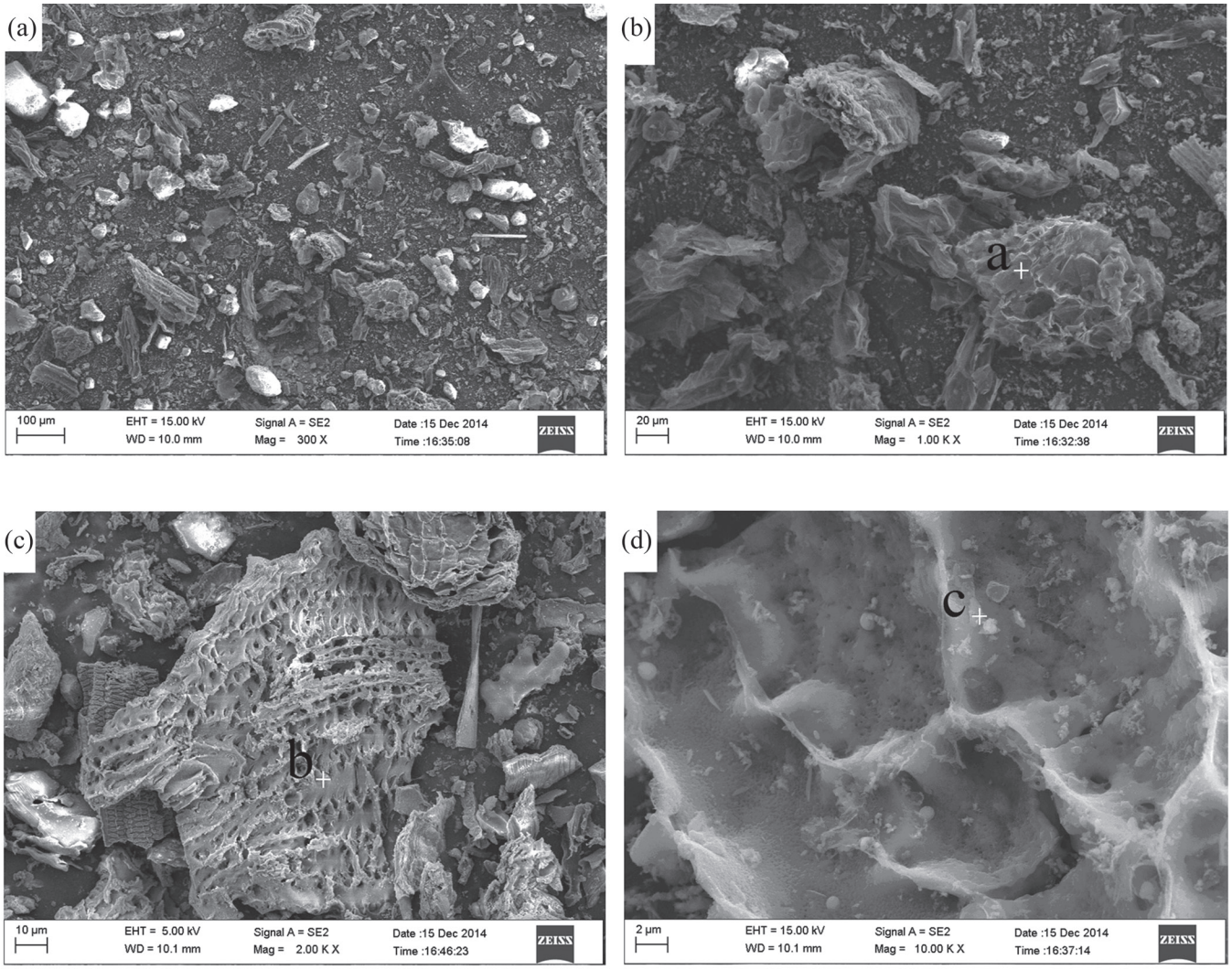

Figure 5. *SEM images at different magnifications of the PSA obtained at 600°C.*

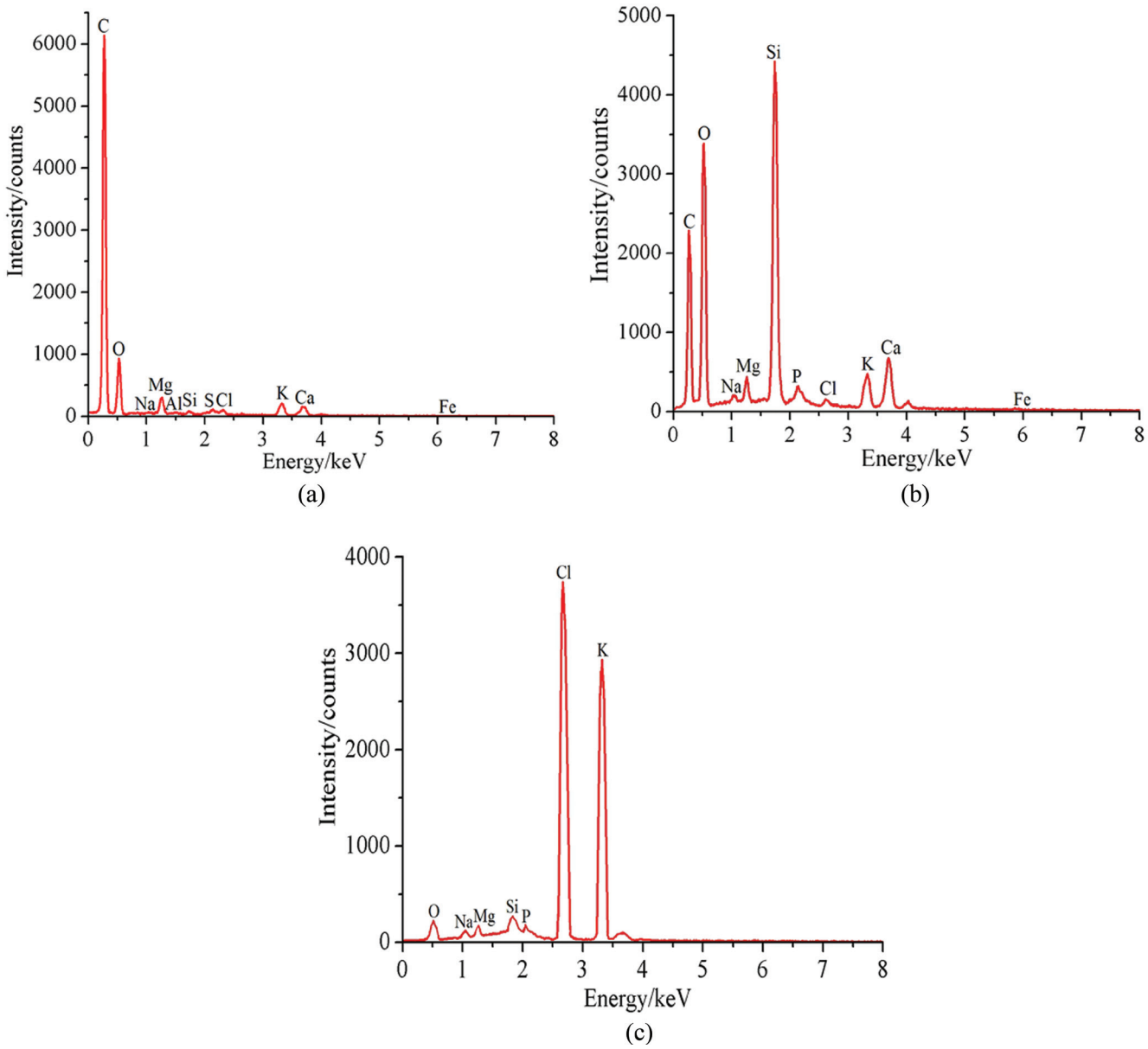

Figure 6. *Spectra of EDX spot analyses in points a-c.*

that could be covered in each one of the suggested industries at present. But with the rapid development of biomass utilization technology, it can be predicted that a reliable estimation of the percentage of PSA used per year in each one of these above mentioned industries will be provided in the near future.

In addition, as determined by XRF analysis, the prepared PSA is devoid of toxic metals, so the ceramic products developed from the ash such as ceramic membrane can be potentially used for clarification or separation in various industries [39]. But such applications are still a ways off, as these applications have not yet been tested on the PSA, needing to be further explored in the near future.

CONCLUSIONS

1. The thermogravimetric analysis of peanut shells indicates that the decomposition of this agricultural waste follows a stepwise mechanism. The starting and peak temperature of main weight loss, the temperature of full width at half maximum, the maximum and mean weight loss rate, and the total weight loss all increase with the increase of heating rate. The activation energy calculated by Flynn-Wall-Ozawa method varies from 58.3 to 88.6 $kJ \cdot mol^{-1}$.
2. During the pyrolysis of peanut shells, the emission concentration of CO and H_2 under 20°C/min was

higher than that case of 10°C/min. The evolution of CO_2 and CH_4 were mainly concentrated above 200°C, corresponding well with the biomass weight loss. The results indicate that high heating rate is suitable for producing biogas.

3. The peanut shell ash has an appreciable content of SiO_2 except for other oxides (K_2O, CaO, MgO, Al_2O_3, etc.) that quite suitable in glass production, indicating its potential as a source for producing high quality glasses and as a mineral admixture in concrete production. Being rich in nutrient elements, the peanut shell ash can also be used as a soil amendment.
4. The peanut shell ash particles are in irregular shapes with size ranging from 1 to 150 μm. Some carbon residues due to inadequate conversion of biomass still exists in the ash. The released volatile matters in pyrolysis create many pores in carbonaceous materials, indicating the potential of carbon residues from peanut shell ash to be used for low-cost adsorbent.

ACKNOWLEDGEMENTS

This work was supported by the Rural Energy Comprehensive Construction Found of the ministry of agriculture of China (No. 2015-36).

REFERENCES

1. Mazlan, M.A.F., Uemura, Y., and Osman, N.B., *et al.*, Fast pyrolysis of hardwood residues using a fixed bed drop-type pyrolyzer, *Energy Conversion and Management.*, Vol. 98, 2015, pp. 208–214. http://dx.doi.org/10.1016/j.enconman.2015.03.102
2. Mikulcic, H., Berg, E.V., and Vujanovic, M., *et al.*, Numerical study of co-firing pulverized coal and biomass inside a cement calciner, *Waste Management & Research*, Vol. 32, No. 7, 2014, pp. 661–669. http://dx.doi.org/ 10.1177/0734242X14538309
3. Mckendry, P., Energy production from biomass (part 1): Overview of biomass, *Bioresource Technology*, Vol. 83, No. 1, 2002, pp. 37–46. http://dx.doi.org/10.1016/S0960-8524(01)00118-3
4. Kumar, A., Wang, L.J., and Dzenis, Y.A., *et al.*, Thermogravimetric characterization of corn stover as gasification and pyrolysis feedstock, *Biomass & Bioenergy*, Vol. 32, No. 5, 2008, pp. 460–467. http://dx.doi.org./10.1016/j.biombioe. 2007.11.004
5. Fu, P., Hu, S., and Xiang, J., *et al.*, FTIR study of pyrolysis products evolving from typical agricultural residues, *Journal of Analytical and Applied Pyrolysis*, Vol. 88, No. 2, 2010, pp. 117–123. http://dx.doi.org/10.1016/j.jaap.2010.03.004
6. Fernando, S., Adhikari, S., and Chandrapal, C., *et al.*, Biorefineries: current Status, challenges, and future direction, *Energy & Fuels*, Vol. 20, No. 4, 2006, pp. 1727–1737. http://dx.doi.org/10.1021/ef060097w
7. Noor, H., Muhammad, A., and Muhammad, S., *et al.*, Synthesis of carboxymethyl cellulose from waste of cotton ginning industry, *Carbohydrate Polymers*, Vol. 113, 2014, pp. 249–255. http://dx.doi.org/10.1016/j.carbpol.2014.07.023
8. Wang, N., Fan, H., and Ai S.Y., Lignin templated synthesis of porous carbon-CeO_2 composites and their application for the photocatalytic desulphuration, *Chemical Engineering Journal*, Vol. 260, 2015, pp. 785–790. http://dx.doi.org/10.1016/j.cej.2014.09.051
9. Vilela, C., Santos, S.A.O., and Villaverde, J.J., *et al.*, Lipophilic phytochemicals from banana fruits of several Musa species, *Food Chemistry*, Vol. 162, 2014, pp. 247–252. http://dx.doi.org/10.1016/j.foodchem.2014.04.050
10. Villaverde, J.J., Vincent, V.D.V., and Santos, S.A.O. *et al.*, Hydroperoxide production from linoleic acid by heterologous Gaeumannomyces graminis tritici lipoxygenase: Optimization and scale-up, *Chemical Engineering Journal*, Vol. 217, 2013, pp. 82-90. http://dx.doi.org/10.1016/j.cej.2012.11.090
11. Mckendry P., Energy production from biomass (part 2): Conversion technologies, *Bioresource Technology*, Vol. 83, No. 1, 2002, pp. 47–54. http://dx.doi.org/10.1016/S0960-8524(01)00119-5
12. Wang, X.H., Chen, H.P., and Yang, H.P., *et al.*, The influence of alkali and alkaline earth metal compounds on pyrolysis of peanut shell, *Asia-Pacific Journal of Chemical Engineering*, Vol. 7, No. 3, 2012, pp. 463–468. http://dx.doi.org/10.1002/apj.595
13. Zhu, G.Y., Zhu, X., and Xiao, Z.B., *et al.*, Kinetics of peanut shell pyrolysis and hydrolysis in subcritical water, *Journal of Material Cycles and Waste Management*, Vol. 16, No. 3, 2014, pp. 546–556. http://dx.doi.org/10.1007/s10163-013-0209-7
14. Wilson, K., Yang, H., and Seo, C.W., *et al.*, Select metal adsorption by activated carbon made from peanut shells, *Bioresource Technology*, Vol. 97, No. 18, 2006, pp. 2266–2270. http://dx.doi.org/10.1016/j.biortech.2005.10.043
15. Yang, H.P., Yan, R., and Chen, H.P., *et al.*, Characteristics of hemicellulose, cellulose and lignin pyrolysis, *Fuel*, Vol. 86, No. 12–13, 2007, pp. 1781–1788. http://dx.doi.org/10.1016/j.fuel.2006.12.013
16. Sanchez, M.E., Cuetos, M.J., and Martinez, O., *et al.*, Pilot scale thermolysis of municipal solid waste Combustibility of the products of the process and gas cleaning, *Journal of Analytical and Applied Pyrolysis*, Vol. 78, No. 1, 2007, pp. 125–142. http://dx.doi.org./10.1016/j.jaap.2006.05.005
17. Wafwoyo, W., Seo, C.W., and Marshall, W.E., Utilization of peanut shells as adsorbents for selected metals, *Journal of Chemical Technology and Biotechnology*, Vol. 74, No. 11, 1999, pp. 1117–1121. http://dx.doi.org/10.1002/(SICI)1097-4660(199911)74:11%3C1117::AID-JCTB151%3E3.3.CO;2-I
18. Duan, F., Chyang, C.S., and Wang, Y.J., *et al.*, Effect of secondary gas injection on the peanut shell combustion and its pollutant emissions in a vortexing fluidized bed combustor, *Bioresource Technology*, Vol. 154, 2014, pp. 201–208. http://dx.doi.org/10.1016/j.biortech.2013.11.093
19. Duan, F., Zhang, J.P., and Chyang, C.S., *et al.*, Combustion of crushed and pelletized peanut shells in a pilot-scale fluidized-bed combustor with flue gas recirculation, *Fuel Processing Technology*, Vol. 128, 2014, pp. 28–35. http://dx.doi.org/10.1016/j.fuproc.2014.06.022
20. Arromdee, P., and Kuprianov, V.I., Combustion of peanut shells in a cone-shaped bubbling fluidized-bed combustor using alumina as the bed material, *Applied Energy*, Vol. 97, 2012, pp. 470–482. http://dx.doi.org/10.1016/j.apenergy. 2012.03.048
21. Kuprianov, V.I., and Arromdee, P., Combustion of peanut and tamarind shells in a conical fluidized-bed combustor: A comparative study, *Bioresource Technology*, Vol. 140, 2013, pp. 199–210. http://dx.doi.org/10.1016/j.biortech.2013.04.086
22. Ferreiro, A.I., Rabacal, M., and Costa, M., A combined genetic algorithm and least squares fitting procedure for the estimation of the kinetic parameters of the pyrolysis of agricultural residues, *Energy Conversion and Management*, 2016, In publication.
23. Wu, C.F., Wang, Z.C., and Huang, J., *et al.*, Pyrolysis/gasification of cellulose, hemicellulose and lignin for hydrogen production in the presence of various nickel-based catalysts, *Fuel*, Vol. 106, 2013, pp. 697–706. http://dx.doi.org/10.1016/j.fuel.2012.10.064
24. Braz, C.E.M., Crnkovic, P.M., Physical-Chemical characterisation of biomass samples for application in pyrolysis process, *Chemical Engineering Transactions*, Vol. 37, 2014, No. 523–528.
25. Chen, H.P., Li, B., and Yang, H.P., *et al.*, Experimental investigation of biomass gasification in a fluidized bed reactor, *Energy & Fuels*, Vol. 22, No. 5, 2008, pp. 3493–3498. http://dx.doi.org/10.1021/ef800180e

26. Souza, B.S., Moreira, A.P.D., and Teixeira, A., TG-FTIR coupling to monitor the pyrolysis products from agricultural residues, *Journal of Thermal Analysis and Calorimetry*, Vol. 97, No. 2, 2009, pp. 637–642. http://dx.doi.org/10.1007/s10973-009-0367-y
27. Slopiecka, K., Bartocci, P., and Fantozzi, F., Thermogravimetric analysis and kinetic study of poplar wood pyrolysis, *Applied Energy*, Vol. 97, No. SI, 2012, pp. 491–497. http://dx.doi.org/10.1016/j.apenergy.2011.12.056
28. Naktiyok, J., Bayrakceken, H., and Ozer, A.K., *et al.*, Kinetics of thermal decomposition of phospholipids obtained from phosphate rock, *Fuel Processing Technology*, Vol. 116, 2013, pp. 158–164. http://dx.doi.org/10.1016/j.fuproc.2013.05.007
29. Du, S.L., Yang, H.P., and Qian, K.Z., *et al.*, Fusion and transformation properties of the inorganic components in biomass ash, *Fuel*, Vol. 117, 2014, pp. 1281–1287. http://dx.doi.org./10.1016/j.fuel.2013.07.085
30. Xiao, R.R., Chen, X.L., and Wang, F.C., *et al.*, The physicochemical properties of different biomass ashes at different ashing temperature, *Renewable Energy*, Vol. 36, No. 1, 2011, pp. 244–249. http://dx.doi.org./10.1016/j.renene.2010.06.027
31. Vassilev, S.V., Baxter, D., and Andersen, L.K., *et al.*, An overview of the composition and application of biomass ash. Part 1. Phase-mineral and chemical composition and classification, *Fuel*, Vol. 105, 2013, pp. 40–76. http://dx.doi.org./10.1016/j.fuel.2012.09.041
32. Munir, S., Daood, S.S., and Nimmo, W., *et al.*, Thermal analysis and devolatilization kinetics of cotton stalk, sugar cane bagasse and shea meal under nitrogen and air atmospheres, *Bioresource Technology*, Vol. 100, No. 3, 2009, pp. 1413–1418. http://dx.doi.org./10.1016/j.biortech.2008.07.065
33. Baray Guerrero, M.R., Silva Paula, M.M., and Melendez Zaragoza, M., *et al.*, Thermogravimetric study on the pyrolysis kinetics of apple pomace as waste biomass, *International Journal of Hydrogen Energy*, Vol. 39, No. 29, 2014, pp. 16619–16627. http://dx.doi.org/10.1016/j.ijhydene.2014.06.012
34. Cao, Q., Xie, K.C., and Bao, W.R., *et al.*, Pyrolytic behavior of waste corn cob, *Bioresource Technology*, Vol. 94, No. 1, 2004, pp. 83–89. http://dx.doi.org/10.1016/j.biortech.2003.10.031
35. Meng, A.H., Zhou, H., and Qin, L., *et al.*, Quantitative and kinetic TG-FTIR investigation on three kinds of biomass pyrolysis, *Journal of Analytical and Applied Pyrolysis*, Vol. 104, 2013, 28–37. http://dx.doi.org/10.1016/j.jaap.2013.09.013
36. Liu, Q., Wang, S.R., and Zheng, Y., *et al.*, Mechanism study of wood lignin pyrolysis by using TG–FTIR analysis, *Journal of Analytical and Applied Pyrolysis*, Vol. 82, No. 1, 2008, pp. 170–177. http://dx.doi.org/10.1016/j.jaap.2008.03.007
37. Abraham, R., George, J., and Thomas, J., *et al.*, Physicochemical characterization and possible application of the waste biomass ash from oleoresin industries of India, *Fuel*, Vol. 109, 2013, pp. 366–372. http://dx.doi.org/10.1016/j.fuel.2013.02.067
38. Alothman, Z.A., Naushad, M., and Rahmat, A., Kinetic, equilibrium isotherm and thermodynamic studies of Cr(VI) adsorption onto low-cost adsorbent developed from peanut shell activated with phosphoric acid, *Environmental Science and Pollution Research*, Vol. 20, No. 5, 2013, 3351–3365. http://dx.doi.org/10.1007/s11356-012-1259-4
39. Umamaheswaran, K., and Batra, V.S., Physico-chemical characterization of Indian biomass ashes, *Fuel*, Vol. 87, No. 6, 2008, pp. 628–638. http://dx.doi.org/10.1016/j.fuel.2007.05.045

The Effects of Secondary-Phosphorus Release on Biological-Phosphorus Removal in a Pre-anoxic Process

RENJIAN DENG[1,*], RANG SHAO[1], JINSONG ZHANG[2], BOZHI REN[1] and PENG ZHANG[1]
[1]*School of Civil Engineering, Hunan University of Science and Technology, Xiangtan Hunan 411201, China*
[2]*Shenzhen Water (Group) Co.Ltd., Shenzhen 518030, China*

ABSTRACT: In this study, a sequencing batch reactor (SBR) with fill, anaerobic, oxic1, anoxic, oxic2, settle, decant and sludge pre-anoxic process, was used to investigate the performance efficiency of biological nutrient removal which occurs secondary- phosphorus release during different pre-anoxic hydraulic time (PAHRT). The results of the study showed that the processes of secondary-phosphorus release and secondary-phosphorus removal were significantly affected by PAHRT, whereas the removal of chemical oxygen demand (COD), ammonia nitrogen (NH_4^+-N) and total nitrogen (TN) removal were only slightly affected. The research also showed that when PAHRT for 120 min., and MLVSS was 5330 mg/1, the secondary-phosphorus-release concentration was lower than 0.15 mg/L, and the removal efficiency of the total phosphorus (TP) was higher than 80.98%. Moreover, it was found that there is a negative correlation between secondary-phosphorus release and TP removal efficiency and between secondary-phosphorus release and the quantity of released anaerobic phosphorus. The study also showed that phosphate-accumulating organisms (PAOs) can be used to break down poly-p without PHA synthesis during the process of secondary- phosphorus release, resulting in a reduction of PHA content in PAOs. As a result, the rate of anaerobic-phosphorus release and oxic-phosphorous uptake decreases , leading to a duction in phosphate- removal efficiency. It is thus necessary to reduce or, avoid a secondary- phosphorus- release event in a pre-anoxic system. In summation, this project's findings show that a decrease of secondary-phosphorus release in a pre-anoxic process is an effective way of enhancing biological- phosphorus removal.

1. INTRODUCTION

TRADITIONAL biological-phosphorus-removal processes have long been known for their low operating costs and for their small reagent-consumption and low sludge production levels (Kim *et al.*, 2010) However, efforts to update and improve the function of the old systems has recently become one of the "hottest" research topics among pollution experts. The traditional phosphorus-removal theory holds that phosphate-accumulating organisms (PAOs) absorb volatile fatty acids (VFAs) in order to synthesize polyhydroxyalkanoates (PHAs), and that the release of phosphorus in anaerobic environments is a necessary step for the removal of biological phosphorus. Moreover, the theory holds that the more phosphorus released in an anaerobic tank, the higher the removal efficiency.. However, several intrinsic problems have been identified for the simultaneous removal of biological phosphorus and nitrogen, such as an intense competition between nitrifying bacteria and phosphate-accumulating bacteria for carbon resource, when the nitrate concentration in the return sludge is too high, it imposes a severely negative impact on the synthesis of PHAs and the release of phosphorus. Therefore, a pre-anoxic tank is needed during the pre-anoxic process with the endogenous denitrification technique applied, such as MSBR (Deng *et al.*, 2013), Johannesburg (JHB) (Makinia *et al.*, 2006; Shi *et al.*, 2011) and triple oxidation ditch, in order to reduce the effect of nitrate recycling in the anaerobic reactor. Some studies (Du, 2006; Yang*et al.*, 2008) have shown that highly efficient phosphorus removal may be achieved when the concentration of NO_3^--N in the pre-anoxic tank is manipulated to be around 0.5~3.0 mg/L. Deng *et al.* (2014) discovered that phosphorus-removal efficiency decreases if the concentration of NO_3^--N in the pre-anoxic tank of MSBR process is lower than 0.5 mg/L. Meanwhile, different levels of secondary phosphorus release (i.e., when phosphorus is released in the absence of an external carbon source) were observed in pre-anoxic tank. In short, the control of a pre-anoxic

*Author to whom correspondence should be addressed.
Email: 800912deng@sina.com

1544-8053/16/03 307-10

doi:10.12783/issn.1544-8053/13/4/8

tank has been found to be a key step in achieving effective phosphorus removal during the MSBR and JHB process. However, studies on such subjects as themechanisms involved in these procedures, the necessary control measures, and the impact of secondary-phosphorus release on phosphorus removal efficiency, are still very limited (Shi *et al.*, 2011).

The aim of this study was to investigate the relationship between secondary-phosphorus release and pre-anoxic hydraulic time (PAHRT) and MLVSS during the pre-anoxic process in a SBR reactor operated with the sequences of fill anaerobic, oxic1, anoxic, oxic2, settle, decant and sludge pre-anoxic. In addition, the study explores the impact of secondary-phosphorus release on anaerobic phosphorus release, evaluates the process of phosphorus removal, and discusses the possible mechanisms involved in the complex procedure. The results of the investigation can be used as a reference for the operation and management of the pre-anoxic tank in MSBR and JHB processes.

2. MATERIALS AND METHODS

2.1. The Pilot-plant Feeding Systems

The lab batch experiments were carried out in a reactor with an active volume of 5 L (18 cm in diameter and 25 cm in height) as shown in Figure 1. The reactor content was stirred mechanically with a propeller on a vertical axis of 25 ~ 75 rpm. The room temperature was maintained at 25 ± 1°C. Two peristaltic pumps were used for feeding and drawing purposes. A diffused aeration system with a blower capacity of 250 $L.h^{-1}$ was connected to the bottom of the reactor. The anaerobic, anoxic or aerobic environment was achieved by making adjustments between aeration and stirring conditions. The system was controlled by a programmable-logic controller (PLC).

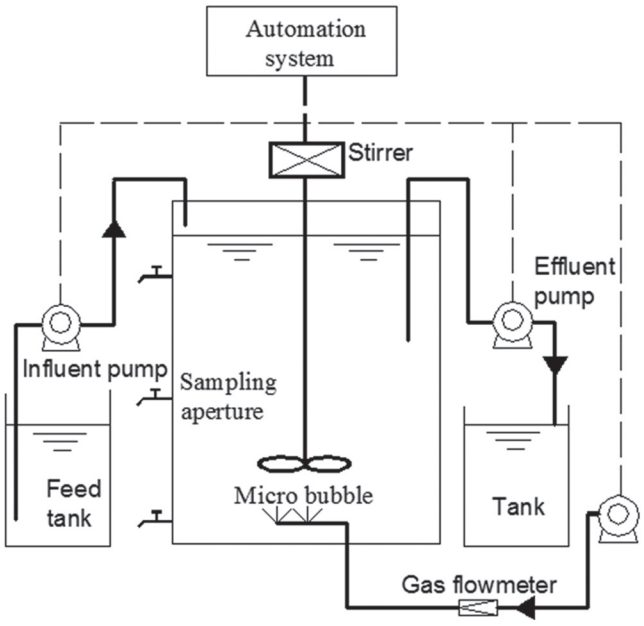

Figure 1. *Schematic diagram of the SBR reactors.*

2.2. Experiment Approach

2.2.1. Batch Tests

Some researchers (Du, 2006; Yang *et al.*, 2008; Shi *et al.*, 2011; Deng *et al.*, 2014) found that the secondary phosphorus release in the pre-anoxic tank was related to factors such as hydraulic residence time (HRT) and MLVSS. For the current study, the experimental procedures and operational conditions lasted for nearly 5 months at 25 ± 1°C (defined as Runs I–IV). The experimental procedures and conditions defined as Runs I–IV are summarized in Figure 2: Fill (5 min) → anaerobic (90 min) → oxic1 → anoxic → oxic2 (30 min) → Settle (30 min) → drain (5 min) → pre-anoxic. The test included 4 operating conditions: Under Runs I-III, the pre-anoxic hydraulic time (PAHRT) was set at 60, 90 and 120 min, respectively, with a fill ratio of 0.5; under condition IV, the pre-anoxia time was 150 min, with a fill ratio of 0.60. The MLVSS of the pre-anoxic process under Run IV was much higher than that under Runs I–III. The operating time for working Runs I–IV was 46 d (including a 15 d for startup), 40 d, 36 d and 31 d, respectively (a total of 153 d). For the experiment, the MLSS in oxic1 was 4000 ± 290 mg/L, the dissolved oxygen (DO) concentration in Oxic1 was 2.5–3.5 mg/L, and the sludge retention time (SRT) was 12–15 d.

2.2.2. Experimental Methods for the Assessment of the Secondary Phosphorus Release

In order to gain insight on the impact of secondary-phosphorus release on the amount of phosphorus released, phosphorus removal efficiency and potential mechanisms, some tests were performed with SBR. The experiments included the following steps: (1) In the absence of external carbon sources and NO_3^--N, 5 L activated sludge from the aerobic tank (MLVSS = 2950 mg/L) was rinsed with distilled water three times. The rinsed samples were then stirred under anaerobic conditions. (2) 700 mL sludge samples were collected at times of 0, 1, 2, … , and 6 h for the following tests,

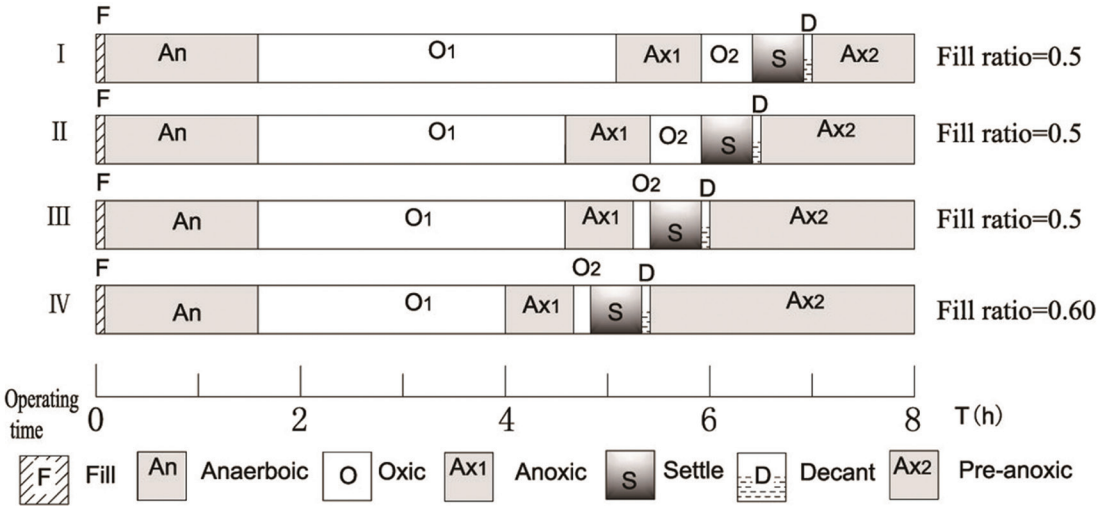

Figure 2. *Operation modes of SBR.*

with 100 mL of each sample used for the determination of orthophosphate and PHA content. (3) 600 mL sludge samples were mixed with 400 mL synthetically sewage Acetic acid was then added to the mixture to achieve an initial concentration of 40 mg COD/L. (4) The mixture was exposed to the anaerobic conditions for 2 h and to the aerobic conditions for 4 h. The concentrations of orthophosphate, PHA and glycogen were measured in order to understand the changing patterns. (5) The organization and analysis of all of the experimental data.

2.2.3. Mathematical Statistics

Multiple regression analysis: Previous studies have shown that factors which might contribute to the reduction in TP removal efficiency and the amount of phosphorous released include secondary phosphorus release, influent COD/TP and residual NO_3^--N in pre-anoxic phase (Wu *et al.*, 2010). Therefore, a multiple regression analysis based on Equations (1)~(2) was conducted to analyze the relationship between those factors and the amount of phosphorous released during the anaerobic phase.

$$Y_1 = a_0 + a_1X_1 + a_2X_2 + a_3X_3 \quad (1)$$

$$Y_2 = b_0 + b_1X_1 + b_2X_2 + b_3X_3 \quad (2)$$

Where Y_1 is the amount of phosphorous released during the anaerobic phase, with the unit as mg/L; Y_2 is TP removal rate, %; X_1 is COD/TP, which is dimensionless; X_2 is NO_3^--N concentration at the end of the pre-anoxic phase, with the unit as mg/L; X_3 is the concentration of released secondary phosphorous at the end of the pre-anoxic phase, with the unit as mg/L.

2.3. Wastewater and Seed Sludge Characteristics

The SBR was fed with domestic wastewater which came from the grit chamber effluents of a municipal wastewater treatment plant, with COD = (307 ± 88) mg/L, TN = (36.5 ± 5.8) mg/L, NH_4^+-N = (31.7 ± 6.2) mg/L, NO_3^--N = (1.1 ± 0.4) mg/L, and TP = (4.6 ± 1.2) mg/L. The seed sludge used for SBR was collected from the oxic tank of a post-denitrification wastewater treatment plant, with a sludge volume index (SVI) of 40–45 mL/g. According to the operation mode maintained in Section 2.2.1, the SBR was operated for 15 d as a start-up period, and then operated normally.

2.4. Analysis Methods

The samples were collected and analyzed according to the protocol developed by Guo *et al.* (2012). The influent flow rates, temperature, pH, and DO were measured on a daily basis. The content of COD, TP, TN, NH_4^+-N, NO_3^--N and MLSS in both influent and effluent were measured two or three times each week. All of the indexes were measured according to Standard Methods (APHA, 1998). The sludge sample mixed with water was centrifuged for 3 min (3000 r/min) prior to the measurement of the supernatant liquid. The DO was measured using a portable DO Meter (HACH HQ30d). The ORP and pH were measured using a portable meter (HACH-sension2). The VFA concentrations were measured via high-performance-liquid chromatography (HPLC), equipped with a Bio Rad Aminex HPX-87H column (Waters2489 UV/RI

detector) with a mobile phase (1.5 mM H_3PO_4) flow-rate of 0.6 mL/min and a temperature of 60°C (Wu, 2010). The PHAs were determined by gas chromatography (GC) using the method described by Takabatake *et al.* (2002), using a Bruker 430-GC gas chromatograph equipped with a FID detector and a BR-S Wax column (60 m, 0.53 mm internal diameter, 1 μm thickness, Bruker, USA). Glycogen was determined as described by Crocetti *et al.* (2002) and Liu *et al.* (2008), using the following conditions during biomass digestion: 2 mg biomass, 0.9 M HCl and 3 h of digestion time. The analysis was performed at 30°C, with 0.005 M H_2SO_4 as eluent, at a flow rate of 0.5 mL min^{-1}, using a Metacarb-87H column (Varian), equipped with an IR detector. All other parameters were measured according to literature (APHA, 1998).

3. RESULTS AND DISCUSSION

3.1. The Influence of PAHRT on Nutrient Removal Efficiency

Table 1 displays the pollutants in influent and effluent as well as the removal efficiencies during the operation periods (Runs I-IV). As shown in Table 1, high COD removal efficiency was achieved under different operating conditions with a range of 90.10–93.03%. Obviously, the data suggests that PAHRT had imposed little effect on the removal efficiency of organics. Excellent NH_4^+-N removal was achieved in Runs I-IV, with the range of effluent NH_4^+-N concentrations and the removal efficiency as 0.25–0.73 mg/L and 97.19–99.24%, respectively, suggesting that both aerobic time and DO played important roles in affecting the removal efficiency of NH_4^+-N, whereas PAHRT did not. The TN removal efficiency remained around 64.0% during Runs I–III, but was down to 57.51%, with the average effluent TN concentration as 12.98 mg/L. This was mainly due to an increase of nitrogen loading from 0.14 kg N/kg vss.d to 0.19 kg N/kg vss.d. Therefore, PAHRT had imposed little impact on the TN removal efficiency. The effect of PAHRT (60, 90, 120, 150 min) on the TP removal efficiency was also studied under different Runs modes. The results showed that the highest TP removal efficiency of 80.98% was achieved with the PAHRT of 120 min (Run III). The effluent phosphorus was able to meet the first-B wastewater-discharge standard in China (TP < 1.5 mg/L). In contrast, in Run IV, the TP removal efficiency decreased rapidly to 59.45% when the MLVSS was 7418 mg/L and the PAHRT increased up to 150 min. Therefore, PAHRT is a critical parameter that determines TP-removal efficiency in the present study.

In this study, the most acceptable removal efficiencies for COD, NH_4^+-N, TN and TP were observed in Run III, which showed removal efficiencies of 92.34%, 99.24%, 64.54%, and 80.89%, respectively. Previous studies have shown that nutrient-removal efficiencies may differ when different types of wastewater are used in the Post-denitrification SBRs (Yt *et al.*, 1997; Umble *et al.*, 1997; Ds *et al.*, 2001; Akin and Ugurlu, 2005; Cybis*et al.*, 2004; Lv *et al.*, 2008; Debik *et al.*, 2010). Table 2 shows a comparison between previous studies and the present study. It can be seen that the COD-, NH_4^+-N- and TP-removal efficiency in Run III of this study was higher or close to the results found in previous studies. But TN-removal efficiency (64.5%) was lower than that which has been reported in the literature (70%~89%). The fill ratio of 0.5–0.65 in the present study was larger than what has been reported in the literature in the range of 0.4–0.35. Therefore, this operation model in Run III has displayed a good removal efficiency of nitrogen and phosphorus, especially when N loading is taken into account.

3.2. The Influence of PAHRT on Anaerobic Phase Phosphorus Release and Secondary Phosphorus Release in Pre-anoxic Phase

Table 3 shows the variations in the content of the residual NO_3^--N during the pre-anoxic phase and the anaerobic phase phosphorus release as well as in the secondary-phosphorus release in the Pre-anoxic phase during the operation periods (Runs I-IV). Generally speaking, It was found thatthe amount of phosphorus released during the anaerobic phase can be negatively affected by the presence of residual nitrate and insufficient influent organic substrates. Meanwhile, the amount of phosphorus released and phosphorus-removal efficiency improved during Runs I–III (Tables 1 and 3), since the content of residual nitrate decreased from 8.69–4.69 mg/L, where the time of PAHRT increased from 60 min to 120 min. Therefore, the maximum amount of phosphorus released during the anaerobic phase reached 13.41 mg/L, and the average removal efficiency rose to 80.98%. Later, a smaller amount of NO_3^--N was removed during the anaerobic phase. As expected, the increasing phosphorus release and removal efficiency was found in Run III. However, when the PAHRT time increased to 150 min (Run IV), and the content of residual nitrate decreased to 3.45 mg/L in Run IV, the amount of phosphorus released during

Table 1. Performance of SBR System Under the Runs I–IV.

Runs Modes	PAHRT (min)	COD			NH_4^+-N			TN			TP		
		Influent (mg/L)	Effluent (mg/L)	Removal Efficiency (%)	Influent (mg/L)	Effluent (mg/L)	Removal Efficiency (%)	Influent (mg/L)	Effluent (mg/L)	Removal Efficiency (%)	Influent (mg/L)	Effluent (mg/L)	Removal Efficiency (%)
I	60	422.5	29.0	93.03	29.37	0.37	98.99	34.84	12.33	65.06	4.44	1.24	71.27
II	90	361.6	27.3	92.49	29.42	0.25	99.11	34.25	11.98	64.44	4.92	1.19	74.86
III	120[a]	438.6	34.1	92.34	30.08	0.25	99.24	35.18	12.48	64.54	4.52	0.86	80.98
IV	150[b]	390.5	38.8	90.10	25.37	0.73	97.19	31.42	12.98	57.51	4.68	1.86	59.45

Notes:
[a]The fill ratio was 0.5.
[b]The fill ratio was 0.60.

Table 2. A Comparison Between Previous Studies and the Present Study.

Water Samples	Operations and Hydraulic Retention Time HRT (h)												Percent Removal (%)			
	F[a]	An[b]	O[c]	*Ax*[d]	O	*Ax*	O	S[e]	D[f]	I[g]	*Ax*[h]	Σ_{HRT}	COD	NH_4^+-N	TN	TP
Domestic sewage (Debik *et al.*, 2010)	0.5	2	2	1	0.75	-	0	1	0.5	0.25	0	8.00	90.8	84.6	78	83
Domestic sewage (Yt *et al.*, 1997)	0.33	2.33	2	–	–	–	–	1	0.17	0.17	0	6.00		90.5	83	86.7
	0.33	3.67	2.83	–	–	–	–	0.8	0.17	0.17	0	8.00		90.1		88.5
	0.33	5.67	4	–	–	–	–	1	0.5	0.5	0	12.00		92.1		75.8
Artificial wastewater (Umble *et al.*, 1997)	–	2	–	1	4.5	1.5	1.5	0.5	0	–	0	11.00	94	84	70	70
Artificial wastewater (Akin and Ugurlu, 2005)	4	–	–	0.5	7	–	–	0.5	0	–	0	12.00	90–98	90–95		70–100
Domestic sewage (Cybis *et al.*, 2004)	1	–	–	2	3	–	–	1	1	–	0	8.00	90			
Artificial wastewater (Lv *et al.*, 2008)	–	1.5	1	1	0.33	1	0.3	1	1	0.84	0	8.00	88		89	99
Artificial wastewater (Lv *et al.*, 2008)	–	1.5	1	1	0.33	1	0.3	1	1	0.84	0	8.00	85		75	99.5
Artificial wastewater (Ds *et al.*, 2001)	–	2	3	–				1	0.17	1.83	0	8.00	92		88	100
Domestic sewage[i]	0.083	1.5	3	0.67	0.17	0	0	0.5	0.083	0	2	8.00	92.3	99.1	64.5	81.0

Notes:
[a]Fill.
[b]Anaerobic.
[c]Oxic.
[d]Anoxic.
[e]Sedimentation.
[f]Drain.
[g]Idle.
[h]Pre-anoxic.
[i]This study.

the anaerobic phase decreased to 11.17 mg/L, with the average removal efficiency falling to 59.45%. Meanwhile, the secondary—phosphorus release during the Pre-anoxic phase reached 0.82 mg/L, which was much higher than it was in Runs I–III (0.03–0.15 mg/L). This suggested that too much PAHRT contributed to secondary phosphorus release but decreased phosphorus removal efficiency. Moreover, statistical analyses were performed to analyze the relationship between PAHRT, MLVSS and secondary phosphorus release, with the relation Equation (3) shown as follows.

$$Y = 1.468 - 7.863e^{-4} \times t - 3.089e^{-4} \times MLVSS \qquad R^2 = 0.73 \qquad P = 5.11e^{-6} \tag{3}$$

Where Y is the secondary phosphorus release concentration, mg/L; t is PAHRT, h; MLVSS is the volatile solids concentration in a sample of mixed liquor, mg/L.

It can be seen from Equation (3) that the impact of PAHRT and MLVSS on secondary phosphorus release was significant, and the relative importance of PAHRT was greater than that of MLVSS. Therefore, in order to prevent the occurrence of secondary phosphorus release, HRT in the pre-anoxic tank should be controlled as a priority, followed by the MLVSS in the pre-anoxic tank. Based on our findings, PAHRT was a critical parameter for the increase of phosphorus release and secondary phosphorus release.

3.3. The Impact of Secondary Phosphorus Release on Phosphorous Removal Efficiency and Mechanisms Involved

3.3.1. The Relationship Between Secondary Phosphorus Release and Phosphorus Removal Efficiency

In Run IV, the maximum amount of released secondary phosphorus was up to 0.82 mg/L, and the TP removal efficiency rapidly decreased to 59.45%. In order to further test the relationship between secondary-phosphorus release, anaerobic-phosphorus release and biological-phosphorus removal efficiency, multiple regression and univariate analysis were conducted in this study.

According the Equations (1) and (2), the results of multiple regression analysis are shown in Equation (1a)–(2a), with $\alpha 0 = 0$, $\alpha 1 = 0.08$, $\alpha 2 = 0.39$, $\alpha 3 = 3.19$, $b0 = 0$, $b1 = 0.32$, $b2 = -6.04$, $b3 = 8.80$.

$$Y_1 = 0 + 0.08X_1 + 0.39X_2 + 3.19X_3 \qquad R^2 = 0.80 \qquad P = 8.5e^{-7} < 0.01 \tag{1a}$$

$$Y_2 = 0 + 0.32X_1 - 6.04X_2 + 8.80X_3 \qquad R^2 = 0.95 \qquad P = 1.6e^{-11} < 0.01 \tag{2a}$$

It can be seen from Equations (1a)–(2a) that the amount of phosphorus released and the phosphorous removal efficiency during the anaerobic phase was affected by the above mentioned factors. These factors are ranked in descending order according to their relative importance: the secondary phosphorus release ≥ residual NO_3^--N_{in} pre-anoxic phase ≥ COD/TP.

In order to gain insight into the impact that secondary-phosphorus release has on the amount of phosphorus released and the phosphorus-removal efficiency in the absence of carbon resource and NO_3^--N, some tests as described in Section 2.2.2 were conducted. Data obtained from step (2) were used to plot a graph, which reflected the changes of the amount of released secondary phosphorus and PHA content in the absence of carbon resource [Figure 3(a)]. Also, data obtained from step (4) were used to plot a graph, which showed the level of anaerobic phosphorus release and the oxic phosphorus uptake [Figure 3(b)]. It can be seen from Figure 3(a) that the relationship between the anaerobic hydraulic time in the absence of carbon resource

Table 3. The Variations of TP and NO3-N Under Different Operational Conditions.

Operation Modes	PAHRT (min)	MLVSS in Pre-anoxic Phase (mg/L)	Residual NO_3^--N_{in} Pre-anoxic Phase (mg/L)	NO_3^--N_{in} Removal During Pre-anoxic Phase (mg/L)	Pre-anoxic Phase Secondary Phosphorus Release (mg/L)	Anaerobic Phase Phosphorus Release (mg/L)
I	60	5185	8.69	2.29	0.04	8.23
II	90	5360	8.19	2.70	0.03	9.17
III	120a	5330	4.69	6.07	0.15	13.41
IV	150b	7418	3.45	8.71	0.82	11.17

Notes:
[a]The fill ratio was 0.5.
[b]The fill ratio was 0.60.

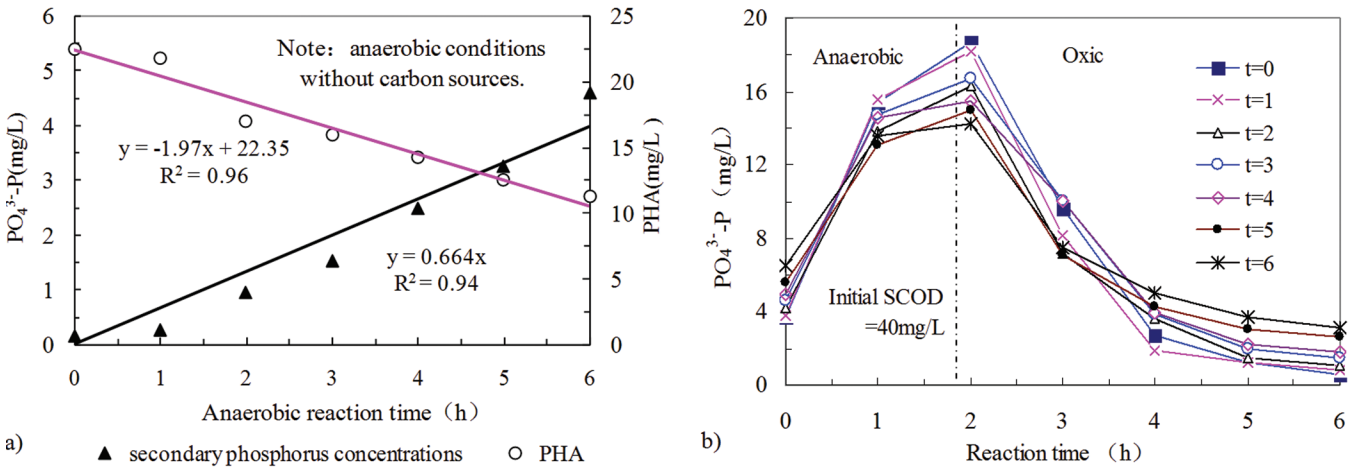

Figure 3. *Effect of secondary phosphorus release on anaerobic phosphorus release and aerobic phosphorus uptake.*

and the secondary phosphorus release was linear (R^2 = 0.94). In other words, the secondary phosphorus release increased with anaerobic hydraulic time. Meanwhile, the PHA content in the sludge increased linearly with anaerobic hydraulic time (R^2 = 0.88). Clearly, secondary phosphorus release during the pre-anoxic phase could reduce the cellular PHA content of PAOs.

Details regarding anaerobic phosphorus release and aerobic phosphorus uptake during the different phases of secondary phosphorus release were shown in Figure 3(b). The amount of anaerobic phosphorus released decreased from 18.68–14.25 mg/L, with the time of secondary phosphorus release increasing from 0 h to 6 h. After the 4 h oxic, the corresponding orthophosphate concentration increased from 0.86–3.16 mg/L, and the phosphorous removal efficiency was reduced from 93.75–67.08%. Moreover, the amount of anaerobic phosphorus released was negatively related to secondary phosphorus release ($y = -0.919x + 18.05$, R^2 = 0.86). Similarly, phosphorous removal efficiency was also negatively related to secondary phosphorus release as shown in Figure 4 ($y = -5.92x + 93.64$, R^2 = 0.98). Therefore, secondary phosphorus release had imposed a negative impact on anaerobic phosphorus release and phosphorous removal efficiency. For the actual practice of the MSBR- or the JHB-based technique, it is necessary to reduce or avoid the occurrence of secondary phosphorus release in the pre-anoxic or SBR tank.

3.3.2. Mechanisms of Secondary Phosphorus Release on Biological Phosphorus Removal Efficiency

Biological phosphorus removal from activated sludge is mainly carried out through the metabolic activities of PAOs, with polyphosphate (poly-P), glycogen and PHA playing important roles in the metabolic process of PAOs. In order to reveal the mechanisms involved inhow secondary-phosphorus release might influence anaerobic-phosphorus release and oxic-phosphorus uptake, the synthesis, decomposition and transformation of poly-P, glycogen and PHA were calculated using SBR-measured data as described in Section 2.2.2. Results of the stoichiometry of substrates of PAOs during the anaerobic and the aerobic phases were summarized in Table 4, including the PHA/acetic-acid rate during anaerobicphase ($R_{PHA,AA}$), Phosphorous release/acetic acid in anaerobic ($R_{P,AA}$), Glycogen/ acetic acid in anaerobic ($R_{G,AA}$), Uptake phosphorous/PHA rate during aerobic phase ($R_{UP,PHA}$), Glycogen/PHA rate during aerobic phase ($R_{G,PHA}$), PHA-consumption rate during aerobic (R_{PHA}).

There was a satisfactory level of phosphorus-removal stoichiometry (metabolic efficiency) when the

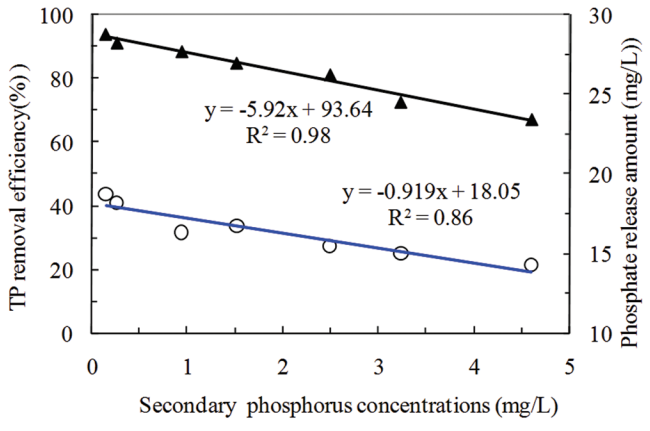

Figure 4. *The relationship between the secondary phosphorous and anaerobic phosphorus release or aerobic phosphorus uptake.*

anaerobic-hydraulic time was 0 h and secondary-phosphorus release was 0.15 mg/L in the absence of carbon resource, with normal $R_{PHA,AA}$ (1.30 mmol-C/mmol-C), $R_{P,AA}$ (0.387 mmol-P/mmol-C), $R_{G,AA}$ (0.53 mmol-C/mmol-C), $R_{UP,PHA}$ (0.365 mmol-P/mmol-C), $R_{G,PHA}$ (0.528 mmol-C/mmol-C), R_{PHA} (0.098 mg-PHA/mg-VSS.d). In addition, Table 4 also showed a comparison of corresponding phosphorus-removal-stoichiometry parameters with several similar BNR process with a UCT, A^2/O configuration. Obviously, the values of $R_{PHA,AA}$, $R_{P,AA}$, $R_{G,AA}$, $R_{UP,PHA}$ and $R_{G,PHA}$ were very close to previous studies (Shi *et al.*, 2011; Wang, *et al.*, 2010; Wu, *et al.*, 2010), with a good phosphorous-removal efficiency of 93.75% (Figure 4).

When the secondary phosphorus release increased (from 0.15 to 4.60 mg/L), the value of $R_{PHA,AA}$ also increased (from 1.30 to 1.35 mmol-C/mmol-C). The results showed that the utilizing rate of degradable substrates to synthesize PHAs during the anaerobic phase decreased with an increase of the secondary phosphorus release. Under the anaerobic condition, PAOs could rapidly uptake the degradable substrates in order to synthesize the PHAs, with the stored polyphosphate (poly-p) serving as the energy source (Peng yongzhen, Ge shijian, 2011). With an increase in the secondary-phosphorus release, the amount of hydrolyzed poly-P decreased under the anaerobic condition. In order to gain more energy, the PAOs would preferentially use acetic acid to synthesize the PHA through the metabolic pathways of acetyl CoA and propionyl CoA condensation reactions (Monica, 2014). However, this metabolic pathway also consumed more glycogen and released a limited amount of phosphorous (Wu, 2010), causing the $R_{PHA,AA}$ and $R_{G,AA}$ to dramatically decrease , with the minimum value of 0.200 mmol-P/mmol-C and 0.50 mmol-C/mmol-C, respectively (Table 4). This suggests that secondary-phosphorus release had imposed a significant impact on the PHAs synthesis and the poly-P hydrolyzing of the PAOs under the anaerobic condition. Afterwards, the amount of phosphorous release and the PHA content decreased as the secondary-phosphorus release increased.

As shown in the Table 4, $R_{UP,PHA}$ and $R_{G,PHA}$ decreased during the aerobic phase as the secondary-phosphorus release increased, with the minimum value as 0.270 mmol-P/mmol-C and 0.494 mmol-C/mmol-C, respectively. Meanwhile, the secondary-phosphorus release had imposed little influence over the synthesis and decomposition of glycogen. Moreover, the content of $R_{UP,PHA}$ was much lower than 0.375 mmol-P/mmol-C, which has been commonly reported in the literature,

Table 4. Stoichiometry of Substrates of PAOs During Anaerobic and Aerobic Phase.

		Anaerobic Reactions (0–2h)			Oxic Reactions (2–6 h)		
Test No. or References	**Secondary Phosphorous (mg/L)**	**$R_{PHA,AA}$ (mm ol-C/mmol-C)**	**$R_{P,AA}$ (mmol-P/mmol-C)**	**$R_{G,AA}$ (mmol-C /mmol-C)**	**$R_{UP,PHA}$ (mmol-P/mmol-C)**	**$R_{G,PHA}$ (mmol-C/mmol-C)**	**R_{pHA} (mg-PHA/mg-vss.d)**
0*	0.15	1.30	0.387	0.53	0.365	0.528	0.098
1	0.26	1.29	0.371	0.52	0.351	0.508	0.097
2	0.94	1.31	0.310	0.51	0.337	0.509	0.089
3	1.52	1.30	0.310	0.51	0.349	0.500	0.086
4	2.49	1.34	0.272	0.51	0.315	0.497	0.085
5	3.24	1.35	0.242	0.50	0.294	0.489	0.083
6	4.60	1.35	0.200	0.50	0.270	0.494	0.080
Shi *et al.*, 2011	–	1.33	0.35–0.75	0.50	0.375	0.375	–
Wang, *et al.*, 2010	–	1.22–1.34	0.47–0.36	0.50	0.65–0.51	0.35–0.27	–
Wu, *et al.*, 2010	–	1.31	0.56	0.77	–	–	–

Note:
*The numbers also indicate the anaerobic hydraulic time without external carbon sources, h.

and was lower than the range of 0.51–0.65 mmol-P/mmol-C, which has been suggested as a standard reference for nitrogen and phosphorus removal systems (Wang, 2010). The main reason for the lower $R_{UP,PHA}$ value might be due to less uptake of phosphorous under the secondary-phosphorus release condition. Another reason for the lower RG,PHA value might be due to the low PHA content in the PAOs under the secondary-phosphorus release condition [Figure 3(a)]. In the aerobic phase, the PAOs could help to reduce the $R_{G,PHA}$ (from 0.098 to 0.080 mg-PHA/mg-vss.d) if the PHA content is low in PAOs (Emmanouel, 2016). As a result, the phosphorus uptake of the sludge decreased, and phosphorous removal efficiency also decreased as the effluent TP concentration increased (Figure 4). Additionally, the rate constant for bacteriolysis of the PAOs (bPAO) was only 0.2 d^{-1}. Therefore, the longer the anaerobic hydraulic time was in the absence of the external carbon resource, the more PAOs tended to die or dissolve, resulting in a lower proportion of effective PAOs in the activated sludge and phosphorous removal efficiency. In sum, PAOs would break down poly-p without PHA synthesis during the process of secondary-phosphorus release. Also, the PHA synthesis rate during the anaerobic process, and the PHA consumption rate during the aerobic process have been influenced by the secondary-phosphorus release. As a result, both the anaerobic-phosphorus release and the oxic-phosphorous-uptake rate decreased, which led further to phosphate removal efficiency. Given that the metabolic processes of polyphosphates, glycogen and PHA are very complicated, and that there are many conflicting research findings, further studies are urgently needed on this subject.

4. CONCLUSIONS

In the pre-anoxic system, the secondary-phosphorus release and phosphorus removal were significantly affected by the pre-anoxic hydraulic time (PAHRT). The secondary-phosphorus release had a negative impact on the anaerobic phosphorus release and the phosphorous-removal efficiency. According to the characteristic of the secondary-phosphorus release and mechanisms, the PAOs break down poly-p without synthesis PHA during the secondary-phosphorus release process, which leads to the decrease of PHA content in PAOs. As a result, both the anaerobic-phosphorus release and the oxic-phosphorous uptake rate decreased, which led to the decreased efficiency of phosphate removal. It is, therefore, of vital necessity to reduce or avoid the occurrence of secondary phosphorus release in a pre-anoxic system.

ACKNOWLEDGEMENTS

This study was financially supported by the National Science Foundation of China Hunan Province (No.2016JJ6041), the scientific research project of Hunan Provincial Education Department (No. 15C0556, No. 10C0705) and Optional subjects of Shenzhen Water (Group) Co., Ltd.

REFERENCES

1. Kim H. G., Jang H. N., Kim H. M., *et al.* Effect of an electro phosphorous removal process on phosphorous removal and membrane permeability in a pilot-scale MBR[J]. *Desalination*. 2010, 25 0(2): 629–633.
2. Deng Renjian, Zhang Jinsong, Qu Zhijun, *et al.* Study on the enhanced bio-denitrification in a full-scale WWTP with MSBR process[J]. *Advanced Materials Research*. 2013, 610–613(1): 1551–1555.
3. Makinia J., Rosenwinkel K. H., Spering A. V., Comparison of Two Model Concepts for Simulation of Nitrogen Removal at a Full-Scale Biological Nutrient Removal Pilot Plant[J]. *Journal Of Environmental Engineering*. 2006, 101(7): 476–487. http://dx.doi.org/10.1061/(ASCE)0733-9372(2006)132:4(476)
4. Shi Hang-chuang, Hu zhi-rong, Zhou Jun, *et al.* Biological Wastewater Treatment: principles, Modelling and Design[M].*China Architecture & Building Press*, Beijing, 2011.09
5. Du Ying-hao. Operation Management of MSBR System[J]. *China Water & Wastewater*, 2006,22(2):90–92.
6. Yang Xing, Leng Han, Hu Linlong, *et al.* Experimental study on phosphorus removal influencing factors in 7-tank process of MSBR[J]. *Chinese Journal of Environmental Engineering*, 2008,2(8):1053–1056.
7. Deng Ren-jian, Zhang Jin-song, Qu Zhi-jun,*et al.* Full-scale Experiment of Enhanced Biological Nitrogen Removal in MSBR Process [J]. *China Water & Wastewater*. 2014,30(7):9–13.
8. Guo Haiyang, Guo G., Liu Z G., *et al.* 2012. Characteristics of nitrogen and phosphorus removal in SBR and SBMBBR with diferent aeration rates[J]. *Acta Scientiae Circumstantiae, 32*(3) :568–576.
9. Wu Changyong, Peng Yongzheng, Xiao-Ling Li E A. Effect of Carbon Source on Biological Nitrogen and Phosphorus Removal in an Anaerobic-Anoxic-Oxic (A2O) Process[J]. *Environmental Engineering. 2010, 12*(1): 1248–1254. http://dx.doi.org/10.1061/(ASCE)EE.1943-7870.0000262
10. Takabatake H., Satoh H., Mino T., *et al.* PHA (polyhydroxyalkanoate) production potential of activated sludge treating wastewater[J]. Water Science And Technology. 2002, 45(12): 119–126.
11. Crocetti G. R., Banfield J. F., Keller J., *et al.* Glycogen-accumulating organisms in laboratory-scale and full-scale wastewater treatment processes[J]. *Microbiology-SGM*. 2002, 148(Part 11): 3353–3364.
12. Liu Xiao-ying, Zhao Hong-mei, Peng Dang-cong1,Sui Xian-jie. Denitrifying Phosphate Uptake of Biological Phosphorous Removal Granular Sludgein SBR[J]. *Environmentalscience*, 2008, 29(8):2254–2259.
13. APHA. Standard Methods for the Examination of Water and Wastewater[S]. Washington DC, USA, 1998.
14. Fan J., Vanrolleghem P. A., Lu S. A kinetic modeling for carbon metabolism in sequencing batch reactor under multiple aerobic/anoxic conditions[J]. *Applied Microbiology and Biotechnology*. 2012, 96(1): 241–252. http://dx.doi.org/10.1007/s00253-011-3729-x
15. Debik E., Manav N. Sequence optimization in a sequencing batch reactor for biological nutrient removal from domestic wastewater[J]. *Bioprocess Biosyst Eng.* 2010, 33(12): 533–540. http://dx.doi.org/10.1007/s00449-009-0366-1

16. Yt R., Hj Y., Ch Y., *et al.* A full-scale test of a biological nutrients removal system using the sequencing batch reactor activated sludge process.[J]. *Water Sci Technol.* 1997, (2) 241–247).
17. Umble. A.K., Ketchum. L.H. A strategy for coupling municipal wastewater treatment using the sequencing batch reactor with effluent nutrient recovery through aquaculture[J]. *Water Sci Technol.* 1997, 35(1): 177–184. http://dx.doi.org/10.1016/S0273-1223(96)00894-3
18. Akin B.S., Ugurlu A. Monitoring and control of biological nutrient removal in a sequencing batch reactor[J]. *Process Biochem.* 2005, 40(12): 2873–2878. http://dx.doi.org/10.1016/j.procbio.2005.01.001
19. Cybis L.F., Santos A.V., Gehling G.R. The sequencing batch reactor (SBR) efficiency in the removal of nitrogen on the treatment of domestic sewage with low COD[J]. *Eng Sanit Ambient.* 2004, 9(1): 260–264. http://dx.doi.org/10.1590/S1413-41522004000300012
20. Lv Juan, CHEN Yinguang, G.U. Guowei. Biological nitrogen and phosphorus removal in the anaerobic-aerobic-anoxic-aerobic -anoxic-aerobic sequencing batch reactors[J]. *Environmental Science*, 2008,29(4):937–941.
21. Ds L., Co J., Jm P. Biological nitrogen removal with enhanced phosphorus uptake in a sequence batch reactor using single sludge system[J]. *Water Res.* 2001, 35(23): 3968–3976.
22. Monica Carvalheira, Adrian Oehmen, Gilda Carvalho,*et al.* Survival strategies of polyphosphate accumulating organismsand glycogen accumulating organisms under conditions of loworganic loading[J]. *Bioresource Technology*, 2014,172 (4) :290–296. http://dx.doi.org/10.1016/j.biortech.2014.09.059
23. Wang Lin. The Dynamic Principles of Denitrifying Simultaneous Phosphorus Removal and Application to Improving the Performance of MSBR Operation[D].Chongqing. Chongqing University, 2010:113–115.
24. Peng yongzhen, Ge shijian. Enhanced nutrient removal in three types of step feeding process from municipal wastewater[J]. *Bioresource Technology*, 2011, 102(5):6405–6413.
25. Sanket Ray, Vimal Prajapati, Kamlesh Patel,*et al.* Optimization and characterization of PHA from isolate Pannonibacterphragmitetus ERC8 using glycerol waste[J]. *International Journal of Biological Macromolecules*, 2016, 86 (7) :741–749. http://dx.doi.org/10.1016/j.ijbiomac.2016.02.002
26. Emmanouel Korkakaki, Michel Mulders, Adrie Veeken, *et al.* PHA production from the organic fraction of municipal solid waste(OFMSW): Overcoming the inhibitory matrix[J]. *Water Research*, 2016, 96 (8) 74–83. http://dx.doi.org/10.1016/j.watres.2016.03.033

Effects of Abiotic Factors on Microbial Characteristics of Petroleum Contaminated Soils in Northern China

KAI ZHANG[1], MAO-GUAN HU[2], YU-HUA LI[3], JIA-JUN YANG[1] and JIAN-LI JIA[4,*]

[1]*China University of Mining &Technology (Beijing), Beijing, 100083, China*

[2]*CSD water service Co., Ltd., 100192, China*

[3]*Guizhou University of Engineering Science, 551700, China*

[4]*School of Chemical & Environmental Engineering, China University of Mining & Technology (Beijing), Beijing, 100083, PR China*

ABSTRACT: In this study, the microbial community and the physico-chemical properties of soil samples from seven oil-fields in the north of China were analyzed using multiple methods. The study's purpose was to analyze the influence of abiotic factors on the microbial activity and the biotic community. By using the Ultrasonic- Soxhle extraction method of hydrocarbon in oil composition were analyzed, and column chromatography combined with GC-MS was used to analyze the contaminant composition. The results showed that the highest oil concentrations in the soil reached 97.3 g/kg dry soil, which amounts to about 500–1,000 times higher than the background in uncontaminated soil. Moreover, the average nutrient content of contaminated soils was lower than the unpolluted controls. The total bacterial load in the soil was measured using the most probable number (MPN) method and the microbial activity was determined by fluorescein diacetate (FDA) activity. The results showed that soil contaminated with oil seriously affects and limits the microbial populations and their activities. The water content of the soil was the key limiting factor of the microbial populations and the FDA activity. With a water content of 6%, oil content below 15%, and a pH of 7.5–8.0, the conditions supported the highest levels of microbial growth and activity. Microbial populations were 10–100 times and the FDA activity was 2–5 times lower in samples originating from the arid Northwest of China compared to samples from Northwest China. In the northwestern region the microbial diversity was 3 times higher. The microbial communities were limited and suppressed whereby the local environment, the temperature, the water content and the oil content were the key factors that induced the biodiversity of the soil contaminated with oil in different analyses of the geography and the climate environment.

INTRODUCTION

PETROLEUM is a complex compound containing a mixture of saturated and unsaturated alkanes, polyaromatic hydrocarbons (PAHs) and, in minor amounts, inorganic compounds like sulfides and nitrates [1–5].

With the development of the oil industry in China, and the occurrence of frequent oil spills from the many wells scattered throughout the county, oil contamination in the soil and in the groundwater has become an important environmental issue [6–8]. During an oil spill, the hydrophobic hydrocarbons plug the porous soil and reduce its permeability, thus changing its nutrient-transport capacity [9]. Petrochemical pollution has a destructive effect on the aquatic ecological environment of oil fields, and such pollution is considered ecotoxic, increasing the vulnerability of the ecosystem and causing physiological disorders to plants and animals alike. Polluted soil undergoes changes in the microbial communities and their compositions and on the ecological function of the soil and the efficiency of bioremediation.

Microbial ecosystem of soil which has been polluted with petrochemical hydrocarbons is influenced by both biotic and abiotic factors [10,11]. The biotic factors influencing the microbial ecosystem are the nature, the relative numbers and the microbial communities and populations. The abiotic factors at play include the soil composition, and concentration of contaminants, as well as other soil properties. Lastly, environmental factors such as weather and local climate play a role.

It has been shown that the biodegradation rates and the dynamics thereof are limited by the interactions of

*Author to whom correspondence should be addressed.
Email: jjl@cumtb.edu.cn

1544-8053/16/03 317-08

doi:10.12783/issn.1544-8053/13/4/9

the biotic and abiotic factors at play. Thus, the microbial communities can be either induced or suppressed by hydrocarbon pollutants, while the microbial community profiles and their activities are remarkably changed and affected by the contaminants in the soil. The microbial activities, the functions and the communities thus change in order to adapt to the pollution [12–14].

In this paper the role of some of the abiotic factors present in soils contaminated with oil were investigated. A range of geographically, widely distant oil fields was assessed. The microbiological diversity in the soils was examined in terms of its aerobic and oil-degrading bacteria content and, later, evaluated by means of denatured gradient gel electrophoresis (DGGE). The findings reported here are relevant for the purpose of developing dynamic biodegradation models, investigating biodegradation processes, and improving the biodegradation rates of petroleum pollution in soils.

2. MATERIAL AND METHODS

2.1. Soil Sampling and Characterization

Soil samples were collected from 7 different oilfields located in various parts of northern China, at approximately 10–25 cm in soil depth. Wherever possible, both polluted and unpolluted samples were collected from the same site. Samples were stored in polypropylene bags, transported to the laboratory and stored at 4°C awaiting further analysis. The sampled locations are shown on a map in Figure 1. The seven oil fields are distributed all over the country, covering a large geographic range of China.

The basic physical properties of the contaminated soil samples including the pH levels, the nitrogen and the phosphorus content were determined on the basis of a soil-agricultural-chemical process [15,16]. Ultrasonic-Soxhle extraction method of hydrocarbon in oil were analyzed, and column chromatography in combination with gas chromatography-mass spectrometry (GC-MS) was used to analyze the pollutant compositions [19]. The GC-MS analysis of extracted oil hydrocarbon was performed on a HP 5890 GC-5922 MSD. Capillary columns were used of 30 m × 0.25 mm × 0.25 μm HP 5 MAS. Chromatography conditions were as follows: the carrier gas was helium (1.0 ml/min), the temperature program for the hydrocarbon distribution was 100°C for 3 min, then 10°C/min increase to 250°C, followed by 5 10°C/min to 280°C, with a final hold for 20 min.

2.2. Microbial Quantitation and Activity Analysis

The total bacterial load present in the soil was determined by using the most probable number (MPN) method and the microbial activities were measured by fluorescein diacetate (FDA)[17,18].

2.3. DGGE Analysis of Total Microbial DNA

The total DNA was extracted from the soil samples according to Zhou *et al.* [20]. The extracted DNA was checked by electrophoresis (BIORAD, Canada) after which a region of 470 bp of the 16S rDNA gene was amplified using the universal primers b341GC(5′-CG CCCGCCGCGCGCGGCGGGCGGGGCGGGGGC ACGGGGGGCCTACGGGAGGCAGCAG-3′) and b758(5′-CTACCAGGGTATCTAATCC-3′) [21,22]. The amplified fragments were detected by electrophoresis in 1%agarose. DGGE analysis was carried out using the BIORAD D code system (BIORAD, Canada), as described in the system specification.

3. RESULTS AND DISCUSSION

3.1. Analysis of Abiotic Factors of the Contaminated Soils

The sampled oilfields are located in different climate zones and are subject to different and geographical characteristics. Thus, environmental factors such as temperature, humidity, and chemical composition obviously differ between the samples, which mean that variable factors have acted on the microbial ecosystems which are distinct among the respective locations. In order to analyze and compare the biotic and abiotic factors of the microbial ecosystems in the polluted soils at the different sampling locations, measurements were performed on polluted and unpolluted samples from the sites. The determined abiotic variables the oil content, the water content, and the nutrient concentrations of the samples are listed in Table 1.

The results show that the oil concentrations in the samples reached up to 97,300 mg/kg of dry soil, which is approximately 500–1,000 times higher than background levels. Most of the contaminated samples contained petroleum quantities in the range of 20–70 g/kg of dry soil. The average nutrient contents of the contaminated soils were lower than that of the unpolluted control samples around the sites. Especially in the agricultural areas, as shown in samples 5 and 6, the effective nitrogen and phosphorus loads were less than 30

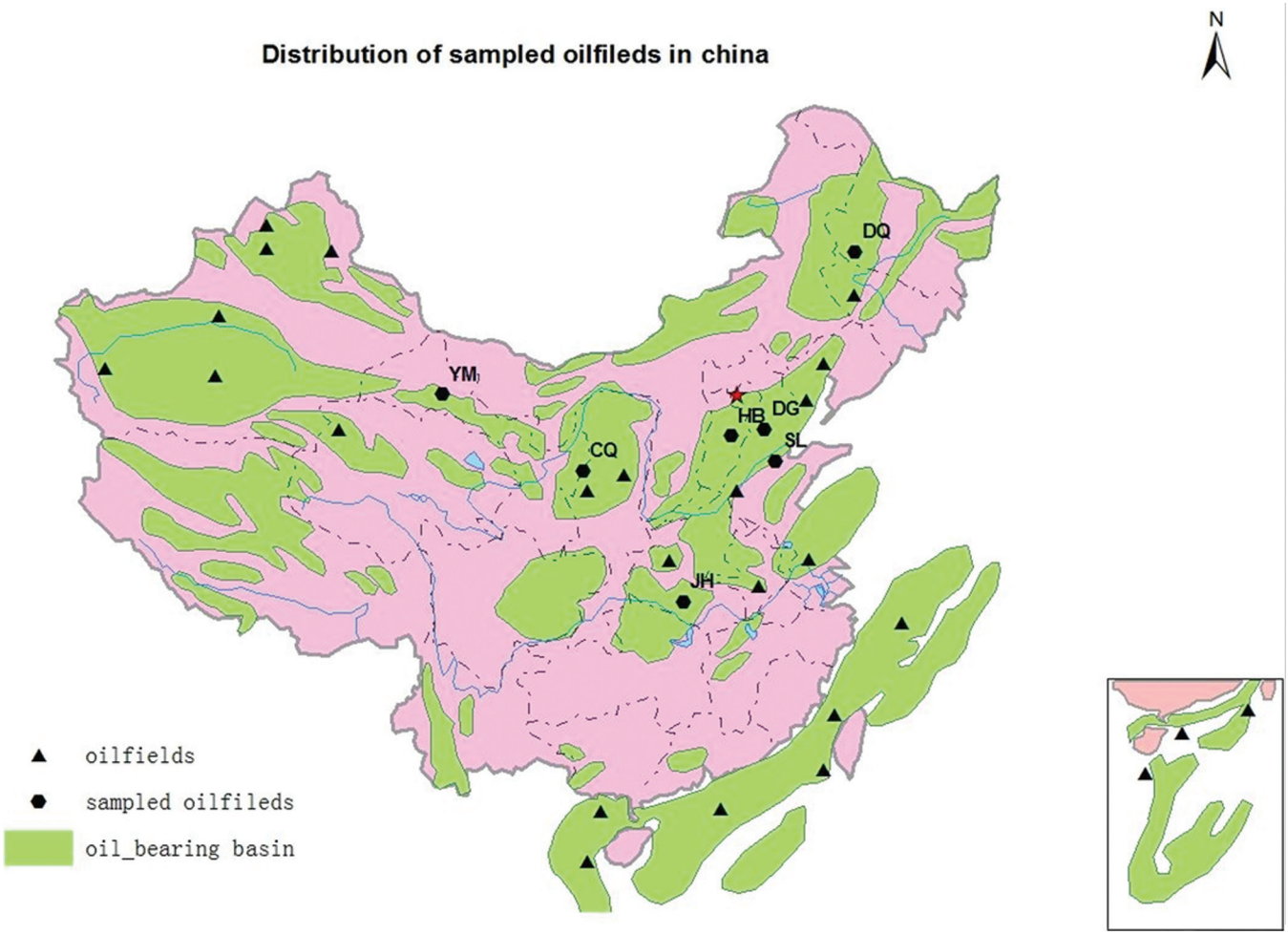

Figure 1. *Map of China showing the location of the oil-fields and the sampling sites used for this study. Abbreviations used are YM: Yumen Oil-field, CQ: Changqing Oil-field, JH: Jianghan Oil-field, DQ: Daqing Oil-field, DG: Dagang Oil-field, HB: Huabei Oil-field, SL:Shengli Oil-field. The inlay shown to the bottom right is located to the south of the main map.*

and 10 mg/kg of dry soil, respectively, accounting for about 5% of the total levels of nitrogen or phosphorus. This was most likely due to thatduring the processes of hydrocarbons biodegradation, which obviously limited the biodegradation rates and the microorganism activities.

3.2. The Effects of Abiotic Factors on the Microbial Community

The different abiotic factors of the soils, created by such local environmental conditions as natural geography and climate, affected the microbial profiles in

Table 1. The Abiotic Variables of the Soils Under Study.

Sample No.	Content*		Water Content (%)	pH	Total N*	Effective N*	Total P*	Effective P*
	Unpolluted Controls	Polluted Samples						
1	51.5	69900	2.18	7.60	1627	93.8	677.3	5.2
2	40.6	21730	3.07	7.92	–	88	–	17.1
3	48.36	60200	5.15	7.75	–	34	–	5.7
4	–	77300	12.95	7.96	1300	40.7	480.3	5.0
5	117.2	55300	14.58	7.17	620	27.9	198.5	9.6
6	23.64–35.19	20539	17.23	8.18	490	12.9	518.5	7.3
7	–	97300	1.08	7.90	733	131.9	321.6	3.6

*mg/kg dry soil.

remarkable ways. The relationship between the microbial activities and the abiotic factors was investigated in the different geographical areas.

The results indicated that the sum total of microorganisms in the soil samples was relatively stable, with typically 10^7–10^9 cells present per g of dry soil. The microbial communities of polluted soils, in terms of their numbers and nature, had changed in comparison with the unpolluted samples. Various analyses were carried out to investigate the relationships between the abiotic factors and the observed changes. Figure 2 shows the effect of the oil content in the various soil samples on the total numbers of aerobic bacteria and the numbers of oil-removing bacteria. The FDA activity of the bacteria is also shown.

As can be seen from Figure 2, the number of aerobic bacteria present in the soil was higher than the number of oil-degrading bacteria, for all of the samples tested. There was a general decrease in their numbers of a factor of 10 to 100 with increasing oil contamination, though there were relatively few samples with high oil content. Samples with an oil content of 0–7%(w/w) contained the highest number of aerobic bacteria, while the numbers of oil-removing bacteria were highest in samples containing 0–15% oil. Samples with an oil content of 2–13% had the highest FDA activity. These findings indicate that oil content below 15% has limited inhibitory effects on total microbial growth.

Figure 3 shows the relationship between the microbial communities and the water content of the selected soils. The number of microbes varied surprisingly little between the samples with different levels of water content. In the polluted samples, which contained less than 6% water, the oi-degrading bacteria amounted to less than 10^3 cells/g of dry soil. With water content higher than 6%, the oil content apparently became the key limiting factor for microbial activity. Figure 2 shows, for example, that the microbial amounts were well below this level in soils with an oil content of less than 0.1%. Under optimal abiotic environmental conditions, oil-degrading microbes can reach levels of 10^5–10^6 cells/g of dry soil, which is 100 to 1000 times higher than is found in soils with low water content.

Figure 4 shows the correlation of the pH levels and the microbial communities. The pH levels varied between 7.2 and 8.8 in the various samples. In the samples with a pH level between 7.4 and 7.9 the number of aerobic bacteria in the soil was at its highest. In the samples with a light alkaline pH (between 7.5 and 8.0), the number of oil-degrading bacteria reached its highest numbers, while the soil samples with a pH 7.7–7.9 produced the highest FDA activity. These results indicate that very strong levels of acidity or alkalinity (i.e., extremely low or high pH levels) produce limiting factors for bacterial growth and diversity. A pH level between 7.5–8.0 is most suitable for microbial growth and activity.

The results presented here showed that abiotic factors dramatically affected the microorganism activity of the FDA in polluted soils. The FDA activities were lower than 0.3 in the arid soil samples with water content lower than 6%, indicating that water content is an important limiting factor for microbial activity. On the

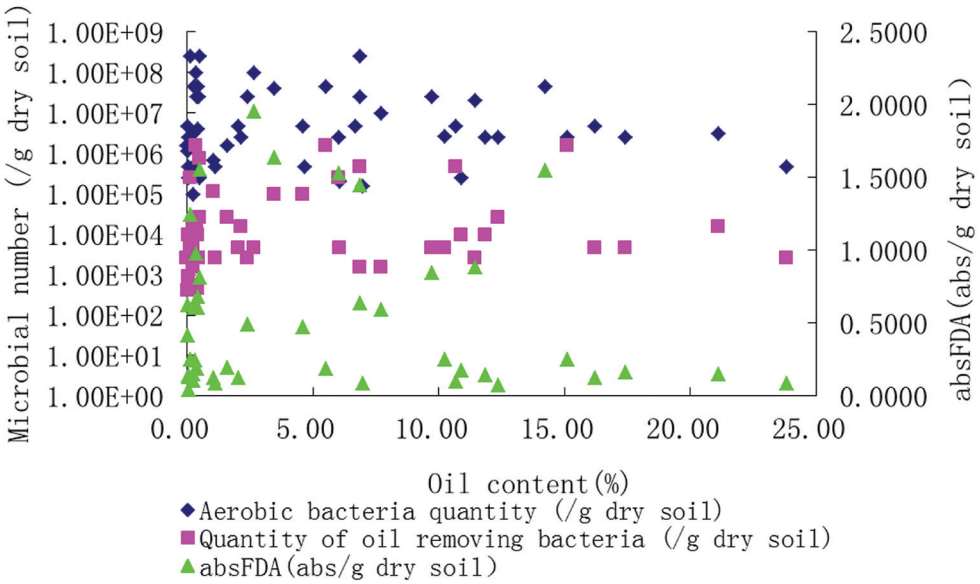

Figure 2. *Effect of oil content on the numbers and nature of microorganisms.*

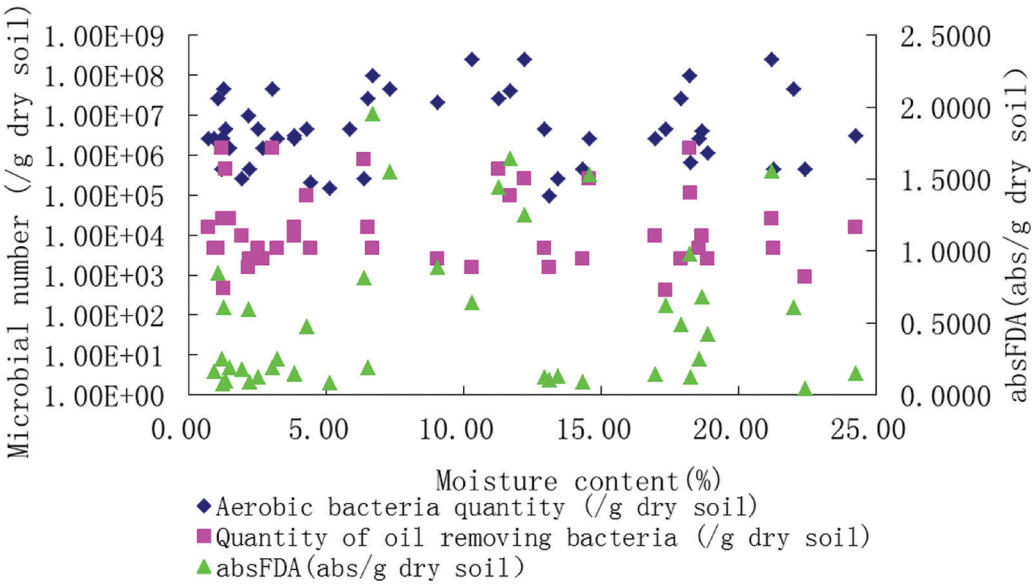

Figure 3. *The effects of water content on the number and nature of microorganisms.*

contrary, oil content in the soil is the main limiting factors affecting microbial activity. In this case, the trends of the FDA activity of microorganism were consistent with the hydrocarbon concentrations.

In conclusion, the microbial activities explored in this study were restricted and induced by the micro-ecosystem of the polluted soil samples. The abiotic factors exercised a strong influence on them. Water content was the key restricting factor over the microbial population and the FDA activity. The oil content was a main variable causing changes in the microbial population. Under optimal abiotic conditions in the microbial eco-system, the presence of hydrocarbons in affected soils could significantly stimulate microbial growth of oil-degrading bacteria.

3.3. The Effects of Biological Factors on Microbial Communities

This study showed that in unpolluted soil environments, the microbial community is very complex, while in, polluted soil environments, the microbial populations produce profiles that are distinct because of the differences between the soil matrix and the variations of the environment [23,24]. Natural selection would result in populations with adapted microbial

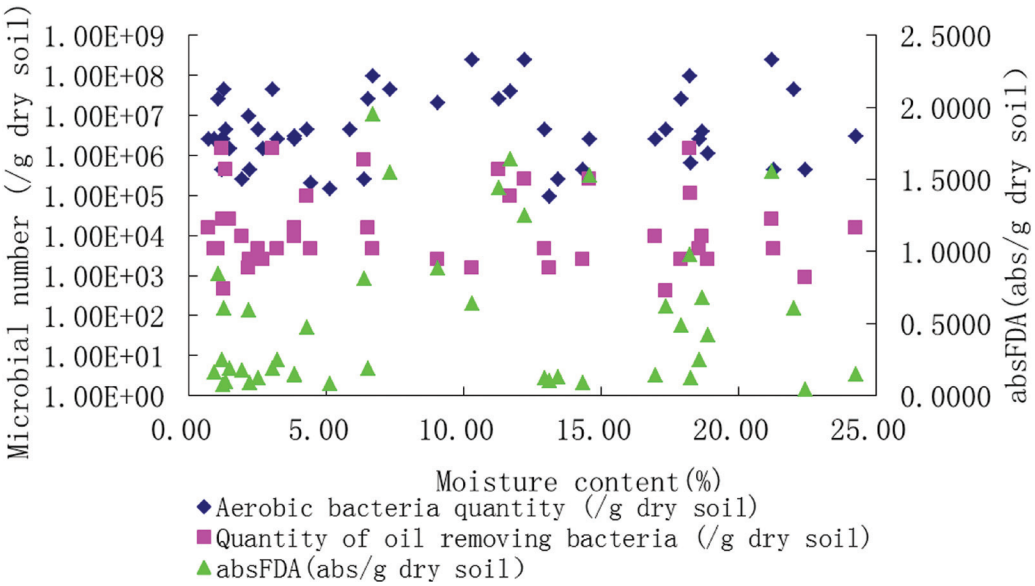

Figure 4. *The effects of pH on the quantity and nature of microorganisms.*

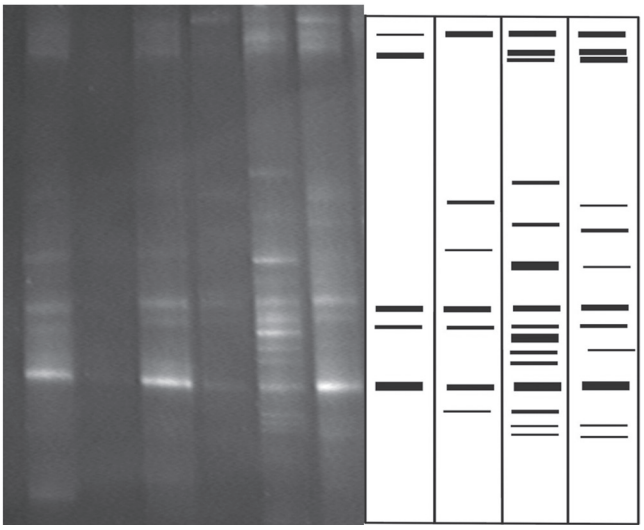

Figure 5. *The DGGE profile of 16S rDNA amplification fragments.*

enzyme activities. The resulting microbial communities vary in microbial profiles, in relative abundance and in the variation of activities and functions. These factors affect the efficiency of the biodegradation processes where different degrading bacteria both compete with each other and stimulate each other's growth. Other factors that affect the microbial eco-system are the presence of heavy metals such as Zn, which, according to the research of Bruce [25,26], can reduce the amount of land reclamation in soil microbial communities. Likewise, environmental pollution with petroleum hydrocarbon has caused changes in microbial diversity in soils in northern Canada [27].

In order to study the microbial diversity in polluted oil soils with different geological, physiognomy, and climate conditions, DNA fingerprint methods such as PCR-DGGE, PCR-SSCP and PCR-RFLP [28–30] are now being used. These can be as sensitive as traditional methods [31].

When the bands of amplified DNA fragments obtained from the contaminated soil samples were compared by DGGE (Figure 5), the weakest signal was obtained with the sample from the drought-ridden area in Northwest China (sample number 7). Strong signals were obtained with the polluted soils from the oil fields of North and Northeast China. From this we can conclude that the microbial diversity in Northwest China (sample 7) was lower than that in the other areas. In sample 6, the microbial diversity was the highest among all of the samples, with 2–5 times more bands than were obtained with any of the other samples. Interestingly, the microbial numbers in samples obtained from Northeast China was 10–100 times higher and their microbial FDA activities 2–5 times higher, when compared to the samples collected from Northwest China. The microbial diversity as determined by DGGE was also more abundant since samples from Northeast China produced 3 times more bands. This illustrates that the microbial diversity of contaminated soils is restricted. Such restriction can be due to local environmental factors such as temperature, but also due to the kinds of abiotic factors i which have been laid out here (This sentence seems repetitive and unnecessary since it reflects the subject matter of your paper: "e.g., the influence of microbial diversity of soils contaminated with petroleum hydrocarbons in different geological and climate conditions). The authors of this project have concluded that more heed should be paid to the exploration of the variations in microbial communities which are being created by different geological and climatic factors, as well as measurable abiotic factors. Such research would lead to more exact predictions on bio-degradation and bio-remediation efficiencies.

4. CONCLUSIONS

The pollution levels, soil properties, microbial populations, DGGE profiles and FDA activities found in soil samples from oil fields in seven locations in China were highly diverse. The average nutrient levels in the soil samples polluted with petroleum were lower than in the control soils from these areas. The effective nitrogen content was lower than 30 mg/kg dry of soil, and the phosphorus content was under 10 mg/kg of dry soil. This only accounted for about 5% of the total nitrogen and phosphorus levels, respectively. Through the analysis of the level of nutrients in the soil samples, these findings showed that the levels of nutrients in the contaminated soils were significantly lower.

In general, in the contaminated soils, microorganism quantity and activity were very low. When the water content was below 6%, the oil degradation bacteria number was less than 10^3 cells/g of dry soil, and the FDA activity was under 0.3%. On the contrary, the oil content was the main factor affecting the microbial quantity and activity. This study's findings revealed that soil with oil content below 15% and a pH level between 7.5–8.0 best supports the growth and activity of microorganisms.

This project also showed that the key factors affecting microbial communities are local temperatures, water content and oil content These factors, in turn, induced the microbial diversities of oil-contaminated

soils in different geographical locations and under diverse climatic conditions. Finally, the project revealed that at lower oil-contamination levels, the growth of oil degrading bacteria is stimulated in the soil, and these accumulate in the microbial communities.

5. ACKNOWLEDGEMENTS

The authors are grateful to the National Basic Research Program of China (973 Program, No. 2014CB238906).

6. REFERENCES

1. Jonker, MTO., Candido, A., Varbie, CM., Scarlett, AG., Rowland, SJ., Synergistic androgenic effect of a petroleum product caused by the joint action of at least three different types of compounds. *Chemosphere*, vol. 144, 2016, pp. 1142–1147. http://dx.doi.org/10.1016/j.chemosphere.2015.09.094
2. Asadov, ZH., Tantawy, AH., Zarbaliyeva, IA., Rahimov, RA., Petroleum-Collecting and Dispersing Complexes Based on Oleic Acid and Nitrogenous Compounds as Surface-Active Agents for Removing Thin Petroleum Films from Water Surface. *Journal of Oleo Science*, vol. 61,No. 11, 2012, pp. 621–630. http://dx.doi.org/10.5650/jos.61.621
3. Li, Y., Li, FM., Li, FX., Yuan, FQ., Wei, PF., Effect of the ultrasound-Fenton oxidation process with the addition of a chelating agent on the removal of petroleum-based contaminants from soil, *Environmental Science and Pollution Research*, vol. 22, No. 23, 2015, pp. 18446–18455. http://dx.doi.org/10.1007/s11356-015-5137-8
4. Vendramel, S., Bassin, JP., Dezotti, M;Sant., Anna, GL., Treatment of petroleum refinery wastewater containing heavily polluting substances in an aerobic submerged fixed-bed reactor. *Environmental Technology*, vol. 36, No. 16, 2015, pp. 2052–2059. http://dx.doi.org/10.1080/09593330.2015.1019933
5. Kafilzadeh, F., Khaledi, Z., Nejad, M.J.N., Evaluation of the bioaugmentation of contaminated soils with petroleum products by isolated bacteria from activated sludge obtained from municipal wastewater treatment in Asalouyeh region in Iran. *Fresenius Environmental Bulletin*, vol. 23, No. 3A, 2014, pp.941–946.
6. Liu, XS., Cai, W.T., Li S.T., Suvey of soil and groundwater contamination in oil pollution site. *Hydrogeology & Engineering Geology*, vol. 37, No. 4, 2010, pp. 121–125.
7. Gao, Y., Pmao, L., Zhi, Y.E., Shi, W.J., Assessment of effects of heavy metals combined pollution on soil enzyme activities and microbial community structure: modified ecological does-response model and PCR-RAPD. *Environmental Earth Sciences*, vol. 60, No. 3, 2010, pp. 603–612. http://dx.doi.org/10.1007/s12665-009-0200-8
8. Laha S., Tansel B., Ussawrujikulchai A., Surfactant-soil interactions during surfactant-amended remediation of contaminated soils by hydrophobic organic compounds: A review. *Journal Of Environmental Management*, vol. 90, No. 1, 2008, pp. 95–100. http://dx.doi.org/10.1016/j.jenvman.2008.08.006
9. Banat IM., Rancich I., Casaring P.,Biosurfactants and environmental improvement in the oil and petrochemical industry and the ecosystem, *Remediation and Beneficial Reuse of Contaminated Sediments*, pp. 95–102.
10. Rajaei S., Seyedi SM.,Raiesi F.,Shiran B.,Raheb J., Characterization and Potentials of Indigenous Oil-Degrading Bacteria Inhabiting the Rhizosphere of Wild Oat (*AvenaFatua* L.) in South West of Iran, *IranianJouranal of Biotechnology*, vol. 11, No. 1, 2013, pp. 32–40. http://dx.doi.org/10.5812/ijb.9334
11. Jia JL., Li GH, Zhong Y., The relationship between abiotic factors and microbial activities of microbial eco-system in contaminated soil with petroleum hydrocarbons, *Environmental Science*, vol. 25, No. 3, 2004, pp. 110–114.
12. M. T Balba., N Al-Awadhi, R Al-Daher. Bioremediation of oil-contaminated soil: microbiological methods for feasibility assessment and field evaluation, *Journal of Microbiological Methods*, vol. 32, 1998, pp. 155–164. http://dx.doi.org/10.1016/S0167-7012(98)00020-7
13. Nakatani AS., Siqueira JO., Soares CRF., Lambais MR., Microbial communities, enzymatic activity and mycorrhizal fungi in rhizospheric soil used for land farming of petrochemical waste, *Revista Brasileira De Ciencia Solo*, vol. 32,No. 4, 2008, pp. 1501–1512. http://dx.doi.org/10.1590/S0100-06832008000400014
14. Tang F., Hu HQ., Su XJ., Fu Qing-ling., Zhu Jun., Effects of Phosphate Rock and Decomposed Rice Straw Application on Lead Immobilization in a Contaminated Soil, *Huanjingke xue*, vol. 36, No. 8, 2015, pp. 3062–3067.
15. Buss W., Graham MC., Shepherd JG., Masek O., Suitability of marginal biomass-derived biochars for soil amendment, *Science of The Total Environment*, vol. 547, 2016, pp. 314–322. http://dx.doi.org/10.1016/j.scitotenv.2015.11.148
16. Freitas ND., Yano-Melo AM., da Silva FSB., de Melo NF., Maia LC., Soil biochemistry and microbial activity in vineyards under conventional and organic management at Northeast Brazil, *Scientia Agricola*, vol. 68, No. 2,2011, pp. 223–229. http://dx.doi.org/10.1590/S0103-90162011000200013
17. Araujo ASF., Monteiro RTR., Abarkeli RB., Effect of glyphosate on the microbial activity of two Brazilian soils, *Chemosphere*, vol. 52, No. 5, 2003, pp. 799–804. http://dx.doi.org/10.1016/S0045-6535(03)00266-2
18. L.G. Whyte., B.Goalen., J.Hawari., D.Labbé., C.W Greer., M.Nahir. Bioremediation treatbility assessment of hydrocarbon-contaminated soils from Eureka, Nunavut, *Cold Regions and Technology*, vol. 32, 2011, pp. 121–132. http://dx.doi.org/10.1016/S0165-232X(00)00025-2
19. Watanabe K., Baker P W., Environmentally relevant microorganisms, *Journal of Bioscience and Bioengineering*, vol. 89, No. 1, 2000, pp. 1–11. http://dx.doi.org/10.1016/S1389-1723(00)88043-3
20. Zhou J., Bruns M A., Tiedje J M.,DNA recovery from soils of diverse composition, *Appl and Envirl Microbiology*, vol. 6,No. 2,1996, pp. 316–322.
21. Rolleke S., Muyzer G., Wawer C., Wanner G., Lubitz W., Identification of bacteria in a biodegraded wall painting by denaturing gradient gel electrophoresis of PCR-amplified gene fragments coding for 16S rRNA, *Applied and Environmental Microbiology*, vol. 62, No. 6, 1996, pp. 2059–2065.
22. Abbasian F., Lockington R., Palanisami T., Megharaj M., Naidu R., Multiwall carbon nanotubes increase the microbial community in crude oil contaminated fresh water sediments, *Science of The Total Environment*, vol. 539, 2016, pp. 370–380. http://dx.doi.org/10.1016/j.scitotenv.2015.09.031
23. Sprocati AR., Alisi C., Tasso F., Marconi P., Sciullo A., Pinto V., Chiavarini S., Ubaldi C., Cremisini C., Effectiveness of a microbial formula, as a bioaugmentation agent, tailored for bioremediation of diesel oil and heavy metal co-contaminated soil, *Process Biochemistry*, vol. 47, No. 11, 2012, pp. 1649–1655. http://dx.doi.org/10.1016/j.procbio.2011.10.001
24. Li GH., Zhang X., Huang W., Characteristics of degrading microorganism distribution in polluted soil with petroleum hydrocarbons, *Environmental Science*, vol. 21, no. 4, 2000, pp.61–64.
25. De La Cueva SC., Rodiguez CH., Cruz NOS., Contreras JAR., Miranda JL., Changes in Bacterial Populations During Bioremediation of Soil Contaminated with Petroleum Hydrocarbons, *Water Air And Soil Pollution*, vol. 227, No. 3, 2016. http://dx.doi.org/10.1007/s11270-016-2789-z
26. Bruce F., Moffett, Fiona A., Nicholson., Nnanna C., Uwakwe., Zinc contamination decreases thebacterial diversity of agricultural soil, *FEMS Microbiology Ecology*, vol. 43, 2003, pp. 13–19. http://dx.doi.org/10.1111/j.1574-6941.2003.tb01041.x
27. D Juck.,WLG Cw., T Charles, Polyphasic microbial community analysis of petroleum hydrocarbon-contaminated soils from two northern Canadian communities, *FEMS Microbiology Ecology*, vol. 33, No. 3,2000, pp. 241–249. http://dx.doi.org/10.1111/j.1574-6941.2000.tb00746.x
28. Gerard M., Ellen C. DE Waal.,Andre G., Uitterlinden. Profiling of complex microbial populations by denaturing gradient gel electropho-

resis analysis of polymerase chain reaction-amplified genes coding for 16S rRNA, *Appl and Envir Microbiology*, vol. 59, 1993, pp. 695–700.

29. Frank S., Christoph C T., A new approach to utilize PCR single strand conformation polymorphism for 16S rRNA gene based microbial community analysis, *Appl Envir Microbiol.*, vol. 64, 1998, pp. 4870–4876.
30. Thomas L., Peter FD., Werner L., Use of the T-RFLP technique to assess spatial and temporal changes in the bacterial community structure within an agricultural soil planted with transgenic and non-transgenic potato plants, *FEMS Microbiology Ecology*, vol. 32, 2000, pp. 241–247. http://dx.doi.org/10.1111/j.1574-6941.2000.tb00717.x

GUIDE TO AUTHORS

1. Manuscripts shall be sent electronically to the Editor-in-Chief, Dr. P. Brent Duncan at pduncan@unt.edu using Microsoft Word in an IBM/PC format. If electronic submission is not possible, three paper copies of double-spaced manuscripts may be sent to Dr. P. Brent Duncan, (Editor of the *Journal of Residuals Science & Technology,* University of North Texas, Biology Building, Rm 210, 1510 Chestnut St., Denton, TX 76203-5017) (Tel: 940-565-4350). Manuscripts should normally be limited to the space equivalent of 6,000 words. The editormay waive this requirement in special occasions. As a guideline, each page of a double-spaced manuscript contains about 300 words. Include on the title page the names, affiliations, and addresses of all the authors, and identify one author as the corresponding author. Because communication between the editor and the authors will be electronic, the email address of the corresponding author is required. Papers under review, accepted for publication, or published elsewhere in journals are normally not accepted for publication in the *Journal of Residuals Science & Technology*. Papers published as proceedings of conferences are welcomed.
2. Article titles should be brief, followed by the author's name(s), affiliation, address, country, and postal code (zip) of author(s). Indicate to whom correspondence and proofs should be sent, including telephone and fax numbers and e-mail address.
3. Include a 100-word or less abstract and at least six keywords.
4. If electronic art files are not supplied, submit three copies of camera-ready drawings and glossy photographs. Drawings should be uniformly sized, if possible, planned for 50% reduction. Art that is sent electronically should be saved in either a .tif or .JPEG files for superior reproduction. All illustrations of any kind must be numbered and mentioned in the text. Captions for illustrations should all be typed on a separate sheet(s) and should be understandable without reference to the text.
5. DEStech uses a numbered reference system consisting of two elements: a numbered list of all references and (in the text itself) numbers in brackets that correspond to the list. At the end of your article, please supply a numbered list of all references (books, journals, web sites etc.). References on the list should be in the form given below. In the text write the number in brackets corresponding to the reference on the list. Place the number in brackets inside the final period of the sentence cited by the reference. Here is an example [2].

   Journal: 1. Halpin, J. C., "article title", *J. Cellular Plastics,* Vol. 3, No. 2, 1997, pp. 432–435.

   Book: 2. Kececioglu, D. B. and F.-B. Sun. 2002. *Burn-In Testing: Its Quantification and Optimization,* Lancaster, PA: DEStech Publications, Inc.
6. Tables. Number consecutively and insert closest to where firstmentioned in text or type on a numbered, separate page. Please use Arabic numerals and supply a heading. Column headings should be explanatory and carry units. (See example at right.)
7. Units & Abbreviations. Metric units are preferred. English units or other equivalents should appear in parentheses if necessary.
8. Symbols. A list of symbols used and their meanings should be included.

Table 5. Comparison of state-of-the-art matrix resins with VPSP/BMI copolymers.

Resin System	Core Temp. (DSC peak)	T_E	Char Yield, %
Epoxy (MY720)	235	250	30
Bismaleimide (H795)	282	>400	48
VPSP/Bismaleimide copolymer			
C379: H795 = 1.9	245	>400	50
C379: H795 = 1.4	285	>400	53

9. Page proofs. Authors will receive page proofs by E-mail. Proof pages will be in a .PDF file, which can be read by Acrobat Reader. Corrections on proof pages should be limited to the correction of errors. Authors should print out pages that require corrections and mark the corrections on the printed pages. Pages with corrections should be returned by FAX (717-509-6100) or mail to the publisher (DEStech Publications, Inc., 439 North Duke Street, Lancaster, PA 17602, USA). If authors cannot handle proofs in a .PDF file format, please notify the Editor, Dr. P. Brent Duncan at pduncan@unt.edu.
10. Index terms.With proof pages authors will receive a form for listing key words that will appear in the index. Please fill out this form with index terms and return it.
11. Copyright Information. All original journal articles are copyrighted in the name of DEStech Publications, Inc. All original articles accepted for publication must be accompanied by a signed copyright transfer agreement available from the journal editor. Previously copyrighted material used in an article can be published with the *written* permission of the copyright holder (see #14 below).
12. Headings. Your article should be structured with unnumbered headings. Normally two headings are used as follows:

    Main Subhead: DESIGN OF A MICROWAVE INSTALLATION Secondary Subhead: Principle of the Design Method

    If further subordination is required, please limit to no more than one (*Third Subhead*).
13. Equations. Number equations with Arabic numbers enclosed in parentheses at the right-hand margin. Type superscripts and subscripts clearly above or below the baseline, or mark them with a caret. Be sure that all symbols, letters, and numbers are distinguishable (e.g., "oh" or zero, one or lowercase "el," "vee" or Greek nu).
14. Permissions. The author of a paper is responsible for obtaining releases for the use of copyrighted figures, tables, or excerpts longer than 200 words used in his/her paper. Copyright releases are permissions to reprint previously copyrighted material. Releases must be obtained from the copyright holder, which is usually a publisher. Forms for copyright release will be sent by the editor to authors on request.

General: The *Journal of Residuals Science & Technology* and DEStech Publications, Inc. are not responsible for the views expressed by individual contributors in articles published in the journal.